

# CITATION REPORT

List of articles citing

The SIESTA method for ab initio order-N materials simulation

DOI: 10.1088/0953-8984/14/11/302

Journal of Physics Condensed Matter, 2002, 14, 2745-2779.

**Source:** <https://exaly.com/paper-pdf/34791253/citation-report.pdf>

**Version:** 2024-04-19

This report has been generated based on the citations recorded by exaly.com for the above article. For the latest version of this publication list, visit the link given above.

The third column is the impact factor (IF) of the journal, and the fourth column is the number of citations of the article.

#	Paper	IF	Citations
2285	A Combined Theoretical and Experimental Approach for Platinum Catalyzed 1,2-Propanediol Aqueous Phase Reforming.		
2284	Colossal Increase in Electric Current and High Rectification Ratio in a Photoconducting, Self-Cleaning, and Luminescent Schottky Barrier NMOF Diode.		
2283	Tuning the Crystal Packing and Semiconductor Electronic Properties of 7,7-Diazaisoindigo by Side-Chain Length and Halogenation.		
2282	Zero-Dimensional Hybrid OrganicInorganic Halide Perovskite Modeling: Insights from First Principles.		
2281	Reversible Polymorphism, Liquid Crystallinity, and Stimuli-Responsive Luminescence in a Bola-amphiphilic System: StructureProperty Correlations Through Nanoindentation and DFT Calculations.		
2280	Enhanced Cooperativity in Supported Spin-Crossover MetalOrganic Frameworks.		
2279	Theoretical Evaluation of $[VIV(C3S5)3]_2$ as Nuclear-Spin-Sensitive Single-Molecule Spin Transistor.		
2278	Chirality-Dependent Electron Spin Filtering by Molecular Monolayers of Helicenes.		
2277	Nonadiabatic Hydrogen Dissociation on Copper Nanoclusters.		
2276	Crystal Phase Effects in Si Nanowire Polytypes and Their Homojunctions.		
2275	Controlling the Conductance of a GrapheneMolecule Nanojunction by Proton Transfer.		
2274	Ferroelectric Control of the Spin Texture in GeTe.		
2273	Understanding and Engineering Phonon-Mediated Tunneling into Graphene on Metal Surfaces.		
2272	Facet-Controlling Agents Free Synthesis of Hematite Crystals with High-Index Planes: Excellent Photodegradation Performance and Mechanism Insight.		
2271	Importance of Vacancies and Doping in the Hole-Transporting Nickel Oxide Interface with Halide Perovskites.		
2270	DNA Sequencing with Single-Stranded DNA Rectification in a Nanogap Gated by NTerminated Carbon Nanotube Electrodes.		
2269	Molecular Arrangement and Charge Transfer in C60/Graphene Heterostructures.		

2268 Doping of Graphene Nanoribbons via Functional Group Edge Modification.

2267 Ultrahigh-Performance Optoelectronics Demonstrated in Ultrathin Perovskite-Based Vertical Semiconductor Heterostructures.

2266 Plasmonic Response of Metallic Nanojunctions Driven by Single Atom Motion: Quantum Transport Revealed in Optics.

2265 Single-Molecule Conductance through an Isoelectronic BN Substituted Phenanthrene Junction.

2264 .

2263 First-Principles Approach to the Conductance of Covalently Bound Molecular Junctions.

2262 Synthetic Control of Quantum Interference by Regulating Charge on a Single Atom in Heteroaromatic Molecular Junctions.

2261 Concept of Lattice Mismatch and Emergence of Surface States in Two-dimensional Hybrid Perovskite Quantum Wells.

2260 Thermal Transport through Single-Molecule Junctions.

2259 Ferromagnet/Two-Dimensional Semiconducting Transition-Metal Dichalcogenide Interface with Perpendicular Magnetic Anisotropy.

2258 Water-Stable 1D Hybrid Tin(II) Iodide Emits Broad Light with 36% Photoluminescence Quantum Efficiency.

2257 Chemical Vapor-Deposited Hexagonal Boron Nitride as a Scalable Template for High-Performance Organic Field-Effect Transistors.

2256 Experimental and Theoretical Study of a Cadmium Coordination Polymer Based on Aminonicotinate with Second-Timescale Blue/Green Photoluminescent Emission.

2255 Ab initio study of C60silicon clusters. **2002**, 117, 10627-10634 17

2254 Electronic, magnetic and spectroscopic properties of manganese nanostructures. **2002**, 65, 1679-1739 58

2253 Current-voltage curves of atomic-sized transition metal contacts: an explanation of why Au is Ohmic and Pt is not. **2002**, 89, 066804 88

2252 Nonorthogonal generalized Wannier function pseudopotential plane-wave method. **2002**, 66, 131

2251 Vibrations of Methane in Structure I Clathrate Hydrateñ ab initio Density Functional Molecular Dynamics Study. **2002**, 2, 429-433 30

2250	Density functional simulation of small Fe nanoparticles. <b>2003</b> , 25, 261-270	54
2249	TransIESTA: a spice for molecular electronics. <b>2003</b> , 1006, 212-26	175
2248	Catalytic role of metal oxides in gold-based catalysts: a first principles study of CO oxidation on TiO <sub>2</sub> supported Au. <b>2003</b> , 91, 266102	358
2247	Microscopic theory of nanostructured semiconductor devices: beyond the envelope-function approximation. <b>2003</b> , 18, R1-R31	90
2246	Modulation of the NO trans effect in heme proteins: implications for the activation of soluble guanylate cyclase. <b>2003</b> , 8, 595-600	39
2245	Computational design of multifunctional materials. <b>2003</b> , 176, 615-632	61
2244	Quantitative vs. qualitative approaches to the electronic structure of solids. <b>2003</b> , 176, 375-389	8
2243	First principles calculation of the geometric and electronic structure of (Al <sub>2</sub> O <sub>3</sub> ) <sub>n</sub> (O <sub>x</sub> ) clusters with n. <b>2003</b> , 428, 206-210	8
2242	Compressibility of CO adsorbed on Ni from 10 <sup>-8</sup> mbar to 1.2 bar ambient CO pressures investigated with X-ray diffraction. <b>2003</b> , 522, 161-166	26
2241	Si <sub>160</sub> bond in cluster-based materials. <b>2003</b> , 532-535, 875-879	5
2240	First principles study of the Si(5 5 7)/Au surface. <b>2003</b> , 532-535, 655-660	40
2239	Charge confinement in epitaxial metallic islands: a study at semiempirical level. <b>2003</b> , 542, 283-292	1
2238	The role of localized states in the degradation of thin gate oxides. <b>2003</b> , 69, 118-129	7
2237	Dependence of the tip-surface interaction on the surface electronic structure. <b>2003</b> , 210, 146-152	18
2236	On the catalytic activity of palladium clusters generated with the electrochemical scanning tunnelling microscope. <b>2003</b> , 5, 584-586	15
2235	Oxygen vacancies at Ni/c-ZrO <sub>2</sub> interfaces. <b>2003</b> , 23, 2737-2740	17
2234	Binary phosphorus-carbon compounds: The series P <sub>4</sub> C <sub>3+8n</sub> . <b>2003</b> , 95, 546-553	15
2233	Critical thickness for ferroelectricity in perovskite ultrathin films. <b>2003</b> , 422, 506-9	1219

2232	Atomistic calculation of leakage current through ultra-thin metal-oxide barriers. <b>2003</b> , 69, 130-137	5
2231	Defect theory: elusive state-of-the-art. <b>2003</b> , 6, 26-35	40
2230	Small polarons in dry DNA. <b>2003</b> , 91, 108105	88
2229	Experimental and Theoretical Electron Density Studies in Large Molecules: NAD <sup>+</sup> , Nicotinamide Adenine Dinucleotide. <b>2003</b> , 107, 9109-9121	29
2228	A DFT-Based QM-MM Approach Designed for the Treatment of Large Molecular Systems: Application to Chorismate Mutase. <b>2003</b> , 107, 13728-13736	110
2227	A Theoretical Study of the Structure and Spectra of Nitric Acid Hydrates Crystals. <b>2003</b> , 107, 10608-10614	26
2226	Electrostatic complementarity in an aldose reductase complex from ultra-high-resolution crystallography and first-principles calculations. <b>2003</b> , 100, 8742-7	97
2225	First principles studies of the surface of galena PbS. <b>2003</b> , 67, 799-805	22
2224	Membrane protein simulations: ion channels and bacterial outer membrane proteins. <b>2003</b> , 66, 159-93	44
2223	Development and implementation of the exact exchange method for semiconductors using a localized basis set. <b>2003</b> , 28, 274-286	21
2222	Density-functional calculations of the structures, binding energies, and spin multiplicities of Fe <sub>n</sub> clusters. <b>2003</b> , 119, 11130-11134	42
2221	Hexagonal diamond from single-walled carbon nanotubes. <b>2003</b> ,	1
2220	Electronic structure calculations of low-dimensional transition metals. <b>2003</b> , 15, 199-288	8
2219	Electrons in dry DNA from density functional calculations. <b>2003</b> , 101, 1587-1594	82
2218	Epitaxial Metallic Islands: Charge Confinement And Templates For Atomic Wires. <b>2003</b> , 794, 136	
2217	Interatomic Forces in Condensed Matter. <b>2003</b> ,	181
2216	First-Principles Studies of N and P Dopant Interactions in SiC: Implications for Co-Doping. <b>2003</b> , 433-436, 649-652	2
2215	Ab initio quantum transport study of metal-molecule-metal structures.	

2214	Density functional calculations of the structures and binding energies of Ni <sub>2</sub> Cn clusters (n=7-11). <b>2003</b> , 118, 10349-10350		7
2213	Low-energy electron diffraction and resonances in DNA and other helical macromolecules. <b>2003</b> , 91, 113201		86
2212	Preconditioned iterative minimization for linear-scaling electronic structure calculations. <b>2003</b> , 119, 8842-8848	107	
2211	First-principles study of n-type dopants and their clustering in SiC. <b>2003</b> , 82, 4298-4300		21
2210	Density functional theory calculations of quantum electron transport: carbon nanotubes-gold contacts. <b>2003</b> , 299-314		5
2209	Models of defects in wide-gap oxides. <b>2003</b> , 151-222		15
2208	Optimized basis sets for the collinear and non-collinear phases of iron. <i>Journal of Physics Condensed Matter</i> , <b>2004</b> , 16, 5453-5459	1.8	38
2207	Realistic model tips in simulations of nc-AFM. <b>2004</b> , 15, S60-S64		18
2206	Theoretical simulation of non-contact atomic force microscopy imaging of the $\alpha$ -alumina(0001) surface. <b>2004</b> , 15, S108-S114		1
2205	MPI parallelization of the first-principles pseudopotential method program with respect to each band. <b>2004</b> , 12, 945-957		18
2204	Linear-scaling quantum Monte Carlo technique with non-orthogonal localized orbitals. <i>Journal of Physics Condensed Matter</i> , <b>2004</b> , 16, L305-L311	1.8	33
2203	Thermally driven hopping and electron transport in amorphous materials from density functional calculations. <i>Journal of Physics Condensed Matter</i> , <b>2004</b> , 16, S5289-S5296	1.8	1
2202	Interaction of silicon dangling bonds with insulating surfaces. <b>2004</b> , 92, 036101		25
2201	Variationally optimized basis orbitals for biological molecules. <b>2004</b> , 121, 10879-88		34
2200	Short-range repulsive interatomic interactions in energetic processes in solids. <b>2004</b> , 70,		11
2199	Projection method for rapid ab initio calculations of metals. <b>2004</b> , 70,		4
2198	Atomic force algorithms in density functional theory electronic-structure techniques based on local orbitals. <b>2004</b> , 121, 6186-94		32
2197	Prediction of new phases of nitrogen at high pressure from first-principles simulations. <b>2004</b> , 93, 125501		127

2196	Adsorption of acetic and trifluoroacetic acid on the TiO <sub>2</sub> (110) surface. <b>2004</b> , 121, 9039-42	22
2195	Fully transferable interatomic potentials for large-scale computer simulations of simple metal oxides: Application to MgO. <b>2004</b> , 70,	35
2194	Electron transport through molecules: Self-consistent and non-self-consistent approaches. <b>2004</b> , 70,	195
2193	Hydrogen-bridge bonding on semiconductor surfaces: Density-functional calculations. <b>2004</b> , 70,	13
2192	Electron transport in carbon nanotube shuttles and telescopes. <b>2004</b> , 70,	25
2191	Network equilibration and first-principles liquid water. <b>2004</b> , 121, 11136-44	148
2190	Electron-phonon interactions in C <sub>28</sub> -derived molecular solids. <b>2004</b> , 70,	8
2189	Role of spin-orbit splitting and dynamical fluctuations in the Si(557)-Au surface. <b>2004</b> , 93, 146803	86
2188	Geometric structure and electronic properties of neutral and anionic Fe <sub>2</sub> C <sub>3</sub> and Fe <sub>2</sub> C <sub>4</sub> clusters, as obtained by density-functional calculations. <b>2004</b> , 120, 2069-70	5
2187	Inelastic scattering and local heating in atomic gold wires. <b>2004</b> , 93, 256601	194
2186	Step barrier for gold adatoms and small clusters diffusing on graphite: An ab initio study. <b>2004</b> , 70,	13
2185	Intrinsic point defects and volume swelling in ZrSiO <sub>4</sub> under irradiation. <b>2004</b> , 70,	23
2184	Diffusion-reaction mechanisms of nitriding species in SiO <sub>2</sub> . <b>2004</b> , 70,	20
2183	Parallel, linear-scaling building-block and embedding method based on localized orbitals and orbital-specific basis sets. <b>2004</b> , 121, 6698-709	26
2182	Lattice density functional theory of molecular diffusion. <b>2004</b> , 121, 426-35	46
2181	Recent Advances in Point Defect Studies Driven by Density Functional Theory. <b>2004</b> , 233-234, 77-86	4
2180	Surface structure determination of zeolites. <b>2004</b> , 154, 1197-1203	3
2179	Bottom-up silicon nanoelectronics.	

2178	Ammonium cyanate: a DFT study of crystal structure, rotational barriers and vibrational spectrum. <b>2004</b> , 102, 869-876	5
2177	THE EFFECTS OF METALLIC CONTACTS ON SILICON NANOSTRUCTURES STUDIED QUANTUM MECHANICALLY. <b>2004</b> , 15, 447-458	
2176	Codoping and Grain-Boundary Cosegregation of Substitutional Cations in $\beta$ -Al <sub>2</sub> O <sub>3</sub> : A Density-Functional-Theory Study. <b>2004</b> , 88, 1-14	13
2175	Ab initio study of novel crystals based on fullerene C <sub>60</sub> and carbynes. <b>2004</b> , 46, 2317-2322	2
2174	Lattice dynamics and stability of CuInSe <sub>2</sub> . <b>2004</b> , 451-452, 141-144	15
2173	First principles simulations of the magnetic and structural properties of Iron. <b>2004</b> , 40, 371-377	29
2172	Defects in nanocrystalline SnO <sub>2</sub> studied by Tight Binding. <b>2004</b> , 42, 435-440	4
2171	Phonon dispersion in graphite. <b>2004</b> , 92, 075501	410
2170	Density-functional study of charge doping in WO <sub>3</sub> . <b>2004</b> , 70,	74
2169	Atomistic theory of transport in organic and inorganic nanostructures. <b>2004</b> , 67, 1497-1561	246
2168	Stability and mobility of mono- and di-interstitials in alpha-Fe. <b>2004</b> , 92, 175503	369
2167	The phonon dispersion of graphite revisited. <b>2004</b> , 131, 141-152	277
2166	Effect of oxygen on the magnetic coupling of a Mn thin film on Fe(001) substrate. <b>2004</b> , 564, 12-20	10
2165	Electron spectroscopy and density-functional study of ferric wheel molecules. <b>2004</b> , 65, 813-817	17
2164	Ultra-high-resolution X-ray structure of proteins. <b>2004</b> , 61, 774-82	24
2163	Self-passivation mechanisms in clusters of N dopants in SiC. <b>2004</b> , 1, 274-277	1
2162	Car-Parrinello simulations with a real space method. <b>2004</b> , 25, 799-812	16
2161	A scaled quantum mechanical force field for the alanine-alanine zwitterions in water based on scale factors for alanine, glycine, N-methylacetamide, acetate, formate, and methylamine. <b>2004</b> , 697, 81-95	4



2160	First principles study of gold adsorption and diffusion on graphite. <b>2004</b> , 564, 173-178	58
2159	Theoretical study of exchange coupling constants in an Fe <sub>19</sub> complex. <b>2004</b> , 65, 799-803	41
2158	Inhibition of copper corrosion in chloride solutions by amino-mercapto-thiadiazol and methyl-mercapto-thiadiazol: an impedance spectroscopy and a quantum-chemical investigation. <b>2004</b> , 49, 2761-2770	80
2157	The HCl hexahydrate: RAIR spectra and theoretical investigation. <b>2004</b> , 396, 335-340	13
2156	Electronic structure, magnetic interactions, and the role of ligands in Mn <sub>n</sub> (n=4,12) single-molecule magnets. <b>2004</b> , 70,	44
2155	Ab initio Simulations of Fe and TiC clusters. <b>2004</b> , 77, 149-159	7
2154	Field-evaporation from first-principles. <b>2004</b> , 102, 1045-1055	60
2153	Internal Ceramic Reconstruction Weakens Metal/Al <sub>2</sub> O <sub>3</sub> Adhesion. <b>2004</b> , 108, 15439-15442	8
2152	The unexpected preference for the fac-isomer with the tris(5-ester-substituted-2,2'-bipyridine) complexes of ruthenium(II). <b>2004</b> , 43, 1714-22	20
2151	Dynamical Criteria for Cs Ion Insertion and Adsorption at Cap and Stem of Carbon Nanotubes: Ab Initio Study and Comparison with Experiment. <b>2004</b> , 108, 15529-15535	20
2150	Thermal Properties of Impurity-Doped Clusters: Orbital-Free Molecular Dynamics Simulations of the Meltinglike Transition in Li <sub>1</sub> Na <sub>54</sub> and Cs <sub>1</sub> Na <sub>54</sub> . <b>2004</b> , 108, 11722-11731	42
2149	First-Principles Infrared Spectrum of Nitric Acid and Nitric Acid Monohydrate Crystals. <b>2004</b> , 108, 10535-10541	39
2148	Stable tetrahedral structure of the silica cluster (SiO <sub>2</sub> ) <sub>10</sub> . <b>2004</b> , 70,	14
2147	A scaled quantum mechanical force field for the alanine/alanine zwitterions in water based on scale factors for alanine, glycine, N-methylacetamide, acetate, formate, and methylamine. <b>2004</b> ,	
2146	Adsorption of C <sub>60</sub> on the Si(001) surface calculated within the generalized gradient approximation. <b>2004</b> , 15, S1-S4	25
2145	Atomic-scale nanowires: physical and electronic structure. <i>Journal of Physics Condensed Matter</i> , <b>2004</b> , 16, R721-R754	1.8 66
2144	Electron-phonon coupling is large for localized states. <b>2004</b> , 69,	50
2143	QM/MM Study of Nitrite Reduction by Nitrite Reductase of <i>Pseudomonas aeruginosa</i> . <b>2004</b> , 108, 18073-18080	37

2142	Multiscale modelling of nanostructures. <i>Journal of Physics Condensed Matter</i> , <b>2004</b> , 16, R1537-R1576	1.8	79
2141	Single-component magnetic conductors based on Mo <sub>3</sub> S <sub>7</sub> trinuclear clusters with outer dithiolate ligands. <b>2004</b> , 126, 12076-83		83
2140	Different origins of the ferromagnetic order in (Ga,Mn)As and (Ga,Mn)N. <b>2004</b> , 70,		111
2139	Stacking-fault based microscopic model for platelets in diamond. <b>2004</b> , 93, 265502		7
2138	Molecular Nanowires and Other Quantum Objects. <b>2004</b> ,		2
2137	Silicon monoxide clusters: the favorable precursors for forming silicon nanostructures. <b>2004</b> , 93, 095503		51
2136	Vacancy-like defects in a-Si: a first principles study. <b>2004</b> , 338-340, 400-402		9
2135	Computing the Properties of Materials from First Principles with SIESTA. <b>2004</b> , 103-170		96
2134	Trends in the structure and bonding of noble metal clusters. <b>2004</b> , 70,		472
2133	Sampling the diffusion paths of a neutral vacancy in silicon with quantum mechanical calculations. <b>2004</b> , 70,		70
2132	Multiscale modelling of defect kinetics in irradiated iron. <b>2004</b> , 4, 68-74		389
2131	Nanotubes and nanowires: the effect of impurities and defects on their electronic properties. <b>2005</b> , 2, 114		10
2130	Structural models for the interaction of Cd(II) with DNA: trans-[Cd(9-RGH-N7) <sub>2</sub> (H <sub>2</sub> O) <sub>4</sub> ] <sub>2</sub> <sup>+</sup> . <b>2005</b> , 99, 1540-7		24
2129	The structure and vibrational frequencies of crystalline HCl trihydrate. <b>2005</b> , 742, 147-152		14
2128	Structural and electronic properties of silicon nanograins with aluminum contacts: a density functional study. <b>2005</b> , 27, 204-209		7
2127	Electronic and magnetic properties of ring-like Fe <sub>6</sub> and Fe <sub>6</sub> @Si <sub>12</sub> clusters. <b>2005</b> , 341, 256-260		
2126	An Fe <sub>11</sub> complex showing single-molecule magnet behavior: Theoretical study using density functional methods and Monte Carlo simulations. <b>2005</b> , 24, 2364-2367		8
2125	First-principle calculations on gate/dielectric interfaces: on the origin of work function shifts. <b>2005</b> , 80, 272-279		30

2124	Stability and mobility of self-interstitials and small interstitial clusters in $\beta$ -iron: ab initio and empirical potential calculations. <b>2005</b> , 228, 92-99	118
2123	Electronic transport property of 4,4'-bipyridine molecular junction. <b>2005</b> , 105, 293-298	12
2122	Structural and dielectric properties of crystalline and amorphous ZrO <sub>2</sub> . <b>2005</b> , 486, 125-128	142
2121	Structural and electronic properties of 9R diamond polytype. <b>2005</b> , 136, 41-44	8
2120	Ab initio study of pentacene on Au(001) surface. <b>2005</b> , 589, 8-18	52
2119	An ab initio study of C <sub>60</sub> adsorption on the Si(001) surface. <b>2005</b> , 591, 45-55	58
2118	Adsorption of atomic and molecular oxygen on Cu(100). <b>2005</b> , 100, 403-406	28
2117	Electron transport and optical properties of carbon nanostructures from first principles. <b>2005</b> , 169, 1-8	16
2116	A quantum mechanically study of silicon nanograins with an aluminum overlayer: structural properties and electronic charge. <b>2005</b> , 43, 549-555	6
2115	Magnetic interactions in a Cu-containing heterospin polymer. <b>2005</b> , 78, 689-699	9
2114	Physics of thin-film ferroelectric oxides. <b>2005</b> , 77, 1083-1130	1700
2113	Anomalous size dependence in the melting temperatures of free sodium clusters: an explanation for the calorimetry experiments. <b>2005</b> , 94, 233-401	65
2112	Efficient projector expansion for the ab initio LCAO method. <b>2005</b> , 72,	283
2111	Electronic Structure Calculations with Localized Orbitals: The Siesta Method. <b>2005</b> , 77-91	3
2110	Electronic structure of FCC carbon. <b>2005</b> , 82, 120-123	5
2109	Towards molecular spintronics. <b>2005</b> , 4, 335-9	1096
2108	Direct observation of electron dynamics in the attosecond domain. <b>2005</b> , 436, 373-6	266
2107	Theoretical study of the magnetic behavior of ferric wheels. <b>2005</b> , 6, 1094-9	18

2106	From Coordination Polymer Macrocrystals to Nanometric Individual Chains. <b>2005</b> , 17, 1761-1765		70
2105	Density functional study of exchange coupling constants in single-molecule magnets: the Fe <sub>8</sub> complex. <b>2005</b> , 11, 4767-71		42
2104	Survey of intermediate band material candidates. <b>2005</b> , 133, 97-101		38
2103	The effect of surface symmetry on the adsorption energetics of SCH <sub>3</sub> on gold surfaces studied using Density Functional Theory. <b>2005</b> , 580, 19-29		35
2102	Hexagonal adenine networks constructed from their homopairings. <b>2005</b> , 589, 139-152		29
2101	Proximal effects in the modulation of nitric oxide synthase reactivity: a QM-MM study. <b>2005</b> , 10, 595-604		14
2100	Ab-initio spin polarized electronic structure calculations for TixGanAsm photovoltaic materials. <b>2005</b> , 40, 1383-1386		23
2099	Ferroelastic phase transitions: structure and microstructure. <b>2005</b> , 61, 3-18		56
2098	Quantum software interfaced with crystal-structure databases: tools, results and perspectives. <b>2005</b> , 38, 697-705		31
2097	Frontier example in experimental charge density research: Experimental electrostatics of proteins. <b>2005</b> , 101, 624-634		17
2096	Two distinct heme distal site states define Cerebratulus lacteus mini-hemoglobin oxygen affinity. <b>2006</b> , 62, 641-8		20
2095	Exchange interactions and magnetic anisotropy in the Ni <sub>4</sub> magnetic molecule. <b>2005</b> , 78, 47-59		8
2094	A Theoretical Study of Dislocation Formation at Surfaces in Covalent Materials: Effect of Step Geometry and Reactivity. <b>2005</b> , 108-109, 193-198		
2093	The Search for Near Interface Oxide Traps - First-Principles Calculations on Intrinsic SiO <sub>2</sub> Defects. <b>2005</b> , 483-485, 569-572		7
2092	Stability of Sr adatom model structures for SrTiO <sub>3</sub> (001) surface reconstructions. <i>Journal of Physics Condensed Matter</i> , <b>2005</b> , 17, L223-L230	1.8	24
2091	Nonlinear algorithm for the solution of the Kohn-Sham equations in solids. <i>Journal of Physics Condensed Matter</i> , <b>2005</b> , 17, 3701-15	1.8	5
2090	On the properties of surface reconstructed silicon nanowires. <b>2005</b> , 16, S250-S253		31
2089	Structural models for Si(553)Au atomic chain reconstruction. <b>2005</b> , 16, S218-S223		27

2088	Zirconia/nickel interfaces in micro- and nanocomposites. <b>2005</b> , 96, 507-514	16
2087	Noncollinear magnetic order in the six-atom Mn cluster. <b>2005</b> , 122, 226102	19
2086	Correlation effects and electronic properties of Cr-substituted SZn with an intermediate band. <b>2005</b> , 123, 114709	21
2085	Scalability of phononic crystal heterostructures. <b>2005</b> , 87, 111101	35
2084	Ab initio calculations of surface phase diagrams of silica polymorphs. <b>2005</b> , 71,	17
2083	Energetic stability, equilibrium geometry, and the electronic properties of CaBi(111) surfaces. <b>2005</b> , 72,	18
2082	Effects of contact geometry on transport properties of a Si <sub>4</sub> cluster. <b>2005</b> , 72,	63
2081	Structure and formation energy of carbon nanotube caps. <b>2005</b> , 72,	105
2080	First-principles investigation of Au-covered carbon fullerenes. <b>2005</b> , 72,	12
2079	Mutual orientation of two C <sub>60</sub> molecules: an ab initio study. <b>2005</b> , 122, 094315	33
2078	Single-channel conductance of H <sub>2</sub> molecules attached to platinum or palladium electrodes. <b>2005</b> , 72,	41
2077	Electron tunneling of photochemical reactions on metal surfaces: nonequilibrium Green's function-density functional theory approach to photon energy dependence of reaction probability. <b>2005</b> , 122, 194706	9
2076	Conductance oscillations in zigzag platinum chains. <b>2005</b> , 95, 256804	50
2075	Electron transport through molecules: Gate-induced polarization and potential shift. <b>2005</b> , 71,	44
2074	Strength of radial breathing mode in single-walled carbon nanotubes. <b>2005</b> , 71,	104
2073	Analysis of the electronic properties of intermediate band materials as a function of impurity concentration. <b>2005</b> , 72,	26
2072	Composition-dependent structural properties in ScGaN alloy films: A combined experimental and theoretical study. <b>2005</b> , 98, 123501	33
2071	Small Pd clusters: A comparison of phenomenological and ab initio approaches. <b>2005</b> , 72,	58

2070	First-principles study of the (112̄0)hBN(112̄0)cBN interface. <b>2005</b> , 71,	6
2069	Bond breaking coupled with translation in rolling of covalently bound molecules. <b>2005</b> , 94, 146104	81
2068	Geometry optimization of periodic systems using internal coordinates. <b>2005</b> , 122, 124508	106
2067	Comment on "Molecular distortions and chemical bonding of a large pi-conjugated molecule on a metal surface". <b>2005</b> , 95, 209601; author reply 209602	66
2066	Fullerene in a metal-organic matrix: design of the electronic structure. <b>2005</b> , 95, 146403	14
2065	Self-assembly of base-functionalized carbon nanotubes. <b>2005</b> , 72,	7
2064	Valence-band electron-tunneling measurement of the gate work function: Application to the high- $\gamma$ polycrystalline-silicon interface. <b>2005</b> , 98, 053712	15
2063	The planar-to-tubular structural transition in boron clusters from optical absorption. <b>2005</b> , 123, 014310	45
2062	STRUCTURAL PROPERTIES OF BIMETALLIC CLUSTERS FROM DENSITY FUNCTIONAL CALCULATIONS. <b>2005</b> , 19, 2339-2344	31
2061	Manipulating the electronic structures of silicon carbide nanotubes by selected hydrogenation. <b>2005</b> , 122, 214707	68
2060	Field emission patterns from first-principles electronic structures: application to pristine and cesium-doped carbon nanotubes. <b>2005</b> , 95, 177602	44
2059	Simple model of microscopic rolling friction. <b>2005</b> , 95, 126104	31
2058	Dielectric properties of ultrathin SiO <sub>2</sub> slabs. <b>2005</b> , 87, 262102	17
2057	Optoelectronic properties analysis of Ti-substituted GaP. <b>2005</b> , 123, 184703	5
2056	Fast computation of the Kohn-Sham susceptibility of large systems. <b>2005</b> , 72,	4
2055	Contact atomic structure and electron transport through molecules. <b>2005</b> , 122, 074704	118
2054	Oxygen-induced atomic desorptions in oxynitrides: Density functional calculations. <b>2005</b> , 72,	5
2053	Relationship between strain and the surface electronic structure of Cu(111) films on Ru(0001): Theory and experiment. <b>2005</b> , 71,	26

2052	Electronic structure and vibrational properties of Ba <sub>8</sub> Si <sub>46</sub> , Ba <sub>8</sub> Ag <sub>n</sub> Si <sub>46</sub> , and Ba <sub>8</sub> Au <sub>n</sub> Si <sub>46</sub> . <b>2005</b> , 72,	39
2051	Substrate-dependent electronic properties of an armchair carbon nanotube adsorbed on Hf(001). <b>2005</b> , 86, 213111	33
2050	Ab initio study of transport properties of multiwalled carbon nanotubes. <b>2005</b> , 72,	46
2049	Neutral self-defects in a silica model: A first-principles study. <b>2005</b> , 71,	50
2048	Ab initio study of helium in Hf: Dissolution, migration, and clustering with vacancies. <b>2005</b> , 72,	377
2047	Chemisorption of C <sub>28</sub> fullerene on c(4×4) reconstructed GaAs(001) surface: A density functional theory study. <b>2005</b> , 71,	4
2046	Coadsorption phases of CO and oxygen on Pd(111) studied by scanning tunneling microscopy. <b>2005</b> , 71,	36
2045	Theoretical study of the mechanism of dry oxidation of 4H-SiC. <b>2005</b> , 71,	122
2044	Defect passivation with fluorine in a Ta/sub x/C/ high-K gate stack for enhanced device threshold voltage stability and performance.	10
2043	Role of elastic scattering in electron dynamics at ordered alkali overlayers on Cu(111). <b>2005</b> , 95, 176802	67
2042	Molecular dynamics simulations of the meltinglike transition in Li <sub>13</sub> Na <sub>42</sub> and Na <sub>13</sub> Cs <sub>42</sub> clusters. <b>2005</b> , 71,	38
2041	First-principles study of the atomic and electronic structure of the Si(111)(5×5)Au surface reconstruction. <b>2005</b> , 71,	42
2040	Fully unconstrained density-functional study of the structures and magnetic moments of small Mn <sub>n</sub> clusters (n=2-7). <b>2005</b> , 72,	39
2039	Scanning tunneling microscopy and surface simulation of zinc-blende GaN(001) intrinsic 4x reconstruction: linear gallium tetramers?. <b>2005</b> , 95, 146102	12
2038	Tip and surface determination from experiments and simulations of scanning tunneling microscopy and spectroscopy. <b>2005</b> , 94, 056103	46
2037	Density-functional calculations of defect formation energies using the supercell method: Brillouin-zone sampling. <b>2005</b> , 71,	21
2036	Temperature dependence of the band gap of semiconducting carbon nanotubes. <b>2005</b> , 94, 036801	105
2035	Electrical switching in metallic carbon nanotubes. <b>2005</b> , 95, 216602	86

2034	1D lattice distortions as the origin of the (2 x 2)p4gm reconstruction in gamma'-Fe4N(100): a magnetism-induced surface reconstruction. <b>2005</b> , 95, 136102		26
2033	ACCELERATING CONVERGENCE OF MOLECULAR DYNAMICS-BASED STRUCTURAL RELAXATION. <b>2005</b> , 16, 193-223		1
2032	Ab initio localized basis set study of structural parameters and elastic properties of HfO polymorphs. <i>Journal of Physics Condensed Matter</i> , <b>2005</b> , 17, 5795-5811	1.8	33
2031	Calculation of the effect of intrinsic point defects and volume swelling in the nuclear magnetic resonance spectra of ZrSiO4. <b>2005</b> , 31, 349-354		8
2030	Isolated modes and percolation in the lattice dynamics of (Be, Zn)Se. <b>2005</b> , 78, 219-228		11
2029	Nanosopic modeling of a carbon nanotube force-measuring biosensor. <b>2005</b> , 31, 123-133		5
2028	Theory of sodium ordering in NaxCoO2. <b>2005</b> , 71,		98
2027	Defect energies of graphite: Density-functional calculations. <b>2005</b> , 72,		280
2026	Ab initio study of benzene adsorption on carbon nanotubes. <b>2005</b> , 71,		217
2025	First-principles study of Ti-doped sodium alanate surfaces. <b>2005</b> , 86, 103109		58
2024	Theoretical study of ethynylbenzene adsorption on Au(111) and implications for a new class of self-assembled monolayer. <b>2005</b> , 109, 20387-92		58
2023	High-resolution valence-band XPS spectra of the nonconductors quartz and olivine. <b>2005</b> , 72,		62
2022	Magnetism and half-metallicity at the O surfaces of ceramic oxides. <i>Journal of Physics Condensed Matter</i> , <b>2005</b> , 17, L451-L457	1.8	58
2021	Dielectric properties of nanoscale HfO2 slabs. <b>2005</b> , 72,		38
2020	Energetics of intrinsic point defects in ZrSiO4. <b>2005</b> , 71,		33
2019	Two exchange-correlation functionals compared for first-principles liquid water. <b>2005</b> , 31, 361-366		31
2018	Linear Response Properties Required to Simulate Vibrational Spectra of Biomolecules in Various Media: (R)-Phenyloxirane (A Comparative Theoretical and Spectroscopic Vibrational Study). <b>2005</b> , 91-124		11
2017	Measuring site-specific cluster-surface bond formation. <b>2005</b> , 127, 17863-6		28



2016	Structural and thermal behavior of compact core-shell nanoparticles: Core instabilities and dynamic contributions to surface thermal stability. <b>2005</b> , 72,	32
2015	Structural, electronic, and vibrational properties of (4,4) picotube crystals. <b>2005</b> , 72,	11
2014	Effect of electron correlations in Pd, Ni, and Co monowires. <b>2005</b> , 72,	30
2013	Concerning the Structure of Hydrogen Molybdenum Bronze Phase III. A Combined Theoretical/Experimental Study. <b>2005</b> , 17, 5957-5969	41
2012	Defect generation in high $\epsilon_r$ gate dielectric stacks under electrical stress: the impact of hydrogen. <i>Journal of Physics Condensed Matter</i> , <b>2005</b> , 17, S2075-S2088	1.8 29
2011	New insights into the melting behavior of MgO from molecular dynamics simulations: the importance of premelting effects. <b>2005</b> , 94, 068501	50
2010	Structural refinement of the high-pressure phase of aluminum trihydroxide: in-situ high-pressure angle dispersive synchrotron X-ray diffraction and theoretical studies. <b>2005</b> , 109, 8857-60	20
2009	First-principles analyses and predictions on the reactivity of barrier layers of Ta and TaN toward organometallic precursors for deposition of copper films. <b>2005</b> , 21, 7608-14	31
2008	Changes of coupling between the electrodes and the molecule under external bias bring negative differential resistance. <b>2005</b> , 109, 3334-9	85
2007	Layered single-bonded nonmolecular phase of nitrogen from first-principles simulation. <b>2005</b> , 72,	63
2006	Discrimination of nitroxyl and nitric oxide by water-soluble Mn(III) porphyrins. <b>2005</b> , 127, 4680-4	102
2005	Nitric oxide interaction with cytochrome c' and its relevance to guanylate cyclase. Why does the iron histidine bond break?. <b>2005</b> , 127, 7721-8	61
2004	Melting-like Transition in a Ternary Alkali Nanoalloy: Li <sub>13</sub> Na <sub>30</sub> Cs <sub>12</sub> . <b>2005</b> , 1, 299-306	28
2003	Band structure of the four pentacene polymorphs and effect on the hole mobility at low temperature. <b>2005</b> , 109, 1849-56	152
2002	Modulation of the electronic structure of semiconducting nanotubes resulting from different metal contacts. <b>2005</b> , 109, 7601-4	17
2001	Finite element methods in ab initio electronic structure calculations. <b>2005</b> , 13, R71-R96	157
2000	Theoretical study of the truncated hemoglobin HbN: exploring the molecular basis of the NO detoxification mechanism. <b>2005</b> , 127, 4433-44	102
1999	Homopairing possibilities of the DNA bases cytosine and guanine: an ab initio DFT study. <b>2005</b> , 109, 22045-52	45

1998	Probing organic layers on the TiO <sub>2</sub> (110) surface. <b>2005</b> , 109, 4554-60	21
1997	Electronic structure of the K <sub>3</sub> Bi <sub>2</sub> metallic phase. <b>2005</b> , 44, 1644-6	7
1996	Photoisomerization of azobenzene from first-principles constrained density-functional calculations. <b>2005</b> , 122, 094311	108
1995	Strain-dependence of the electronic properties in periodic quadruple helical G <sub>4</sub> -wires. <b>2005</b> , 109, 22301-7	28
1994	Charge density research: from inorganic and molecular materials to proteins. <b>2005</b> , 220,	11
1993	Ferromagnetism driven by intrinsic point defects in HfO <sub>2</sub> . <b>2005</b> , 94, 217205	383
1992	Ab initio molecular dynamics simulation of a room temperature ionic liquid. <b>2005</b> , 109, 5895-902	256
1991	Exchange coupling in transition-metal complexes via density-functional theory: comparison and reliability of different basis set approaches. <b>2005</b> , 123, 074102	98
1990	Derivation of an Interatomic Potential for Fluoride-Containing Microporous Silicates and Germanates. <b>2005</b> , 17, 730-740	17
1989	Introducing ONETEP: linear-scaling density functional simulations on parallel computers. <b>2005</b> , 122, 84119	457
1988	A Tight Binding study of defects in nanocrystalline SnO <sub>2</sub> . <b>2005</b> , 33, 346-350	2
1987	First stages of the oxidation of the Si-rich 3C <sub>2</sub> BiC(0 0 1) surface. <b>2005</b> , 33, 13-19	9
1986	Ab initio phonon dispersion calculations for TixGanAsm and TixGanPm compounds. <b>2005</b> , 33, 118-124	12
1985	Modelling of nanoscale ferroelectrics from atomistic simulations. <b>2005</b> , 9, 114-121	20
1984	Single-molecule manipulation and chemistry with the STM. <i>Journal of Physics Condensed Matter</i> , <b>2005</b> , 17, S1049-S1074	1.8 59
1983	Crystal symmetry and pressure effects on the valence band structure of E <sub>n</sub> Se and E <sub>n</sub> GaSe: Transport measurements and electronic structure calculations. <b>2005</b> , 71,	54
1982	Designing meaningful density functional theory calculations in materials science—primer. <b>2005</b> , 13, R1-R31	282
1981	Deep-level emissions influenced by O and Zn implantations in ZnO. <b>2005</b> , 87, 211912	243

1980	Metallic and semimetallic silicon 100 nanowires. <b>2005</b> , 94, 026805	153
1979	Lattice distortion effects on the magnetostructural phase transition of MnAs. <b>2005</b> , 95, 077203	22
1978	Lattice dynamics of the mixed semiconductors (Be,Zn)Se from first-principles calculations. <b>2005</b> , 71,	72
1977	Theoretical study of structural, electronic, and magnetic properties of $AunM^+$ clusters (M=Sc, Ti, V, Cr, Mn, Fe, Au; $n \geq 9$ ). <b>2005</b> , 71,	105
1976	Models and modeling schemes for binary IV-VI glasses. <b>2005</b> , 71,	45
1975	Molecular distortions and chemical bonding of a large pi-conjugated molecule on a metal surface. <b>2005</b> , 94, 036106	249
1974	Defects in SiO <sub>2</sub> as the possible origin of near interface traps in the SiC/BiO <sub>2</sub> system: A systematic theoretical study. <b>2005</b> , 72,	134
1973	Electronic structure and magnetic properties of small manganese oxide clusters. <b>2005</b> , 123, 34306	28
1972	Intermolecular effect in molecular electronics. <b>2005</b> , 122, 44703	49
1971	Models of electrodes and contacts in molecular electronics. <b>2005</b> , 123, 114701	78
1970	Structure and electronic properties of zirconium and hafnium nitrides and oxynitrides. <b>2005</b> , 97, 044108	65
1969	Organometallic spintronics: dicobaltocene switch. <b>2005</b> , 5, 1959-62	104
1968	Self-vacancies in gallium arsenide: An ab initio calculation. <b>2005</b> , 71,	51
1967	Determination of the structure of $\gamma$ -alumina from interatomic potential and first-principles calculations: The requirement of significant numbers of nonspinel positions to achieve an accurate structural model. <b>2005</b> , 71,	120
1966	Impact of oxygen on the work functions of Mo in vacuum and on ZrO <sub>2</sub> . <b>2005</b> , 97, 064911	32
1965	Theoretical insights into bone grafting silicon-stabilized alpha-tricalcium phosphate. <b>2005</b> , 122, 024709	21
1964	Reactions and clustering of water with silica surface. <b>2005</b> , 122, 144709	66
1963	First-principles study of structural, elastic, and bonding properties of pyrochlores. <b>2005</b> , 72,	106

1962	First-principles calculations of the electrical properties of LaAlO <sub>3</sub> and its interface with Si. <b>2005</b> , 72,	45
1961	Electronic and structural properties of silicon carbide nanowires. <b>2005</b> , 71,	59
1960	Distribution patterns and controllable transport of water inside and outside charged single-walled carbon nanotubes. <b>2005</b> , 122, 84708	44
1959	Prediction of ordered phases of encapsulated C <sub>60</sub> , C <sub>70</sub> , and C <sub>78</sub> inside carbon nanotubes. <b>2005</b> , 5, 349-55	80
1958	Strain energy and electronic structures of silicon carbide nanotubes: Density functional calculations. <b>2005</b> , 71,	224
1957	Homopairing possibilities of the DNA base adenine. <b>2005</b> , 109, 11933-9	61
1956	An Efficient Real Space Multigrid QM/MM Electrostatic Coupling. <b>2005</b> , 1, 1176-84	186
1955	A density-functional study of the structures, binding energies and total spins of Ni-Fe clusters using nonlocal norm-conserving pseudopotentials and the generalized gradient approximation. <b>2005</b> , 122, 84311	11
1954	Studies of silicon dihydride and its potential role in light-induced metastability in hydrogenated amorphous silicon. <b>2005</b> , 86, 241916	11
1953	Spin-unrestricted linear-scaling electronic structure theory and its application to magnetic carbon-doped boron nitride nanotubes. <b>2005</b> , 123, 124105	25
1952	Enhancement of hydrogen physisorption on single-walled carbon nanotubes resulting from defects created by carbon bombardment. <b>2005</b> , 71,	17
1951	Real-space formulation of the electrostatic potential and total energy of solids. <b>2005</b> , 71,	47
1950	Multiple-steering QM-MM calculation of the free energy profile in chorismate mutase. <b>2005</b> , 127, 6940-1	103
1949	Density-functional theory calculations of XH <sub>3</sub> -decorated SiC nanotubes (X={C,Si}): Structures, energetics, and electronic structures. <b>2005</b> , 97, 104311	32
1948	Spintronic properties of carbon-based one-dimensional molecular structures. <b>2006</b> , 74,	21
1947	Structure, bonding nature, and binding energy of alkanethiolate on As-rich GaAs (001) surface: a density functional theory study. <b>2006</b> , 110, 23619-22	30
1946	Polarizability of phthalocyanine based molecular systems: A first-principles electronic structure study. <b>2006</b> , 88, 222903	26
1945	Theory of electrochemical monoatomic nanowires. <b>2006</b> , 74,	16

1944	Ab Initio Simulation of Si-Doped Hydroxyapatite. <b>2006</b> , 18, 413-422	47
1943	Adsorption and dimerisation of thiol molecules on Au(111) using a Z-matrix approach in density functional theory. <b>2006</b> , 32, 1219-1225	19
1942	First principles modeling of tunnel magnetoresistance of Fe/MgO/Fe trilayers. <b>2006</b> , 97, 226802	107
1941	Electronic and magnetic properties of ZnS doped with Cr. <b>2006</b> , 74,	61
1940	Effect of the atomic configuration of gold electrodes on the electrical conduction of alkanedithiol molecules. <b>2006</b> , 73,	121
1939	Adsorption of Benzene on Copper, Silver, and Gold Surfaces. <b>2006</b> , 2, 1093-105	130
1938	Negative differential resistance and hysteresis through an organometallic molecule from molecular-level crossing. <b>2006</b> , 128, 6274-5	66
1937	Amorphization induced by pressure: results for zeolites and general implications. <b>2006</b> , 97, 225502	42
1936	The atomic and electronic structure of dislocations in Ga-based nitride semiconductors. <b>2006</b> , 86, 2241-2269	17
1935	Conductance, surface traps, and passivation in doped silicon nanowires. <b>2006</b> , 6, 2674-8	91
1934	Computational design of SiBiO <sub>2</sub> interfaces: Stress and strain on the atomic scale. <b>2006</b> , 73,	32
1933	Electrons and hydrogen-bond connectivity in liquid water. <b>2006</b> , 96, 016404	87
1932	Identifying an O <sub>2</sub> supply pathway in CO oxidation on Au/TiO <sub>2</sub> (110): a density functional theory study on the intrinsic role of water. <b>2006</b> , 128, 4017-22	225
1931	Assisted desolvation as a key kinetic step for crystal growth. <b>2006</b> , 128, 13568-74	125
1930	Electron paramagnetic resonance and theoretical studies of shallow phosphorous centers in 3C-, 4H-, and 6H-BiC. <b>2006</b> , 73,	29
1929	Electronic Structure. <b>2006</b> , 199-276	2
1928	New Carbyne-Fullerene-Based Structures: Stability and Electronic Characteristics. <b>2006</b> , 14, 489-498	2
1927	Theoretical study of the electronic transport property of the hydrogen-Pt contact system. <b>2006</b> , 89, 182119	3

1926	Implementation of a Z-matrix approach within the SIESTA periodic boundary conditions code and its application to surface adsorption. <b>2006</b> , 32, 595-600	9
1925	Diameter-dependent spin polarization of injected carriers in carbon-doped zigzag boron nitride nanotubes. <b>2006</b> , 89, 123103	20
1924	Nanotube-metal junctions: 2- and 3-terminal electrical transport. <b>2006</b> , 124, 181102	19
1923	Extended Hückel theory for band structure, chemistry, and transport. I. Carbon nanotubes. <b>2006</b> , 100, 043714	80
1922	Electron Scattering in Narrow Metal Wires. <b>2006</b> ,	1
1921	Information Delivery in Computational Mineral Science: The eMinerals Data Handling System. <b>2006</b> ,	0
1920	Electronic Properties of Metallocene Wires. <b>2006</b> ,	0
1919	Ab initio study of the magnetostructural properties of MnAs. <b>2006</b> , 74,	39
1918	Crystal structure prediction using ab initio evolutionary techniques: principles and applications. <b>2006</b> , 124, 244704	1658
1917	Nonlinear spin current and magnetoresistance of molecular tunnel junctions. <b>2006</b> , 96, 166804	280
1916	High-resolution scanning force microscopy of gold nanoclusters on the KBr (001) surface. <b>2006</b> , 73,	35
1915	Insight into the solvent effect: a density functional theory study of cisplatin hydrolysis. <b>2006</b> , 125, 091101	19
1914	Empirical Molecular Dynamics: Possibilities, Requirements, and Limitations. 213-244	2
1913	Unusual sequence of phase transitions in MnAs: First-principles study. <b>2006</b> , 74,	12
1912	Ab initio study of metal-organic framework-5 Zn <sub>4</sub> O(1,4-Benzenedicarboxylate) <sub>3</sub> : An assessment of mechanical and spectroscopic properties. <b>2006</b> , 73,	76
1911	Spherical harmonic expansion of short-range screened Coulomb interactions. <b>2006</b> , 39, 8613-8630	12
1910	Structure and dynamics of dioxygen bound to cobalt and iron heme. <b>2006</b> , 91, 2024-34	20
1909	A mechanism for copper inhibition of infectious prion conversion. <b>2006</b> , 91, L11-3	16

1908	Structural characterization of fully coordinated ultrathin silica nanotubes by first-principles calculations. <b>2006</b> , 73,	20
1907	Electron states in a lattice of Au nanoparticles: the role of strain and functionalization. <b>2006</b> , 96, 116802	14
1906	Structural and dielectric properties of amorphous ZrO <sub>2</sub> and HfO <sub>2</sub> . <b>2006</b> , 74,	135
1905	Spin and molecular electronics in atomically generated orbital landscapes. <b>2006</b> , 73,	551
1904	Electronic excitations in metals and at metal surfaces. <b>2006</b> , 106, 4160-206	206
1903	Ab initio study of TCNQ-doped carbon nanotubes. <b>2006</b> , 73,	21
1902	Theoretical study of iron-filled carbon nanotubes. <b>2006</b> , 73,	61
1901	Dithiocarbamate anchoring in molecular wire junctions: a first principles study. <b>2006</b> , 110, 9893-8	72
1900	Surface segregation and backscattering in doped silicon nanowires. <b>2006</b> , 96, 166805	154
1899	Introducing Molecular Electronics: A Brief Overview. <b>2006</b> , 1-10	9
1898	Electronic structure of semiconductor nanowires. <b>2006</b> , 73,	181
1897	Hydrogen dynamics and light-induced structural changes in hydrogenated amorphous silicon. <b>2006</b> , 74,	17
1896	Filtering a distribution simultaneously in real and Fourier space. <b>2006</b> , 73,	9
1895	Piezoelectricity in ZnO nanowires: A first-principles study. <b>2006</b> , 89, 223111	154
1894	Analysis of scanning tunneling microscopy images of the charge-density-wave phase in quasi-one-dimensional Rb <sub>0.3</sub> MoO <sub>3</sub> . <b>2006</b> , 74,	6
1893	Silica nanoarchitectures with tailored pores based on the hybrid three- and four-membered rings. <b>2006</b> , 110, 15269-74	11
1892	Novel structural features of CDK inhibition revealed by an ab initio computational method combined with dynamic simulations. <b>2006</b> , 49, 5141-53	37
1891	A synthetic route toward well-defined stoichiometric silica fullerene and nanotubes based on metastable four-membered rings. <b>2006</b> , 110, 8992-7	6

1890	The simulation of imidazolium-based ionic liquids <a href="#">View all notes</a> . <b>2006</b> , 32, 1-10	112
1889	Noncovalent interactions between organometallic metallocene complexes and single-walled carbon nanotubes. <b>2006</b> , 125, 154704	41
1888	New route for stabilizing silicon fullerenes. <b>2006</b> , 110, 14619-22	22
1887	First-principles calculations of AlN nanowires and nanotubes: atomic structures, energetics, and surface states. <b>2006</b> , 110, 8764-8	70
1886	Assembling of dimeric entities of Cd(II) with 6-mercaptopurine to afford one-dimensional coordination polymers: synthesis and scanning probe microscopy characterization. <b>2006</b> , 45, 7642-50	52
1885	STM/STS observation of polyoxoanions on HOPG surfaces: the wheel-shaped [Cu <sub>20</sub> Cl(OH) <sub>24</sub> (H <sub>2</sub> O) <sub>12</sub> (P <sub>8</sub> W <sub>48</sub> O <sub>184</sub> )] <sub>25</sub> - and the ball-shaped [Sn(CH <sub>3</sub> ) <sub>2</sub> (H <sub>2</sub> O)] <sub>24</sub> [Sn(CH <sub>3</sub> ) <sub>2</sub> ] <sub>12</sub> (A-PW <sub>9</sub> O <sub>34</sub> ) <sub>12</sub> ] <sub>36</sub> -. <b>2006</b> , 45, 2866-72	46
1884	Hydrogen-bonded PTCDA-melamine networks and mixed phases. <b>2006</b> , 110, 6110-4	52
1883	Structural model of silica nanowire assembled from a highly stable (SiO <sub>2</sub> ) <sub>8</sub> unit. <b>2006</b> , 110, 1338-43	14
1882	Designing cyclophane-based molecular wire sensors. <b>2006</b> , 110, 23806-11	20
1881	Theoretical study of CO adsorption on gold/alumina substrates. <b>2006</b> , 110, 10449-54	9
1880	Ab Initio Simulations of the (101) Surfaces of Potassium Dihydrogenphosphate (KDP). <b>2006</b> , 2, 797-800	5
1879	Homopairing possibilities of the DNA base thymine and the RNA base uracil: an ab initio density functional theory study. <b>2006</b> , 110, 2249-55	43
1878	Ab initio study of nitrogen and boron substitutional impurities in single-wall SiC nanotubes. <b>2006</b> , 73,	127
1877	First-principles approaches to the structure and reactivity of atmospherically relevant aqueous interfaces. <b>2006</b> , 106, 1282-304	66
1876	C <sub>59</sub> Si on the monohydride Si(100):H-(2 x 1) surface. <b>2006</b> , 110, 10849-54	8
1875	A family of stable silica fullerenes with fully coordinated structures. <b>2006</b> , 110, 17757-62	8
1874	Solvation structure and transport of acidic protons in ionic liquids: a first-principles simulation study. <b>2006</b> , 110, 8798-803	58
1873	O(N) LDA+U electronic structure calculation method based on the nonorthogonal pseudoatomic orbital basis. <b>2006</b> , 73,	105



1872	Orbital interaction mechanisms of conductance enhancement and rectification by dithiocarboxylate anchoring group. <b>2006</b> , 110, 19116-20		47
1871	Electronic structure and charge transfer in the ternary intercalated graphite beta-KS0.25C3. <b>2006</b> , 45, 9387-93		
1870	Structure and bonding of the multifunctional amino acid L-DOPA on Au(110). <b>2006</b> , 110, 23756-69		53
1869	Melting in small gold clusters: a density functional molecular dynamics study. <i>Journal of Physics Condensed Matter</i> , <b>2006</b> , 18, 55-74	1.8	35
1868	Nature of the bottom t <sub>2g</sub> -block bands of layered perovskites. Implications for the transport properties of phases where these bands are partially filled. <b>2006</b> , 128, 4318-29		11
1867	Dianhydride-amine hydrogen bonded perylene tetracarboxylic dianhydride and tetraaminobenzene rows. <b>2006</b> , 110, 12207-10		27
1866	Concerning the different roles of cations in metallic Zintl phases: Ba <sub>7</sub> Ga <sub>4</sub> Sb <sub>9</sub> as a test case. <b>2006</b> , 45, 7235-41		20
1865	Molecular dynamics simulation of the melting-like transition in K1Na54. <b>2006</b> , 35, 174-178		12
1864	Acetylene adsorption onto Si(1 0 0): a study of adsorption dynamics and of surface steps. <b>2006</b> , 35, 6-12		4
1863	Exchange parameters in Fe-based molecular magnets. <b>2006</b> , 36, 91-95		13
1862	Time saving techniques for electronic structure calculations of infinite and semi-infinite crystals, interfaces, and slabs of arbitrary thickness. <b>2006</b> , 36, 106-111		
1861	Ag chains deposited onto silicon steps studied by Tight-Binding. <b>2006</b> , 35, 27-34		
1860	Cs doping effects on electronic structure of thin nanotubes. <b>2006</b> , 36, 152-158		8
1859	Analysis of the optical properties for Ga <sub>4</sub> P <sub>3</sub> Ti compound with a metallic intermediate band. <b>2006</b> , 36, 263-267		11
1858	Energetics of phase transitions in BaO through DFT calculations with norm-conserving pseudopotentials: LDA vs. GGA results. <b>2006</b> , 37, 349-354		17
1857	Optoelectronic properties of Cr-substituted II-VI semiconductors. <b>2006</b> , 37, 483-490		16
1856	First-principles modelling of Earth and planetary materials at high pressures and temperatures. <b>2006</b> , 69, 2365-2441		133
1855	Modeling heme proteins using atomistic simulations. <b>2006</b> , 8, 5611-28		72

1854	The catalytic mechanism of peptidylglycine alpha-hydroxylating monooxygenase investigated by computer simulation. <b>2006</b> , 128, 12817-28	126
1853	Adsorption of benzene-1,4-dithiol on the Au(111) surface and its possible role in molecular conductance. <b>2006</b> , 128, 8996-7	63
1852	Endohedral terthiophene in zigzag carbon nanotubes: Density functional calculations. <b>2006</b> , 74,	19
1851	Embedding method for conductance studies of large molecules. <b>2006</b> , 509-533	
1850	The role of the electrodes in a molecular conductor: an eigenchannel analysis. <b>2006</b> , 29, 91-94	2
1849	Unexpected magnetism in low dimensional systems: the role of symmetry. <b>2006</b> , 30, 215-223	1
1848	Atomic pseudopotentials. 143-177	
1847	Basis sets. 178-216	
1846	Electronic structure methods. 217-269	
1845	First-principles molecular dynamics (CarParrinello). 323-338	
1844	Quasi-one-dimensional $S = 1/2$ magnet $\text{Pb}[\text{Cu}(\text{SO}_4)(\text{OH})_2]$ : frustration due to competing in-chain exchange. <b>2006</b> , 3, 220-224	20
1843	Implementation of linear-scaling plane wave density functional theory on parallel computers. <b>2006</b> , 243, 973-988	42
1842	Density functional studies of molecular magnets. <b>2006</b> , 243, 2533-2572	86
1841	Half-metallic graphene nanoribbons. <b>2006</b> , 444, 347-9	3486
1840	USPEX: Evolutionary crystal structure prediction. <b>2006</b> , 175, 713-720	748
1839	A theoretical study of the stability trends of boron nitride fullerenes. <b>2006</b> , 421, 246-250	25
1838	Elimination of basis set superposition error in linear-scaling density-functional calculations with local orbitals optimised in situ. <b>2006</b> , 422, 345-349	47
1837	Prediction of increased tunneling current by bond length stretch in molecular break junctions. <b>2006</b> , 429, 503-506	13

1836	Modeling the silicon/beryllia interface. <b>2006</b> , 9, 928-933	1
1835	Atomic structure of the carbon induced Si(0 0 1)(4 × 4) surface. <b>2006</b> , 252, 5284-5287	4
1834	Structure and electronic property of medium-sized silicon clusters. <b>2006</b> , 31, 86-92	19
1833	The scattering approach: Application to the conductance of silicon nanograins. <b>2006</b> , 31, 204-208	1
1832	Theoretical study of hydrogen atom adsorbed on carbon-doped BN nanotubes. <b>2006</b> , 357, 369-373	52
1831	Functionalization of silicon-doped single walled carbon nanotubes at the doping site: An ab initio study. <b>2006</b> , 358, 166-170	11
1830	Structural, magnetic and electronic properties of Fe encapsulated by silicon clusters. <b>2006</b> , 360, 384-389	10
1829	Resistivity recovery simulations of electron-irradiated iron: Kinetic Monte Carlo versus cluster dynamics. <b>2006</b> , 352, 42-49	29
1828	The influence of oxygen vacancies on the electronic and magnetic properties of perovskite-like SrFeO <sub>3-x</sub> . <b>2006</b> , 67, 1436-1439	19
1827	A computational study on CO adsorption onto SnO <sub>2</sub> small grains. <b>2006</b> , 126, 56-61	5
1826	Dioxygen affinity in heme proteins investigated by computer simulation. <b>2006</b> , 100, 761-70	83
1825	Electrical properties of high- $\epsilon_r$ gate dielectrics: Challenges, current issues, and possible solutions. <b>2006</b> , 51, 37-85	209
1824	Energetics and electronic structure of acetylene molecules encapsulated inside a carbon nanotube: A density functional theory study. <b>2006</b> , 29, 150-152	2
1823	Elastic, electronic, and lattice dynamical properties of CdS, CdSe, and CdTe. <b>2006</b> , 373, 124-130	214
1822	Optical properties for Ga <sub>32</sub> P <sub>31</sub> Cr and Ga <sub>31</sub> P <sub>32</sub> Cr intermediate band materials. <b>2006</b> , 90, 203-212	11
1821	Survey of intermediate band materials based on ZnS and ZnTe semiconductors. <b>2006</b> , 90, 588-596	41
1820	Electronic and optical analysis of high-efficiency photovoltaic materials based on a GaN semiconductor. <b>2006</b> , 90, 1734-1740	6
1819	The structure of an Fe monolayer on the Ni (111) surface. A density-functional study using the generalized gradient approximation. <b>2006</b> , 137, 129-131	3

1818	Spin polarization of the injected carriers in C-doped BN nanotubes. <b>2006</b> , 137, 246-248	17
1817	Influence of sublayer atoms on Si(100) surface reconstructions. <b>2006</b> , 137, 553-556	1
1816	First-principles study of single-walled armchair C <sub>x</sub> (BN) <sub>y</sub> nanotubes. <b>2006</b> , 137, 549-552	15
1815	Magnetic coupling in the cluster Fe <sub>2</sub> Mn <sub>4</sub> : A fully unconstrained density-functional study. <b>2006</b> , 140, 480-482	3
1814	Non-contact AFM images of a C <sub>60</sub> molecule adsorbed on the Si(0 0 1) surface: An ab initio method. <b>2006</b> , 600, 551-558	15
1813	Adsorption dynamics of O <sub>2</sub> on Cu(100). <b>2006</b> , 600, 1574-1578	22
1812	Ab initio study of the double row model of the Si(553)Au reconstruction. <b>2006</b> , 600, 1201-1206	15
1811	Ge adsorption on SiC(0001): An ab initio study. <b>2006</b> , 600, 1107-1112	4
1810	Metal-insulator transition in the In/Si(111) surface. <b>2006</b> , 600, 3821-3824	20
1809	Structural, electronic and magnetic properties of vacancies in single-walled carbon nanotubes. <b>2006</b> , 600, 4305-4309	50
1808	High resolution core and valence band XPS spectra of non-conductor pyroxenes. <b>2006</b> , 600, 3175-3186	50
1807	First-principles study on current through a single conjugate molecule for analysis of carrier injection through an organic/metal interface. <b>2006</b> , 600, 5080-5083	9
1806	Properties of cyclo-tetrapeptide assemblies investigated by means of DFT calculations. <b>2006</b> , 776, 53-59	6
1805	Interaction of single-walled carbon nanotubes with alkylamines: An ab initio study. <b>2006</b> , 499, 256-258	7
1804	First-principles calculation of the TiN effective work function on SiO <sub>2</sub> and on HfO <sub>2</sub> . <b>2006</b> , 74,	27
1803	Ab initio study of semiconducting carbon nanotubes adsorbed on the Si(100) surface: Diameter- and registration-dependent atomic configurations and electronic properties. <b>2006</b> , 100, 124304	20
1802	Structures of 13-atom clusters of fcc transition metals by ab initio and semiempirical calculations. <b>2006</b> , 74,	61
1801	Energy gaps in graphene nanoribbons. <b>2006</b> , 97, 216803	3863

1800	The structural and electronic properties of compound $\text{Sn}_m\text{O}_n$ clusters studied by the Density Functional Theory. <b>2006</b> , 51, 307-313	8
1799	First principles study of CdSe quantum dots: Stability, surface saturations, and experimental validation. <b>2006</b> , 88, 231910	59
1798	Comment on "Magnetism in atomic-size palladium contacts and nanowires". <b>2006</b> , 96, 079701; author reply 079702	30
1797	Computational Design of Silicon Suboxides: Chemical and Mechanical Forces on the Atomic Scale. <b>2006</b> , 13, 185-200	3
1796	Properties of ferroelectric ultrathin films from first principles. <b>2006</b> , 41, 137-145	36
1795	Self-assembled nanowires on semiconductor surfaces. <b>2006</b> , 41, 4568-4603	82
1794	DFT study of the cation arrangements in the octahedral and tetrahedral sheets of dioctahedral 2:1 phyllosilicates. <b>2006</b> , 33, 655-666	41
1793	The SCC-DFTB method and its application to biological systems. <b>2006</b> , 116, 316-325	296
1792	Free Energy Calculations with Non-Equilibrium Methods: Applications of the Jarzynski Relationship. <b>2006</b> , 116, 338-346	65
1791	Adhesion at metal/ $\text{ZrO}_2$ interfaces. <b>2006</b> , 61, 303-344	156
1790	First principles study of vacancies and Al substitutional impurities in $\text{TiN}$ . <b>2006</b> , 515, 2730-2733	8
1789	Ab initio study of $\text{Ti}_3\text{Si}_0.5\text{Ge}_0.5\text{C}_2$ under pressure. <b>2006</b> , 67, 2149-2153	5
1788	DFT study of the conductance of molecular wire: The effect of coupling geometry and intermolecular interaction on the transport properties. <b>2006</b> , 49, 492-498	4
1787	. <b>2006</b> , 53, 1180-1185	6
1786	A periodic density functional study of the location of titanium within TS-1. <b>2006</b> , 8, 234-240	21
1785	A range of spin-crossover temperature $T_{1/2} > 300$ K results from out-of-sphere anion exchange in a series of ferrous materials based on the 4-(4-imidazolylmethyl)-2-(2-imidazolylmethyl)imidazole (trim) ligand, $[\text{Fe}(\text{trim})_2]\text{X}_2$ (X=F, Cl, Br, I): comparison of experimental results with those derived from density functional theory calculations. <b>2006</b> , 12, 7421-32	67
1784	Single gold atoms in heterogeneous catalysis: selective 1,3-butadiene hydrogenation over Au/ $\text{ZrO}_2$ . <b>2006</b> , 45, 6865-8	70
1783	Application of standard DFT theory for nonbonded interactions in soft matter: prototype study of poly-para-phenylene. <b>2006</b> , 27, 217-27	14

1782	Single Gold Atoms in Heterogeneous Catalysis: Selective 1,3-Butadiene Hydrogenation over Au/ZrO <sub>2</sub> . <b>2006</b> , 118, 7019-7022		10
1781	Electronic Structure Calculations for Nanomolecular Systems. <b>2006</b> , 77-116		2
1780	Molecular electrostatic properties of ions in an ionic liquid. <b>2006</b> , 104, 2477-2483		42
1779	Ab Initio Calculation on Self-Assembled Base-Functionalized Single-Walled Carbon Nanotubes. <b>2006</b> , 23, 2210-2212		23
1778	Hydrogen Storage in Benzene Moiety Decorated Single-Walled Carbon Nanotubes. <b>2006</b> , 23, 1536-1539		1
1777	Vibrational properties and superconductivity in Ba <sub>24</sub> Si <sub>100</sub> . <b>2006</b> , 75, 153-159		8
1776	Molecules on vicinal Au surfaces studied by scanning tunnelling microscopy. <i>Journal of Physics Condensed Matter</i> , <b>2006</b> , 18, S51-S66	1.8	17
1775	Large-scale electronic structure theory for simulating nanostructure processes. <i>Journal of Physics Condensed Matter</i> , <b>2006</b> , 18, 10787-10802	1.8	14
1774	Theoretical study of the photodesorption mechanism of nitric oxide on a Ag(111) surface: a nonequilibrium Green's function approach to hot-electron tunneling. <b>2006</b> , 125, 084708		7
1773	Size-dependent alternation of magnetoresistive properties in atomic chains. <b>2006</b> , 125, 121102		11
1772	Hydrogen-bond dynamics and Fermi resonance in high-pressure methane filled ice. <b>2006</b> , 125, 154509		8
1771	Electronic structure study by means of x-ray spectroscopy and theoretical calculations of the "ferric star" single molecule magnet. <b>2006</b> , 124, 044503		18
1770	Orbital-corrected orbital-free density functional theory. <b>2006</b> , 124, 081107		16
1769	Single quintuple bond [PhCrCrPh] molecule as a possible molecular switch. <b>2006</b> , 125, 184713		19
1768	An efficient molecular orbital approach for self-consistent calculations of molecular junctions. <b>2006</b> , 125, 194106		22
1767	Simulation of the Growth of Copper Films for Micro and Nano-Electronics. <b>2006</b> , 51, 167-173		
1766	Computational Investigation Into the Adsorption of Pollutants Onto Mineral Surfaces: Arsenate and Dolomite. <b>2006</b> , 930, 1		
1765	First-principles Study of Adsorption Energetics of Alkanethiols on GaAs(001). <b>2006</b> , 950, 1		

1764	Linear scaling calculation of maximally localized Wannier functions with atomic basis set. <b>2006</b> , 124, 234108	11
1763	Laser Irradiation of Atomic Chains: A Show-Case Study Based on the Density Functional Theory. <b>2006</b> , 960, 1	
1762	DENSITY FUNCTIONAL STUDIES OF NOBLE METAL CLUSTERS. ADSORPTION OF O <sub>2</sub> AND CO ON GOLD AND SILVER CLUSTERS. <b>2006</b> , 407-432	4
1761	Molecular dynamics study of the ternary compound Li <sub>3</sub> AlB <sub>2</sub> O <sub>6</sub> . <b>2006</b> , 15, 428-431	2
1760	Localized orbital description of electronic structures of extended periodic metals, insulators, and confined systems: Density functional theory calculations. <b>2006</b> , 73,	17
1759	How do oxygen molecules move into silver contacts and change their electronic transport properties?. <b>2006</b> , 97, 256101	19
1758	Linear-scaling density matrix perturbation treatment of electric fields in solids. <b>2006</b> , 97, 266402	16
1757	On-site approximation for spin-orbit coupling in linear combination of atomic orbitals density functional methods. <i>Journal of Physics Condensed Matter</i> , <b>2006</b> , 18, 7999-8013	1.8 80
1756	Collinear versus noncollinear magnetic order in Pd atomic clusters: Ab initio calculations. <b>2006</b> , 74,	15
1755	Interplay between structure and magnetism in Mo <sub>12</sub> S <sub>9</sub> I <sub>9</sub> nanowires. <b>2006</b> , 96, 125502	35
1754	Magnetism of two-dimensional defects in Pd: Stacking faults, twin boundaries, and surfaces. <b>2006</b> , 74,	39
1753	Electron transport in stretched monoatomic gold wires. <b>2006</b> , 97, 236807	35
1752	Geometry and electronic structure of M-DNA (M=Zn <sup>2+</sup> , Co <sup>2+</sup> , and Fe <sup>2+</sup> ). <b>2006</b> , 73,	56
1751	Magnetization of electrodeposited nickel: Role of interstitial carbon. <b>2006</b> , 99, 08J301	6
1750	Small sodium clusters that melt gradually: Melting mechanisms in Na <sub>30</sub> . <b>2006</b> , 74,	32
1749	Lateral adsorption geometry and site-specific electronic structure of a large organic chemisorbate on a metal surface. <b>2006</b> , 74,	122
1748	Enantiospecific adsorption of chiral molecules on chiral gold clusters. <b>2006</b> , 97, 233401	63
1747	Origin of p(2 × 1) phase on Si(001) by noncontact atomic force microscopy at 5 k. <b>2006</b> , 96, 106104	47

1746	Electronic transport through Si nanowires: Role of bulk and surface disorder. <b>2006</b> , 74,	89
1745	First-principles investigation of a bistable boron-oxygen interstitial pair in Si. <b>2006</b> , 73,	20
1744	Finite-size effects in BaTiO <sub>3</sub> nanowires. <b>2006</b> , 88, 112906	103
1743	Prediction of giant electroactuation for papyruslike carbon nanoscroll structures: First-principles calculations. <b>2006</b> , 74,	60
1742	Silver-filled single-walled carbon nanotubes: Atomic and electronic structures from first-principles calculations. <b>2006</b> , 74,	13
1741	Extended Hückel theory for band structure, chemistry, and transport. II. Silicon. <b>2006</b> , 100, 043715	39
1740	Toward uniform nanotubular compounds: synthetic approach and ab initio calculations. <b>2006</b> , 124, 121102	6
1739	Surface and adsorption properties of alpha-tricalcium phosphate. <b>2006</b> , 124, 124701	14
1738	First-principles investigation of isolated band formation in half-metallic T <sub>x</sub> Ga <sub>1-x</sub> P (x=0.3125-0.25). <b>2006</b> , 73,	55
1737	Adsorption and Self-Assembly of Alkanethiols on GaAs (001) Surface. <b>2006</b> ,	1
1736	Subsurface structure of epitaxial rare-earth silicides imaged by STM. <b>2006</b> , 74,	20
1735	Transport properties of the Au <sub>32</sub> cluster with fullerene symmetry. <b>2006</b> , 74,	29
1734	Nonuniversal behavior of the parity effect in monovalent atomic wires. <b>2006</b> , 73,	10
1733	Effect of gating on the transport properties of a Si <sub>4</sub> cluster. <b>2006</b> , 73,	10
1732	Size effects in surface-reconstructed <100> and <110> silicon nanowires. <b>2006</b> , 74,	33
1731	Planar and cage-like structures of gold clusters: Density-functional pseudopotential calculations. <b>2006</b> , 73,	104
1730	Electron transport in a Pt <sub>100</sub> Pt nanocontact: Density functional theory calculations. <b>2006</b> , 73,	26
1729	Incorporation of impurity anions into DSP: insights into structure and stability from computer modelling. <b>2006</b> , 32, 35-44	6



1728	TRANSPORT PROPERTY OF TWO ISOELECTRONIC MOLECULES. <b>2006</b> , 05, 841-846	2
1727	Fe adatoms along Bi nanolines on HBi(001). <b>2006</b> , 89, 093105	15
1726	Organometallic molecular rectification. <b>2006</b> , 124, 024718	67
1725	A general and efficient pseudopotential Fourier filtering scheme for real space methods using mask functions. <b>2006</b> , 124, 174102	27
1724	Electron transport via local polarons at interface atoms. <b>2006</b> , 97, 206801	46
1723	Tuning the electrical conductivity of nanotube-encapsulated metallocene wires. <b>2006</b> , 96, 106804	63
1722	Contact dependence of carrier injection in carbon nanotubes: an ab initio study. <b>2006</b> , 96, 076802	168
1721	Mechanical properties of ultrananocrystalline diamond prepared in a nitrogen-rich plasma: A theoretical study. <b>2006</b> , 74,	13
1720	Density-functional geometry optimization of the 150,000-atom photosystem-I trimer. <b>2006</b> , 124, 024301	57
1719	Dislocation formation from a surface step in semiconductors: An ab initio study. <b>2006</b> , 73,	41
1718	Manipulation of C60 on the Si(001) surface: Experiment and theory. <b>2006</b> , 74,	18
1717	Experimental and theoretical identification of adenine monolayers on Ag-terminated Si(111). <b>2006</b> , 73,	44
1716	Theoretical investigation of free-standing CoPd nanoclusters as a function of cluster size and stoichiometry in the Pd-rich phase: Geometry, chemical order, magnetism, and metallic behavior. <b>2006</b> , 74,	46
1715	Electron transport through an interacting region: The case of a nonorthogonal basis set. <b>2006</b> , 73,	59
1714	Interfacial oxide growth at silicon/high-k oxide interfaces: First principles modeling of the Si/HfO2 interface. <b>2006</b> , 100, 043708	44
1713	Bonding modes and electronic properties of single-crystalline silicon nanotubes. <b>2006</b> , 73,	17
1712	O(N) Krylov-subspace method for large-scale ab initio electronic structure calculations. <b>2006</b> , 74,	76
1711	Atomic-scale dielectric permittivity profiles in slabs and multilayers. <b>2006</b> , 74,	50

1710	Density-functional study of oxygen vacancies in monoclinic tungsten oxide. <i>Journal of Physics Condensed Matter</i> , <b>2006</b> , 18, 7361-7371	1.8	32
1709	Control of electron transport through Fano resonances in molecular wires. <b>2006</b> , 74,		106
1708	Double-resonant Raman processes in germanium: Group theory and ab initio calculations. <b>2006</b> , 73,		5
1707	Strongly correlated electron physics in nanotube-encapsulated metallocene chains. <b>2006</b> , 74,		19
1706	Dielectric properties of Cu-phthalocyanine systems from first principles. <b>2006</b> , 89, 102904		28
1705	Probing the Si(001) surface with a Si tip: An ab initio study. <b>2006</b> , 73,		37
1704	(Ga,In)P: A standard alloy in the classification of phonon mode behavior. <b>2006</b> , 73,		17
1703	CO oxidation on AuTiOx/Mo{112}: Structure characterization and catalytic activity studied using ab initio calculations. <b>2006</b> , 73,		14
1702	NO structures adsorbed on Rh(111): Theoretical approach to high-coverage STM images. <b>2006</b> , 73,		19
1701	Adsorption of fullerenes C <sub>n</sub> (n=32,36,40,44,48,60) on the GaAs(001)√(4√) reconstructed surface. <b>2006</b> , 73,		4
1700	Strong electron-phonon coupling of the high-energy modes of carbon nanotubes. <b>2006</b> , 74,		15
1699	Defect passivation and interface engineering for high-K gate dielectric device performance and reliability enhancement. <b>2006</b> ,		
1698	Effect of dipole moment on current-voltage characteristics of single molecules. <b>2006</b> ,		1
1697	Automistic modeling of direct tunnelling in metal-oxide-semiconductor nanostructures. <b>2006</b> ,		2
1696	Controlled Electron Transport Through Single Molecules. <b>2006</b> ,		
1695	Theoretical investigation on the stability and properties of a (10,0) BN-AlN nanotube junction. <b>2006</b> , 17, 1637-41		17
1694	The VA, VCD, Raman and ROA spectra of tri-L-serine in aqueous solution. <b>2006</b> , 3, S63-79		36
1693	Tuning the electronic structures of semiconducting SiC nanotubes by N and NH <sub>x</sub> (x=1,2) groups. <b>2006</b> , 125, 194710		26

1692	High-pressure, high-temperature phase diagram of InSe: A comprehensive study of the electronic and structural properties of the monoclinic phase of InSe under high pressure. <b>2006</b> , 73,	32
1691	FIRST PRINCIPLES SLAB RELAXATION STUDY OF THE TiFe(001) SURFACE. <b>2006</b> , 13, 495-501	1
1690	First-principles study of silicon-doped (5,5) BN nanotubes. <b>2006</b> , 76, 664-669	42
1689	Alternative search strategy for minimal energy nanocluster structures: the case of rhodium, palladium, and silver. <b>2006</b> , 125, 214708	36
1688	Atomistic simulation of light-induced changes in hydrogenated amorphous silicon. <i>Journal of Physics Condensed Matter</i> , <b>2006</b> , 18, L1-L6	1.8 14
1687	Heme protein oxygen affinity regulation exerted by proximal effects. <b>2006</b> , 128, 12455-61	79
1686	Electron transport through single conjugated organic molecules: basis set effects in ab initio calculations. <b>2007</b> , 127, 144107	40
1685	LOW-DIMENSIONAL QUANTUM TRANSPORT PROPERTIES OF CHEMICALLY-DISORDERED CARBON NANOTUBES: FROM WEAK TO STRONG LOCALIZATION REGIMES. <b>2007</b> , 21, 1955-1982	52
1684	Quantum Dot Based on Z-shaped Graphene Nanoribbon: First-principles Study. <b>2007</b> , 20, 489-494	7
1683	Switching mechanism of photochromic diarylethene derivatives molecular junctions. <b>2007</b> , 127, 094705	41
1682	Spin polarized current and Andreev transmission in planar superconducting/ferromagnetic Nb/Ni junctions. <b>2007</b> , 9, 34-34	4
1681	Theory and Practice The Ab Initio Treatment of High-Pressure and -Temperature Mineral Properties and Behavior. <b>2007</b> , 359-387	
1680	First-principles calculation on the conductance of a single 1,4-diisocyanatobenzene molecule with single-walled carbon nanotubes as the electrodes. <b>2007</b> , 126, 084705	28
1679	Local and semilocal density functional computations for crystals of 1-alkyl-3-methyl-imidazolium salts. <b>2007</b> , 126, 144705	19
1678	Linear scaling calculation of band edge states and doped semiconductors. <b>2007</b> , 126, 244707	12
1677	Exchange parameters from approximate self-interaction correction scheme. <b>2007</b> , 127, 034112	9
1676	Design-atom approach for the quantum mechanical/molecular mechanical covalent boundary: a design-carbon atom with five valence electrons. <b>2007</b> , 127, 124102	20
1675	Chapter 3 Computer simulation of the solid-liquid phase transition in alkali metal nanoparticles. <b>2007</b> , 18, 59-83	

1674	Effect of the continuity of the pi conjugation on the conductance of ruthenium-octene-ruthenium molecular junctions. <b>2007</b> , 126, 174706		9
1673	Achieving plane wave accuracy in linear-scaling density functional theory applied to periodic systems: a case study on crystalline silicon. <b>2007</b> , 127, 164712		43
1672	Oscillatory exchange coupling in magnetic molecules. <i>Journal of Physics Condensed Matter</i> , <b>2007</b> , 19, 216205	1.8	2
1671	Accuracy control in ultra-large-scale electronic structure calculations. <i>Journal of Physics Condensed Matter</i> , <b>2007</b> , 19, 365243	1.8	2
1670	Design and First-principles Study of a Fullerene Molecular Device. <b>2007</b> , 24, 2369-2372		1
1669	Small tin oxide grains: structural and electronic properties evaluated using the density functional theory. <i>Journal of Physics Condensed Matter</i> , <b>2007</b> , 19, 026214	1.8	3
1668	Structural and magnetic properties of Fe <sub>4</sub> clusters confined in carbon nanotubes. <i>Journal of Physics Condensed Matter</i> , <b>2007</b> , 19, 466203	1.8	8
1667	Thermally stimulated H emission and diffusion in hydrogenated amorphous silicon. <b>2007</b> , 79, 36001		10
1666	Transport Properties of Binary Clusters. <b>2007</b> , 24, 3570-3573		2
1665	Hydrogen-related catalytic effects of Ti and other light transition metals on NaAlH <sub>4</sub> surfaces. <i>Journal of Physics Condensed Matter</i> , <b>2007</b> , 19, 176007	1.8	8
1664	Evidence of disorder in cubic zirconium tungstate from the temperature dependence of Raman spectra. <i>Journal of Physics Condensed Matter</i> , <b>2007</b> , 19, 226210	1.8	5
1663	Theoretical prediction for the (AlN) <sub>12</sub> fullerene-like cage-based nanomaterials. <i>Journal of Physics Condensed Matter</i> , <b>2007</b> , 19, 346228	1.8	15
1662	First-principles calculation on the zero-bias conductance of a gold/1,4-diaminobenzene/gold molecular junction. <b>2007</b> , 18, 345203		25
1661	Control of electron- and phonon-derived thermal conductances in carbon nanotubes. <b>2007</b> , 9, 245-245		21
1660	Ab initio and empirical studies on the asymmetry of molecular current-voltage characteristics. <i>Journal of Physics Condensed Matter</i> , <b>2007</b> , 19, 215206	1.8	11
1659	DFT based study of Au <sub>n</sub> (4n) clusters: new stabilized geometries. <b>2007</b> , 75, 411-413		8
1658	Mechanical Properties of Single-Walled (5,5) Carbon Nanotubes with Vacancy Defects. <b>2007</b> , 24, 2036-2039		5
1657	Resonant magnetoresistance in organic spin valves (invited). <b>2007</b> , 101, 09B102		17

1656	Characteristic jump in the electrical properties of a Pd <sub>3</sub> AlNiSi-based device on exposure to hydrogen. <b>2007</b> , 75,	3
1655	Determination of Compton profiles at solid surfaces from first-principles calculations. <b>2007</b> , 75,	6
1654	Interplay between electronic and atomic structures in the Si(557)-Au reconstruction from first principles. <b>2007</b> , 76,	32
1653	Mixing of the fully symmetric vibrational modes in carbon nanotubes. <b>2007</b> , 75,	9
1652	Theoretical study of size-dependent properties of BN nanotubes with intrinsic defects. <b>2007</b> , 76,	40
1651	Evolution-operator method for density functional theory. <b>2007</b> , 75,	18
1650	Size dependence of thermal properties of armchair carbon nanotubes: A first-principles study. <b>2007</b> , 91, 023112	12
1649	Inelastic transport theory from first principles: Methodology and application to nanoscale devices. <b>2007</b> , 75,	330
1648	Threshold voltage shifts in Si passivated (100)Ge p-channel field effect transistors: Insights from first-principles modeling. <b>2007</b> , 91, 023506	20
1647	Surface structures and electronic states of silicon nanotubes stabilized by oxygen atoms. <b>2007</b> , 102, 024313	5
1646	Quantum confinement of crystalline silicon nanotubes with nonuniform wall thickness: Implication to modulation doping. <b>2007</b> , 91, 103107	10
1645	The effect of reciprocal-space sampling and basis set quality on the calculated conductance of a molecular junction. <b>2007</b> , 33, 897-904	7
1644	Gallium self-interstitial relaxation in GaAs: An ab initio characterization. <b>2007</b> , 76,	19
1643	Comparison of localized basis and plane-wave basis for density-functional calculations of organic molecules on metals. <b>2007</b> , 75,	62
1642	Interface between a polar perovskite oxide and silicon from monoatomic lines. <b>2007</b> , 90, 072906	5
1641	Atomic-orbital-based approximate self-interaction correction scheme for molecules and solids. <b>2007</b> , 75,	139
1640	Electronic properties of alkali- and alkaline-earth-intercalated silicon nanowires. <b>2007</b> , 75,	9
1639	Semiconducting chains of gold and silver. <b>2007</b> , 91, 223115	16

1638	Formation of gold nanowires with impurities: a first-principles molecular dynamics simulation. <b>2007</b> , 98, 096102	25
1637	Intrinsic dielectric properties of phthalocyanine crystals: An ab initio investigation. <b>2007</b> , 75,	17
1636	Characterization of the anion-ordering transition in (TMTTF) <sub>2</sub> ReO <sub>4</sub> by x-ray absorption and photoemission spectroscopies. <b>2007</b> , 76,	9
1635	Combined Raman study of InGaAsN from the N-impurity and InGaAs-matrix sides. <b>2007</b> , 91, 051910	4
1634	Structure and transport characteristics of modified DNA with magnetic ions. <b>2007</b> , 98, 136601	23
1633	First-principles analysis of the STM image heights of styrene on Si(100). <b>2007</b> , 76,	20
1632	Detection of intrinsic stress in cubic boron nitride films by x-ray absorption near-edge structure: Stress relaxation mechanisms by simultaneous ion implantation during growth. <b>2007</b> , 76,	11
1631	Local dielectric permittivity of HfO <sub>2</sub> based slabs and stacks: A first principles study. <b>2007</b> , 91, 242906	14
1630	Charge transfer composites of bis(cyclopentadienyl) and bis(benzene) transition metal complexes encapsulated in single-walled carbon nanotubes. <b>2007</b> , 75,	17
1629	Identification of P dopants at nonequivalent lattice sites of the Si(111)( $\sqrt{3}\times\sqrt{3}$ ) surface. <b>2007</b> , 76,	18
1628	Nature of well-defined conductance of amine-anchored molecular junctions: Density functional calculations. <b>2007</b> , 76,	71
1627	First-principles calculations of Cu adsorption on an H-terminated Si surface. <b>2007</b> , 76,	18
1626	Density matrix-based variational quantum Monte Carlo providing an asymptotically linear scaling behavior for the local energy. <b>2007</b> , 75,	11
1625	Low-pressure metastable phase of single-bonded polymeric nitrogen from a helical structure motif and first-principles calculations. <b>2007</b> , 75,	39
1624	Density functional calculations of Ge(105): Local basis sets and O(N) methods. <b>2007</b> , 76,	16
1623	Adsorption and diffusion dynamics of atomic and molecular oxygen on reconstructed Cu(100). <b>2007</b> , 75,	29
1622	Soft modes and negative thermal expansion in Zn(CN) <sub>2</sub> from Raman spectroscopy and first-principles calculations. <b>2007</b> , 76,	36
1621	Unique structural and transport properties of molybdenum chalcogenide nanowires. <b>2007</b> , 99, 085503	25

1620	Superconductivity and magnetic order in CeRhIn5: spectra of coexistence. <b>2007</b> , 98, 126406	8
1619	RETRACTED ARTICLE: ONETEP: linear-scaling density-functional theory with plane-waves. <b>2007</b> , 33, 551-555	14
1618	Ferrodistorive instability at the (001) surface of half-metallic manganites. <b>2007</b> , 99, 226101	37
1617	Design of molecular wires based on one-dimensional coordination polymers. <b>2007</b> , 90, 193107	24
1616	Size limit of defect formation in pyramidal Pt nanocontacts. <b>2007</b> , 99, 255501	16
1615	Resistive and rectifying effects of pulling gold atoms at thiol-gold nanocontacts. <b>2007</b> , 75,	17
1614	Electronic structure of ultrathin $\sqrt{3}\times\sqrt{3}$ Fe4N (100) films epitaxially grown on Cu(100). <b>2007</b> , 75,	28
1613	Hydrogen interaction with native defects in SiC nanotubes. <b>2007</b> , 76,	35
1612	Search for magnetoresistance in excess of 1000% in Ni point contacts: Density functional calculations. <b>2007</b> , 76,	22
1611	Role of volume versus defects in the electrical resistivity of lattice-distorted V(001) ultrathin films. <b>2007</b> , 76,	4
1610	Defect-induced spin deterioration of La0.64Sr0.36MnO3: Ab initio study. <b>2007</b> , 76,	11
1609	EL2-like defects in InP nanowires: An ab initio total energy investigation. <b>2007</b> , 75,	6
1608	Ordered arrays of quantum wires through hole patterning: ab initio and empirical electronic structure calculations. <b>2007</b> , 90, 083118	8
1607	Intrinsic surface band bending in Cu3N(100) ultrathin films. <b>2007</b> , 76,	65
1606	Predictions for the formation of atomic chains in mechanically controllable break-junction experiments. <b>2007</b> , 75,	28
1605	First-principles dynamic simulations of field emission from carbon nanotubes on gold substrate. <b>2007</b> , 75,	4
1604	Energy dispersion in graphene and carbon nanotubes and molecular encapsulation in nanotubes. <b>2007</b> , 75,	11
1603	Electron transport in self-assembled monolayers of thiolalkane: Symmetric $I_V$ curves and Fano resonance. <b>2007</b> , 76,	10

1602	Ab initio investigations of the transport properties of a Ge7 cluster. <b>2007</b> , 75,	21
1601	Effect of thickness on the electronic structure of poly(vinylidene fluoride) molecular films from first-principles calculations. <b>2007</b> , 75,	11
1600	From tunneling to contact: Inelastic signals in an atomic gold junction from first principles. <b>2007</b> , 75,	55
1599	First-principles study of the electronic structure of cubic GaS: Metallic versus insulating polymorphs. <b>2007</b> , 75,	4
1598	Effect of electron and hole doping on the structure of C, Si, and S nanowires. <b>2007</b> , 75,	14
1597	First-principles calculations of the effect of Pt on NiAl surface energy and the site preference of Pt. <b>2007</b> , 91, 011907	19
1596	Density functional calculations of the binding energies and adatom diffusion on strained AlN (0001) and GaN (0001) surfaces. <b>2007</b> , 1040, 1	
1595	Anisotropy of the Vacancy Migration in Ti, Zr and Hf Hexagonal Close-Packed Metals from First Principles. <b>2007</b> , 129, 75-81	50
1594	Correlation and nuclear distortion effects of Cr-substituted ZnSe. <b>2007</b> , 126, 164703	11
1593	Electrical characterization of 7 nm long conjugated molecular wires: experimental and theoretical studies. <b>2007</b> , 18, 044005	12
1592	Ab Initio Simulations of the Nucleation of Single-Walled Carbon Nanotubes. <b>2007</b> , 121-123, 1037-1040	1
1591	Insight into the adsorption competition and the relationship between dissociation and association reactions in ammonia synthesis. <b>2007</b> , 127, 234706	14
1590	Rank-ordering protein-ligand binding affinity by a quantum mechanics/molecular mechanics/Poisson-Boltzmann-surface area model. <b>2007</b> , 126, 026101	19
1589	Giant magnetoresistance of nickel-contacted carbon nanotubes. <i>Journal of Physics Condensed Matter</i> , <b>2007</b> , 19, 042201	1.8 6
1588	Magnetism induced by single-atom defects in nanographites. <b>2007</b> , 61, 1294-1298	6
1587	Inhomogenities of the CDW vector at the (-201) surface of Quasi-1D blue bronze Rb0.3MoO3. <b>2007</b> , 61, 140-146	2
1586	Field emission of metal nanowires studied by first-principles methods. <b>2007</b> , 18, 475706	15
1585	Inelastic fingerprints of hydrogen contamination in atomic gold wire systems. <b>2007</b> , 61, 312-316	9



1584	Linearized force constants method for lattice dynamics in mixed semiconductors. <b>2007</b> , 92, 012139	4
1583	Recent Advances in Fullerene Deposition on Semiconductor Surfaces. <b>2007</b> , 533-563	
1582	Theoretical study of isoelectronic $\text{SinM}$ clusters ( $M=\text{Sc,Ti,V}^+$ ; $n=14-18$ ). <b>2007</b> , 75,	80
1581	Titanium substitution mechanisms in forsterite. <b>2007</b> , 242, 176-186	71
1580	CO adsorption onto tin oxide clusters: DFT calculations. <b>2007</b> , 38, 814-823	4
1579	The electronic configuration and the conductance of silicon nanograins: An application of the scattering approach. <b>2007</b> , 38, 830-837	1
1578	Dynamical behaviour of Si clusters studied in real time: Fragmentation and melting. <b>2007</b> , 39, 393-401	
1577	The elastic, electronic, and vibrational properties of pure $\text{CdF}_2$ : A first-principles study. <b>2007</b> , 438, 66-71	7
1576	Contact transparency of nanotube-molecule-nanotube junctions. <b>2007</b> , 99, 146802	47
1575	Density functional theory study of a graphene sheet modified with titanium in contact with different adsorbates. <b>2007</b> , 76,	85
1574	Discrete size series of $\text{CdSe}$ quantum dots: a combined computational and experimental investigation. <b>2007</b> , 14, 167-174	11
1573	WSXM: a software for scanning probe microscopy and a tool for nanotechnology. <b>2007</b> , 78, 013705	5902
1572	Metallic behavior of Pd atomic clusters. <b>2007</b> , 18, 365706	14
1571	Charge Transport in Conjugated Aromatic Molecular Junctions: Molecular Conjugation and Molecule-Electrode Coupling. <b>2007</b> , 111, 14893-14902	89
1570	Conductance oscillation and quantization in monatomic Al wires. <i>Journal of Physics Condensed Matter</i> , <b>2007</b> , 19, 056010	1.8 11
1569	First-principles calculation of charge transfer at surfaces: The case of core-excited $\text{Ar}^*(2p3d4s)$ on $\text{Ru}(0001)$ . <b>2007</b> , 76,	14
1568	Clusters, liquids, and crystals of dialkylimidazolium salts. A combined perspective from ab initio and classical computer simulations. <b>2007</b> , 40, 1156-64	45
1567	Theoretical Study of the Magnetic Properties of an $\text{Mn}_{12}$ Single-Molecule Magnet with a Loop Structure: The Role of the Next-Nearest Neighbor Interactions. <b>2007</b> , 3, 782-8	41

1566	Stress-induced band gap tuning in <112> silicon nanowires. <b>2007</b> , 91, 263107	62
1565	First-principles study of the dependence of ground-state structural properties on the dimensionality and size of ZnO nanostructures. <b>2007</b> , 76,	51
1564	Ab initio molecular dynamics simulations of the static, dynamic, and electronic properties of liquid Pb using real-space pseudopotentials. <b>2007</b> , 76,	31
1563	Impact of bidirectional charge transfer and molecular distortions on the electronic structure of a metal-organic interface. <b>2007</b> , 99, 256801	186
1562	New Solids Based on B <sub>12</sub> N <sub>12</sub> Fullerenes. <b>2007</b> , 111, 13354-13360	58
1561	Metal-organic honeycomb nanomeshes with tunable cavity size. <b>2007</b> , 7, 3813-7	281
1560	Magnetic ordering and exchange interactions in multiferroic GaFeO <sub>3</sub> . <b>2007</b> , 75,	62
1559	Faceted Silicon Nanotubes: Structure, Energetic, and Passivation Effects. <b>2007</b> , 111, 1234-1238	31
1558	Stabilizing Zigzag Single-Walled Silicon Nanotubes and Tailoring the Electronic Structures by Oxygen Atoms: First-Principles Studies. <b>2007</b> , 111, 2942-2946	8
1557	Cobaltocene as a spin filter. <b>2007</b> , 127, 141104	46
1556	The mechanism of defect creation and passivation at the SiC/SiO <sub>2</sub> interface. <b>2007</b> , 40, 6242-6253	120
1555	Magnetic anisotropies of late transition metal atomic clusters. <b>2007</b> , 99, 183401	64
1554	Adsorption structure and scanning tunneling data of a prototype organic-inorganic interface: PTCDA on Ag(111). <b>2007</b> , 76,	128
1553	Massless fermions in multilayer graphitic systems with misoriented layers: Ab initio calculations and experimental fingerprints. <b>2007</b> , 76,	263
1552	Electronic structures and superconductivity of endohedrally doped C <sub>28</sub> solids from first principles. <b>2007</b> , 76,	11
1551	Magnetism and local distortions near carbon impurity in gamma-iron. <b>2007</b> , 99, 247205	69
1550	Adsorption of As(OH) <sub>3</sub> on the (001) Surface of FeS <sub>2</sub> Pyrite: A Quantum-mechanical DFT Study. <b>2007</b> , 111, 11390-11396	43
1549	Hydrogen trapping in oxygen-deficient hafnium silicates. <b>2007</b> , 102, 044108	7

1548	Ab initio models of amorphous Si <sub>1-x</sub> Gex:H. <b>2007</b> , 75,	13
1547	Spin-dependent transport in Fe-doped carbon nanotubes. <b>2007</b> , 75,	68
1546	Early stages of radiation damage in graphite and carbon nanostructures: A first-principles molecular dynamics study. <b>2007</b> , 75,	66
1545	Band gap and density of states of the hydrated C <sub>60</sub> fullerene system at finite temperature. <b>2007</b> , 7, 1526-31	36
1544	Coupled quantum mechanical/molecular mechanical modeling of the fracture of defective carbon nanotubes and graphene sheets. <b>2007</b> , 75,	263
1543	Temperature and composition of the Earth's core. <b>2007</b> , 48, 63-80	67
1542	Efficient density-functional theory integrations by locally augmented radial grids. <b>2007</b> , 127, 164113	45
1541	H <sub>2</sub> S exposure of a (100)Ge surface: Evidences for a (2 $\times$ 1) electrically passivated surface. <b>2007</b> , 90, 222105	31
1540	Photoabsorption spectra of boron nitride fullerenelike structures. <b>2007</b> , 126, 214306	17
1539	Energetic Landscapes and Diffusion Properties in FeCu Alloys. <b>2007</b> , 129, 31-39	13
1538	Electronic Transport in Molecular Junction Based on C <sub>20</sub> Cages. <b>2007</b> , 24, 1042-1045	3
1537	UHV STM I(V) and XPS studies of aryl diazonium molecules assembled on Si(111). <b>2007</b> , 23, 4700-8	17
1536	Electric field effects on spin transport in defective metallic carbon nanotubes. <b>2007</b> , 7, 3518-22	35
1535	Theoretical study of atomic transport via interstitials in dilute FeB alloys. <b>2007</b> , 75,	46
1534	Superconductivity in high-pressure SiH <sub>4</sub> . <b>2007</b> , 78, 37003	82
1533	Morphology and magnetism of Fe monolayers and small Fe clusters (n=2-9) supported on the Ni(111) surface. <b>2007</b> , 18, 055701	1
1532	Effect of Co and O defects on the magnetism in Co-doped ZnO: Experiment and theory. <b>2007</b> , 75,	93
1531	Electronic and transport properties of graphene nanoribbons. <b>2007</b> ,	

1530	Ethynylbenzene monolayers on gold: a metal-molecule binding motif derived from a hydrocarbon. <b>2007</b> , 129, 3533-8	29
1529	Planar Heteropairing Possibilities of the DNA and RNA Bases: An ab Initio Density Functional Theory Study. <b>2007</b> , 111, 3883-3892	20
1528	Multishell Carrier Transport in Multiwalled Carbon Nanotubes. <b>2007</b> , 6, 722-726	19
1527	Exploring the performance of molecular rectifiers: limitations and factors affecting molecular rectification. <b>2007</b> , 7, 3018-22	30
1526	Electronic stopping power in LiF from first principles. <b>2007</b> , 99, 235501	124
1525	Effect of Alteration of Antioxidant by UV Treatment on the Dielectric Strength of BOPP Capacitor Film. <b>2007</b> , 14, 1295-1301	84
1524	Insight into the Synergetic Effect in Ternary Gold-Based Catalysts: Ultrastability and High Activity of Au on Alumina Modified Titania. <b>2007</b> , 111, 13539-13546	23
1523	Controlled contact to a C60 molecule. <b>2007</b> , 98, 065502	119
1522	Origin of Oxide sensitivity in gold-based catalysts: a first principle study of CO oxidation over Au supported on monoclinic and tetragonal ZrO <sub>2</sub> . <b>2007</b> , 129, 2642-7	96
1521	Mechanisms of Dye Incorporation into Potassium Sulfate: Computational and Experimental Studies. <b>2007</b> , 111, 9283-9289	7
1520	Ab initio Monte Carlo simulations applied to a Si <sub>5</sub> cluster. <b>2007</b> , 75,	12
1519	Novel superconductivity in metallic SnH(4) under high pressure. <b>2007</b> , 98, 117004	170
1518	Ab initio estimate of temperature dependence of electrical conductivity in a model amorphous material: Hydrogenated amorphous silicon. <b>2007</b> , 76,	33
1517	Photoswitching of Conductivity through a Diarylperfluorocyclopentene Nanowire. <b>2007</b> , 111, 3517-3521	74
1516	First-Principles Design of Well-Ordered Silica Nanotubes from Silica Monolayers and Nanorings. <b>2007</b> , 111, 9652-9657	9
1515	Honeycomb Networks and Chiral Superstructures Formed by Cyanuric Acid and Melamine on Au(111). <b>2007</b> , 111, 886-893	72
1514	Modeling and Testing of Molecular Wire Sensors To Detect a Nucleic Acid Base. <b>2007</b> , 111, 3495-3504	21
1513	Proton Mobility in the In-Doped CaZrO <sub>3</sub> Perovskite Oxide. <b>2007</b> , 19, 2842-2851	23

1512	Field Emission Signature of Pentagons at Carbon Nanotube Caps. <b>2007</b> , 111, 6690-6693		23
1511	Coexistence of homochiral and heterochiral adenine domains at the liquid/solid interface. <b>2007</b> , 111, 12048-52		47
1510	Ab initio simulation of magnetic tunnel junctions. <b>2007</b> , 18, 424026		47
1509	Supramolecular self-assembled polynuclear complexes from tritopic, tetratopic, and pentatopic ligands: structural, magnetic and surface studies. <b>2007</b> , 46, 7767-81		91
1508	Tuning the electronic structure of graphene nanoribbons through chemical edge modification: A theoretical study. <b>2007</b> , 75,		145
1507	Boron nitride fullerene B <sub>36</sub> N <sub>36</sub> doped with transition metal atoms: First-principles calculations. <b>2007</b> , 75,		32
1506	All-carbon nanoswitch based on C <sub>70</sub> molecule: A first principles study. <b>2007</b> , 102, 064501		20
1505	Vanadium--benzimidazole-modified sDNA: a one-dimensional half-metallic ferromagnet. <b>2007</b> , 111, 13877-80		42
1504	Electronic, elastic, thermodynamical, and dynamical properties of the rock-salt compounds LaAs and LaP. <i>Journal of Physics Condensed Matter</i> , <b>2007</b> , 19, 436204	1.8	22
1503	Density Function Theory Study of Copper Agglomeration on the WN(001) Surface. <b>2007</b> , 111, 9403-9406		16
1502	First-Principles Study of NO <sub>x</sub> and SO <sub>2</sub> Adsorption onto SnO <sub>2</sub> (110). <b>2007</b> , 154, H675		39
1501	Divacancies in graphene and carbon nanotubes. <b>2007</b> , 7, 2459-62		151
1500	L-alanine in a droplet of water: a density-functional molecular dynamics study. <b>2007</b> , 111, 4227-34		73
1499	First-principles study on ZnO nanoclusters with hexagonal prism structures. <b>2007</b> , 90, 223102		53
1498	Surface dangling-bond States and band lineups in hydrogen-terminated Si, Ge, and Ge/si nanowires. <b>2007</b> , 98, 026801		30
1497	Stability and electronic structure of CdSe nanorods from first principles. <b>2007</b> , 76,		16
1496	Quantum-Chemical Interpretation of Current-Induced Forces on Adatoms on Carbon Nanotubes. <b>2007</b> , 111, 12478-12482		6
1495	Magnetic properties of vacancies in a graphitic boron nitride sheet by first-principles pseudopotential calculations. <b>2007</b> , 75,		171

1494	Correlation effects for highly Cr doped ZnSe. <i>Journal of Physics Condensed Matter</i> , <b>2007</b> , 19, 466209	1.8	2
1493	Efficient organometallic spin filter between single-wall carbon nanotube or graphene electrodes. <b>2007</b> , 98, 197202		127
1492	Scaling theory put into practice: first-principles modeling of transport in doped silicon nanowires. <b>2007</b> , 99, 076803		100
1491	Electronic and transport properties of boron-doped graphene nanoribbons. <b>2007</b> , 98, 196803		502
1490	Effect of protonation on the electronic properties of DNA base pairs: applications for molecular electronics. <b>2007</b> , 111, 11614-8		17
1489	First-principles calculations of the diamond (110) surface: A Mott insulator. <b>2007</b> , 75,		5
1488	A comparative ab initio study of the ferroelectric behaviour in KNO <sub>3</sub> and CaCO <sub>3</sub> . <i>Journal of Physics Condensed Matter</i> , <b>2007</b> , 19, 496210	1.8	17
1487	Three water sites in upper mantle olivine and the role of titanium in the water weakening mechanism. <b>2007</b> , 112,		51
1486	Stability and electronic properties of vacancies and antisites in BC <sub>2</sub> N nanotubes. <b>2007</b> , 75,		44
1485	Ab initio study of K adsorption on graphene and carbon nanotubes: Role of long-range ionic forces. <b>2007</b> , 76,		84
1484	Cu-precipitation kinetics in $\beta$ -Fe from atomistic simulations: Vacancy-trapping effects and Cu-cluster mobility. <b>2007</b> , 76,		185
1483	Organic spintronics. <b>2007</b> , 40, R205-R228		395
1482	Silicate chain formation in the nanostructure of cement-based materials. <b>2007</b> , 127, 164710		52
1481	Computational Studies of the Structure, Behavior upon Heating, and Mechanical Properties of Graphite Oxide. <b>2007</b> , 111, 18099-18111		281
1480	Efficient atomic self-interaction correction scheme for nonequilibrium quantum transport. <b>2007</b> , 99, 056801		120
1479	Real-time time-dependent density functional theory approach for frequency-dependent nonlinear optical response in photonic molecules. <b>2007</b> , 127, 154114		132
1478	Negative differential resistance of carbon nanotube electrodes with asymmetric coupling phenomena. <b>2007</b> , 76,		60
1477	Ab initio theoretical study of hydrogen and its interaction with boron acceptors and nitrogen donors in single-wall silicon carbide nanotubes. <b>2007</b> , 75,		40

1476	An efficient nonequilibrium Green's function formalism combined with density functional theory approach for calculating electron transport properties of molecular devices with quasi-one-dimensional electrodes. <b>2007</b> , 127, 194710	47
1475	Theoretical Study of Donor-Bridge-Acceptor Unimolecular Electric Rectifier. <b>2007</b> , 111, 11699-11705	114
1474	Molecular Design of Negative Differential Resistance Device through Intermolecular Interaction. <b>2007</b> , 111, 19098-19102	53
1473	STRUCTURAL AND ELECTRONIC PROPERTIES OF Sr(N3)2 UNDER PRESSURE. <b>2007</b> , 06, 487-494	2
1472	Ab-Initio Modeling of Defects in Germanium. <b>2007</b> , 187-210	1
1471	Control of channel shapes in a microporous manganese(II)-borophosphate framework by variation of size and shape of organic template cations. <b>2007</b> , 13, 1737-45	23
1470	Observation of van der Waals Driven Self-Assembly of MoSI Nanowires into a Low-Symmetry Structure Using Aberration-Corrected Electron Microscopy. <b>2007</b> , 19, 543-547	41
1469	Impurity-host interactions in Cr-substituted ZnSe. <b>2007</b> , 143, 399-402	13
1468	The conductance of SnO2 small nanowires: A study based on density functional and scattering theories. <b>2007</b> , 143, 481-486	3
1467	Ab initio simulations of the mechanics and electrical transport of Pt nanowires. <b>2007</b> , 8, 186-190	2
1466	Structure of the oxidized 4H-BiC(0001)-3B surface. <b>2007</b> , 601, 1048-1053	9
1465	Effects of Cs treatment on field emission properties of capped carbon nanotubes. <b>2007</b> , 601, 1501-1506	14
1464	The low-frequency Raman and IR spectra of nitric acid hydrates. <b>2007</b> , 43, 254-259	10
1463	Ab initio insights into the visible luminescent properties of ZnO. <b>2007</b> , 515, 8670-8673	27
1462	A computational study on nanocrystalline SnO2: Adsorption of CO and O2 onto defective nanograins. <b>2007</b> , 253, 4010-4015	2
1461	PUPIL: A systematic approach to software integration in multi-scale simulations. <b>2007</b> , 177, 265-279	20
1460	Order-N first-principles calculations with the conquest code. <b>2007</b> , 177, 14-18	57
1459	Electric field effects on the reactivity of heme model systems. <b>2007</b> , 434, 121-126	29

1458	Molecular orbital shift of perylenetetracarboxylic-dianhydride on gold. <b>2007</b> , 438, 249-253	60
1457	From a fullerene-like cage (SiC) <sub>12</sub> to novel silicon carbide nanowires: An ab initio study. <b>2007</b> , 442, 384-389	12
1456	Metallic edges in zinc oxide nanoribbons. <b>2007</b> , 448, 258-263	48
1455	First-principles study of Ti <sub>3</sub> AlC <sub>2</sub> (A=Si, Al) (001) surfaces. <b>2007</b> , 55, 4645-4655	70
1454	Charge imbalance at oxide interfaces: How nature deals with it. <b>2007</b> , 144, 1-6	14
1453	Experimental and theoretical study of Ge surface passivation. <b>2007</b> , 84, 2267-2273	18
1452	Density functional theory of high-k dielectric gate stacks. <b>2007</b> , 47, 686-693	6
1451	The electronic transport properties of N@C <sub>60</sub> @(n,m) carbon nanotube peapods. <b>2007</b> , 40, 99-102	5
1450	Design and energetic characterization of ZnO clusters from first-principles calculations. <b>2007</b> , 372, 39-43	51
1449	Theoretical study of the exchange coupling interactions in a polyoxometalate Fe <sub>9</sub> W <sub>12</sub> complex. <b>2007</b> , 26, 2161-2164	5
1448	HNO trapping and assisted decomposition of nitroxyl donors by ferric hemes. <b>2007</b> , 26, 4673-4679	30
1447	Non-periodic finite-element formulation of orbital-free density functional theory. <b>2007</b> , 55, 669-696	46
1446	Interaction between helium and self-defects in $\delta$ -iron from first principles. <b>2007</b> , 367-370, 244-250	78
1445	The first principles study on the Boron antimony compound. <b>2007</b> , 68, 482-489	25
1444	Slab calculations and Green's function recursive methods combined to study the electronic structure of surfaces: application to Cu(111)(4 $\times$ 4)-Na. <b>2007</b> , 82, 313-335	11
1443	Crystal growth of GaN on (0001) face by HVPE-atomistic scale simulation. <b>2007</b> , 303, 37-43	12
1442	Pure and doped boron nitride nanotubes. <b>2007</b> , 10, 30-38	171
1441	Revision of pyrrhotite structures within a common superspace model. <b>2007</b> , 63, 693-702	19



1440	Influence of sequential lithium insertions on the physical properties of spinel manganese oxide. <b>2007</b> , 107, 225-231	3
1439	Basis-set optimization for first-principles simulation of liquid water. <b>2007</b> , 107, 556-566	2
1438	An accurate total energy density functional. <b>2007</b> , 107, 2995-3000	4
1437	Mercury telluride crystals encapsulated within single walled carbon nanotubes: A density functional study. <b>2007</b> , 108, 797-807	13
1436	Probing the hierarchy of thymine-thymine interactions in self-assembled structures by manipulation with scanning tunneling microscopy. <b>2007</b> , 3, 2011-4	94
1435	Oxygen affinity controlled by dynamical distal conformations: the soybean leghemoglobin and the Paramecium caudatum hemoglobin cases. <b>2007</b> , 68, 480-7	30
1434	Transformation of spin information into large electrical signals using carbon nanotubes. <b>2007</b> , 445, 410-3	307
1433	Investigation of n-type donor defects in Co-doped ZnO. <b>2007</b> , 316, e185-e187	8
1432	Magnetic properties of ZrO <sub>2</sub> -diluted magnetic semiconductors. <b>2007</b> , 316, e188-e190	24
1431	Electronic transport through Fe/MgO/Fe(1 0 0) tunnel junctions. <b>2007</b> , 316, 481-483	13
1430	Study of the Reliability Impact of Chlorine Precursor Residues in Thin Atomic-Layer-Deposited $\text{HfO}_2$ Layers. <b>2007</b> , 54, 752-758	16
1429	Defect Passivation With Fluorine and Interface Engineering for Hf-Based High- $k$ /Metal Gate Stack Device Reliability and Performance Enhancement. <b>2007</b> , 54, 3267-3275	42
1428	Atomic structure of pre-Guinier-Breston zones in Al alloys. <b>2007</b> , 1, 172-174	8
1427	Atomic and electron structure of the GaAs (001) surface. <b>2007</b> , 41, 810-817	6
1426	First-Principles Studies of Ferroelectric Oxides. <b>2007</b> , 117-174	47
1425	Two-dimensional semiconducting nanostructures based on single graphene sheets with lines of adsorbed hydrogen atoms. <b>2007</b> , 91, 183103	59
1424	Defect-induced magnetism in graphene. <b>2007</b> , 75,	1107
1423	Mechanical Properties, Thermal Stability and Heat Transport in Carbon Nanotubes. <b>2007</b> , 165-195	16

1422	Theoretical study of the surface energy, stress, and lattice contraction of silver nanoparticles. <b>2007</b> , 75,	123
1421	Scanning tunnelling spectroscopy and ab initio calculations of single-walled carbon nanotubes interfaced with highly doped hydrogen-passivated Si(100) substrates. <b>2007</b> , 18, 095204	19
1420	Ab initio calculation of dc resistivity in liquid Al, Na and Pb. <i>Journal of Physics Condensed Matter</i> , <b>2007</b> , 19, 196105	1.8 16
1419	A first principles study of cubic IrO <sub>2</sub> polymorph. <b>2007</b> , 60, 477-481	4
1418	Relative stability of Si <sub>n</sub> and Si <sub>n</sub> Sc- clusters in the range n = 14-18. <b>2007</b> , 43, 217-220	16
1417	Magnetic properties of Pd atomic clusters from different theoretical approaches. <b>2007</b> , 44, 125-131	25
1416	Identification of fullerene-like CdSe nanoparticles from optical spectroscopy calculations. <b>2007</b> , 75,	45
1415	Order-N and embedded-cluster first-principles DFT calculations using SIESTA/Mosaico. <b>2007</b> , 118, 541-547	9
1414	Dielectric properties of nanoscale multi-component systems: A first principles computational study. <b>2007</b> , 14, 133-139	6
1413	Core structure and Peierls potential of screw dislocations in $\beta$ -Fe from first principles: cluster versus dipole approaches. <b>2007</b> , 14, 85-94	118
1412	Multiscale model of electronic behavior and localization in stretched dry DNA. <b>2007</b> , 42, 8894-8903	5
1411	Small Tin Oxide Grains: Structural and Electronic Properties Evaluated using the Density Functional Theory. <b>2007</b> , 18, 459-471	
1410	The Structural and Electronic Properties of Tin-Based Heteroatom Clusters Studied by the Density Functional Theory. <b>2007</b> , 18, 797-815	1
1409	Hydrocarbon Molecules Deposited onto Silicon Surfaces: A DFT Study of Adsorption and Conductance. <b>2007</b> , 18, 869-881	
1408	Interaction of copper organometallic precursors with barrier layers of Ti, Ta and W and their nitrides: a first-principles molecular dynamics study. <b>2007</b> , 13, 861-4	10
1407	Ab initio study of transport properties of an all-carbon molecular switch based on C <sub>20</sub> molecule. <b>2007</b> , 2, 36-40	1
1406	Hydrocarbon molecules deposited onto monolayer steps on Si(100): A study of adsorption and conductance. <b>2007</b> , 253, 4537-4541	1
1405	Electronic structure and driving forces in $\beta$ -cyclodextrin: Diclofenac inclusion complexes. <b>2007</b> , 366, 454-459	12

1404	Ab initio study of NO <sub>x</sub> compounds adsorption on SnO <sub>2</sub> surface. <b>2007</b> , 126, 62-67	82
1403	Acetylene adsorption on Si(100): A study of the role of surface steps. <b>2007</b> , 601, 218-226	2
1402	O <sub>2</sub> dissociation on Pd(211) and Cu(211) surfaces. <b>2007</b> , 601, 3774-3777	10
1401	Electron tunneling in the presence of adsorbed molecules. <b>2007</b> , 601, 5715-5720	1
1400	Theoretical modelling of intermediate band solar cell materials based on metal-doped chalcopyrite compounds. <b>2007</b> , 515, 6280-6284	88
1399	Stability of the tetrahedral motif for small gold clusters in the size range 16-24 atoms. <b>2007</b> , 140, 177-181	3
1398	Early precipitation stages of aluminum alloys—the role of quenched-in vacancies. <b>2008</b> , 255, 132-135	24
1397	Density-functional molecular dynamics studies of biologically relevant iron and cobalt complexes with macrocyclic ligands. <b>2008</b> , 252, 1497-1513	9
1396	Rapid iterative method for electronic-structure eigenproblems using localised basis functions. <b>2008</b> , 178, 128-134	134
1395	Generating relativistic pseudo-potentials with explicit incorporation of semi-core states using APE, the Atomic Pseudo-potentials Engine. <b>2008</b> , 178, 524-534	102
1394	Introducing PROFESS: A new program for orbital-free density functional theory calculations. <b>2008</b> , 179, 839-854	77
1393	Experimental and theoretical studies of l-cysteine adsorbed at Ag(111) electrodes. <b>2008</b> , 53, 6807-6817	30
1392	Ab initio investigation of the I <sub>V</sub> characteristics of the butadiene nano-molecular wires: A light-driven molecular switch. <b>2008</b> , 372, 3058-3063	6
1391	Electronic structure and driving forces in β-cyclodextrin:butylparaben inclusion complexes. <b>2008</b> , 372, 4257-4262	4
1390	First-principles study of transport of V doped boron nitride nanotube. <b>2008</b> , 372, 5609-5613	46
1389	Ab initio investigation of the characteristics of the phenoxynaphthacenequinone-based optical molecular switch. <b>2008</b> , 372, 5811-5815	11
1388	Toxins by first-principles: Electronic structure mapping structural changes. <b>2008</b> , 853, 58-61	2
1387	Spin-Dependence in Asymmetric, V-Shaped-Notched Graphene Nanoribbons. <b>2008</b> , 153, 393-398	19

1386	Computer simulation of the effective double layer occurring on a catalyst surface under electro-chemical promotion conditions. <b>2008</b> , 38, 1065-1073	14
1385	Transport in silicon nanowires: role of radial dopant profile. <b>2008</b> , 7, 324-327	15
1384	Numerical simulation of electronic transport in zigzag-edged graphene nano-ribbon devices. <b>2008</b> , 7, 390-393	11
1383	trans-1,2-Dicyano-cyclopropane and other cyano-cyclopropane derivatives. <b>2008</b> , 119, 211-229	8
1382	Quantum transport through STM-lifted single PTCDA molecules. <b>2008</b> , 93, 335-343	17
1381	Protonation effects on electron transport through diblock molecular junctions: A theoretical study. <b>2008</b> , 51, 1159-1165	6
1380	Enhanced ferromagnetism in ZnO nanoribbons and clusters passivated with sulfur. <b>2008</b> , 1, 420-426	32
1379	Effect of curvature on structures and vibrations of zigzag carbon nanotubes: A first-principles study. <b>2008</b> , 31, 335-341	15
1378	Carbon nanotubes with an extended line defect. <b>2008</b> , 4, 2209-13	18
1377	An investigation into the interactions between self-assembled adenine molecules and a Au(111) surface. <b>2008</b> , 4, 1494-500	92
1376	On the electronic structures and spectroscopic properties of polyynes and its derivatives. <b>2008</b> , 108, 1565-1571	3
1375	Electronic superlattices and waveguides based on graphene: structures, properties and applications. <b>2008</b> , 245, 2086-2089	12
1374	Vibrational properties of four consecutive carbon picotubes. <b>2008</b> , 245, 2145-2148	3
1373	Effects of a ZnS-shell on the structural and electronic properties of CdSe-nanorods. <b>2008</b> , 245, 2111-2114	6
1372	Folding of coordination polymers into double-stranded helical organization. <b>2008</b> , 14, 3883-8	34
1371	Magnetic endohedral transition-metal-doped semiconducting-nanoclusters. <b>2008</b> , 14, 8547-54	10
1370	Job submission to grid computing environments. <b>2008</b> , 20, 1329-1340	9
1369	Carbon nanotube, graphene, nanowire, and molecule-based electron and spin transport phenomena using the nonequilibrium Green's function method at the level of first principles theory. <b>2008</b> , 29, 1073-83	79

1368	Roles of cations, electronegativity difference, and anionic interlayer interactions in the metallic versus nonmetallic character of Zintl phases related to arsenic. <b>2008</b> , 29, 2144-53	24
1367	Ab-initio simulations of materials using VASP: Density-functional theory and beyond. <b>2008</b> , 29, 2044-78	1671
1366	A Modular Approach to Luminescent Dinuclear Ruthenium(II) and Rhenium(I) Complexes. <b>2008</b> , 2008, 3597-3605	6
1365	Specificity of watson-crick base pairing on a solid surface studied at the atomic scale. <b>2008</b> , 47, 9673-6	60
1364	Reversible Lithium-Ion Insertion in Molybdenum Oxide Nanoparticles. <b>2008</b> , 20, 3627-3632	304
1363	Specificity of Watson-Crick Base Pairing on a Solid Surface Studied at the Atomic Scale. <b>2008</b> , 120, 9819-9822	19
1362	Crystal growth of GaN on (0001) face by HVPE: Ab initio simulations. <b>2008</b> , 310, 900-905	10
1361	Role of chlorine in the dynamics of GaN(0001) surface during HVPE GaN growth—Ab initio study. <b>2008</b> , 310, 1391-1397	6
1360	Density functional non-equilibrium Green's function (DFT-NEGF) study of the smallest nano-molecular switch. <b>2008</b> , 40, 2606-2613	15
1359	Novel structure and electronic property of Sin (21?n?30) clusters. <b>2008</b> , 40, 2884-2889	2
1358	Electron transport phenomenon simulation through the carborane nano-molecular wire. <b>2008</b> , 40, 2965-2972	12
1357	Electronic structure and magnetism in BeO nanotubes induced by boron, carbon and nitrogen doping, and beryllium and oxygen vacancies inside tube walls. <b>2008</b> , 41, 164-168	47
1356	Thickness-dependent electronic and optical properties of faceted hexagonal aluminum nitride nanotubes. <b>2008</b> , 41, 254-257	9
1355	Bond energy and electronic structure in M-bis-terpyridine complexes (, Co and Ru). <b>2008</b> , 372, 1885-1889	5
1354	Theoretical study of the adsorption of CO2 on tungsten carbide nanotubes. <b>2008</b> , 372, 3277-3282	49
1353	First-principles electronic transport properties study of small carbon clusters: Cyclic C6. <b>2008</b> , 372, 4465-4468	6
1352	Simulation of STM technique for electron transport through boron-nitride nanotubes. <b>2008</b> , 372, 4839-4844	6
1351	First-principles study on the transport properties of phenyl dithiol oligomers. <b>2008</b> , 403, 2597-2601	7

1350	On the composition and atomic arrangement of calcium-deficient hydroxyapatite: An ab-initio analysis. <b>2008</b> , 181, 1712-1716	35
1349	Ab-initio approach to the effect of Fe on the diffusion in hcp Zr. <b>2008</b> , 374, 95-100	19
1348	The structural, elastic, and electronic properties of the pyrite-type phase for SnO <sub>2</sub> . <b>2008</b> , 69, 859-864	9
1347	DFT study on the reactivity of iron porphyrins tuned by ring substitution. <b>2008</b> , 102, 70-6	21
1346	Theoretical insight into the hydroxylamine oxidoreductase mechanism. <b>2008</b> , 102, 1523-30	38
1345	Monte Carlo study of oxidation of the 3C <sub>2</sub> BiC(001) surface. <b>2008</b> , 254, 4352-4356	2
1344	First principles calculations in iron: structure and mobility of defect clusters and defect complexes for kinetic modelling. <b>2008</b> , 9, 335-342	37
1343	Theoretical characterization of thioepoxidated single wall carbon nanotubes. <b>2008</b> , 460, 486-491	30
1342	Influence of ceramic-metal interface adhesion on crack growth resistance of ZrO <sub>2</sub> /Nb ceramic matrix composites. <b>2008</b> , 56, 3358-3366	51
1341	The chiral Zn(II)/La(III) coordination polymer: Synthesis, crystal structure, thermal and optical properties. <b>2008</b> , 11, 749-753	12
1340	Methane adsorption inside and outside pristine and N-doped single wall carbon nanotubes. <b>2008</b> , 353, 79-86	47
1339	Laser irradiation of atomic chains: A study based on the Density Functional Theory. <b>2008</b> , 145, 359-363	
1338	Theoretical models of ZnS nanoclusters and nanotubes: First-principles calculations. <b>2008</b> , 147, 165-168	20
1337	Electronic properties of (100)Ge/Ge(Hf)O <sub>2</sub> interfaces: A first-principles study. <b>2008</b> , 602, L25-L28	37
1336	Au on (111) and (110) surfaces of CeO <sub>2</sub> : A density-functional theory study. <b>2008</b> , 602, 1736-1741	78
1335	First principle study of a bimolecular thin film on Ag(111) surface. <b>2008</b> , 602, 2856-2862	15
1334	Investigations of the CN/Cu(1 1 1) system using density functional theory. <b>2008</b> , 602, 3308-3315	3
1333	The role of preadsorbed sulphur and oxygen in O <sub>2</sub> dissociation on Pd(100). <b>2008</b> , 602, 3660-3666	2

1332	Numerical evaluation of overlap integrals between atomic orbitals. <b>2008</b> , 848, 34-39	5
1331	Structural and electronic properties of 2,4,6-trinitrophenol (TNP). <b>2008</b> , 857, 33-37	10
1330	Theoretical study of molecular rectification in porphyrin dimer. <b>2008</b> , 516, 2630-2634	12
1329	First principles study of Si(3 3 5)Au surface. <b>2008</b> , 254, 4318-4321	10
1328	Design of nanoswitch based on C20-bowl molecules: A first principles study. <b>2008</b> , 39, 1499-1503	
1327	Potassium orbiting in fullerene based K(C60)2 nanosystem. <b>2008</b> , 887, 249-252	2
1326	Ab initio study of the diffusion mechanisms of gallium in a silicon matrix. <b>2008</b> , 64, 165-172	11
1325	Fullerene nanocage capacity for hydrogen storage. <b>2008</b> , 8, 767-74	211
1324	Hydrogen on graphene: Electronic structure, total energy, structural distortions and magnetism from first-principles calculations. <b>2008</b> , 77,	657
1323	Behavior of a single nitrogen molecule on the pentagon at a carbon nanotube tip: a first-principles study. <b>2008</b> , 19, 025709	55
1322	Helical [110] gold nanowires make longer linear atomic chains. <b>2008</b> , 101, 125502	21
1321	Heterodoped nanotubes: theory, synthesis, and characterization of phosphorus-nitrogen doped multiwalled carbon nanotubes. <b>2008</b> , 2, 441-8	165
1320	Deformation induced semiconductor-metal transition in single wall carbon nanotubes probed by electric force microscopy. <b>2008</b> , 100, 256804	57
1319	Magnetic correlations at graphene edges: basis for novel spintronics devices. <b>2008</b> , 100, 047209	566
1318	Spatially resolved electronic and vibronic properties of single diamondoid molecules. <b>2008</b> , 7, 38-42	80
1317	A density functional theory study of the $\beta$ -olefin selectivity in Fischer-Tropsch synthesis. <b>2008</b> , 255, 20-28	63
1316	The first principles study on PtC compound. <b>2008</b> , 111, 29-33	37
1315	Optical, magnetic and electronic properties of Ln <sub>2</sub> O <sub>2</sub> Te (Ln=La, Sm and Gd). <b>2008</b> , 43, 312-319	6

1314	Experimental and theoretical studies suggesting the possibility of metallic boron nitride edges in porous nanourchins. <b>2008</b> , 8, 1026-32		79
1313	Transport properties of an armchair carbon nanotube with a double vacancy under stretching. <i>Journal of Physics Condensed Matter</i> , <b>2008</b> , 20, 345225	1.8	2
1312	Nitric oxide reactivity with globins as investigated through computer simulation. <b>2008</b> , 437, 477-98		24
1311	Thermodynamic and kinetic approach in density functional theory studies of microscopic structure of GaN(0001) surface in ammonia-rich conditions. <b>2008</b> , 129, 234705		18
1310	Half-metallicity in undoped and boron doped graphene nanoribbons in the presence of semilocal exchange-correlation interactions. <b>2008</b> , 112, 1333-5		177
1309	Tuning the band structures of single walled silicon carbide nanotubes with uniaxial strain: A first principles study. <b>2008</b> , 92, 183116		28
1308	Phonon transport in isotope-disordered carbon and boron-nitride nanotubes: is localization observable?. <b>2008</b> , 101, 165502		104
1307	Ab initio study of spin-dependent transport in carbon nanotubes with iron and vanadium adatoms. <b>2008</b> , 78,		36
1306	Impact of incorporated Al on the TiN/HfO <sub>2</sub> interface effective work function. <b>2008</b> , 104, 074501		24
1305	Systematic investigation of the structure of the Si(553)-Au surface from first principles. <b>2008</b> , 77,		27
1304	Theoretical models of eumelanin protomolecules and their optical properties. <b>2008</b> , 94, 2095-105		86
1303	Theoretical study of DNA damage recognition via electron transfer from the [4Fe-4S] complex of MutY. <b>2008</b> , 95, 3259-68		18
1302	Mechanisms for ultrafast nonradiative relaxation in electronically excited eumelanin constituents. <b>2008</b> , 95, 4396-402		37
1301	Computational studies of semiconductor quantum dots. <b>2008</b> , 10, 4535-50		33
1300	Magnetism of CoO polymorphs: Density functional theory and Monte Carlo simulations. <b>2008</b> , 78,		33
1299	Impurity-ion pair induced high-temperature ferromagnetism in Co-doped ZnO. <b>2008</b> , 78,		144
1298	Direct observation of the radial breathing mode in CdSe nanorods. <b>2008</b> , 8, 4614-7		33
1297	Dynamic polarization effects on the angular distributions of protons channeled through carbon nanotubes in dielectric media. <b>2008</b> , 77,		21



1296	Evolutionary crystal structure prediction as a tool in materials design. <i>Journal of Physics Condensed Matter</i> , <b>2008</b> , 20, 064210	1.8	73
1295	Natural dyes adsorbed on TiO <sub>2</sub> nanowire for photovoltaic applications: enhanced light absorption and ultrafast electron injection. <b>2008</b> , 8, 3266-72		181
1294	Algorithm for the construction of self-energies for electronic transport calculations based on singularity elimination and singular value decomposition. <b>2008</b> , 78,		251
1293	I <sub>V</sub> curves of Fe/MgO (001) single- and double-barrier tunnel junctions. <b>2008</b> , 78,		19
1292	Influence of functional groups on charge transport in molecular junctions. <b>2008</b> , 128, 111103		107
1291	A theoretical study of the effect of nitrogen, boron and phosphorus impurities on the growth and morphology of diamond surfaces. <b>2008</b> , 17, 1307-1310		18
1290	Modeling extended contacts for nanotube and graphene devices. <b>2008</b> , 77,		61
1289	Adsorbate-limited conductivity of graphene. <b>2008</b> , 101, 196803		177
1288	Complexation of flavonoids with iron: structure and optical signatures. <b>2008</b> , 112, 1845-50		103
1287	Enumeration of not-yet-synthesized zeolitic zinc imidazolate MOF networks: a topological and DFT approach. <b>2008</b> , 112, 9437-43		87
1286	Competing intermediates in the pressure-induced wurtzite to rocksalt phase transition in ZnO. <b>2008</b> , 78,		30
1285	First-principles study of the geometric and electronic structure of Au <sub>13</sub> clusters: Importance of the prism motif. <b>2008</b> , 77,		38
1284	Modeling the destruction of realistic nanotube emitters: Relative role of charging and temperature. <b>2008</b> , 77,		2
1283	Channeling of protons through carbon nanotubes embedded in dielectric media. <i>Journal of Physics Condensed Matter</i> , <b>2008</b> , 20, 474212	1.8	11
1282	Recent progress in linear-scaling density functional calculations with plane waves and pseudopotentials: the ONETEP code. <i>Journal of Physics Condensed Matter</i> , <b>2008</b> , 20, 064209	1.8	17
1281	Surface Species Formed by the Adsorption and Dissociation of Water Molecules on a Ru(0001) Surface Containing a Small Coverage of Carbon Atoms Studied by Scanning Tunneling Microscopy. <b>2008</b> , 112, 7445-7454		43
1280	Semiconductor to metal transition in SWNTs caused by interaction with gold and platinum nanoparticles. <i>Journal of Physics Condensed Matter</i> , <b>2008</b> , 20, 215211	1.8	28
1279	Edge States and magnetism in carbon nanotubes with line defects. <b>2008</b> , 100, 146801		24

1278	First-principles study of ZnS nanostructures: nanotubes, nanowires and nanosheets. <b>2008</b> , 19, 305708		33
1277	Determination of elastic constants of Na <sub>0.5</sub> Bi <sub>0.5</sub> TiO <sub>3</sub> from ab initio calculations. <b>2008</b> , 81, 1117-1124		20
1276	Electronic band structure of carbon nanotube superlattices from first-principles calculations. <b>2008</b> , 77,		27
1275	Theoretical Insight into Faceted ZnS Nanowires and Nanotubes from Interatomic Potential and First-Principles Calculations. <b>2008</b> , 112, 3509-3514		33
1274	Constraints on T <sub>c</sub> for superconductivity in heavily boron-doped diamond. <b>2008</b> , 77,		79
1273	Hydrogenation of single-wall carbon nanotubes using polyamine reagents: combined experimental and theoretical study. <b>2008</b> , 130, 2296-303		48
1272	The structure of mixed H <sub>2</sub> O-OH monolayer films on Ru(0001). <b>2008</b> , 129, 154109		49
1271	Fe <sub>3</sub> C cluster confined in single-walled carbon nanotubes: A first-principles study. <b>2008</b> , 104, 054310		5
1270	Heat conductance is strongly anisotropic for pristine silicon nanowires. <b>2008</b> , 8, 3771-5		82
1269	Conformation dependence of molecular conductance: chemistry versus geometry. <i>Journal of Physics Condensed Matter</i> , <b>2008</b> , 20, 022203	1.8	32
1268	Monovacancy-induced magnetism in graphene bilayers. <i>Journal of Physics Condensed Matter</i> , <b>2008</b> , 20, 235220	1.8	20
1267	A study of the high-pressure polymorphs of L-serine using ab initio structures and PIXEL calculations. <b>2008</b> , 10, 1154		43
1266	The effect of stretching thiylland ethynylAu molecular junctions. <i>Journal of Physics Condensed Matter</i> , <b>2008</b> , 20, 025207	1.8	13
1265	Ferromagneticlike closure domains in ferroelectric ultrathin films: first-principles simulations. <b>2008</b> , 100, 177601		108
1264	The difference of the transport properties of graphene with corrugation structure and with flat structure. <b>2008</b> , 92, 163104		11
1263	First-principles modeling of electron transport. <i>Journal of Physics Condensed Matter</i> , <b>2008</b> , 20, 064216	1.8	57
1262	Origin of anomalous electronic structures of epitaxial graphene on silicon carbide. <b>2008</b> , 100, 176802		314
1261	Microscopic description of light induced defects in amorphous silicon solar cells. <b>2008</b> , 101, 265501		33

1260	Transparent conductive single-walled carbon nanotube networks with precisely tunable ratios of semiconducting and metallic nanotubes. <b>2008</b> , 2, 1266-74	278
1259	Hydrogen adsorption on boron doped graphene: an ab initio study. <b>2008</b> , 19, 155708	80
1258	Modeling bulk and surface Pt using the "Gaussian and plane wave" density functional theory formalism: validation and comparison to k-point plane wave calculations. <b>2008</b> , 129, 234703	33
1257	Substituting a copper atom modifies the melting of aluminum clusters. <b>2008</b> , 129, 124709	20
1256	Excess-silver-induced bridge formation in a silver sulfide atomic switch. <b>2008</b> , 93, 152106	43
1255	From pure C(60) to silicon carbon fullerene-based nanotube: an ab initio study. <b>2008</b> , 128, 154719	10
1254	Vacancy-induced magnetism in SnO <sub>2</sub> : A density functional study. <b>2008</b> , 78,	182
1253	Atomic and electronic structure of divacancies in carbon nanotubes. <b>2008</b> , 77,	39
1252	Direct observation of optically induced transient structures in graphite using ultrafast electron crystallography. <b>2008</b> , 101, 077401	116
1251	Approximation to density functional theory for the calculation of band gaps of semiconductors. <b>2008</b> , 78,	284
1250	Switching on magnetism in Ni-doped graphene: Density functional calculations. <b>2008</b> , 78,	80
1249	Network structure and dynamics of hydrogenated amorphous silicon. <b>2008</b> , 354, 2149-2154	12
1248	Electrical conductivity and Meyer-Neldel rule: The role of localized states in hydrogenated amorphous silicon. <b>2008</b> , 354, 2909-2913	27
1247	Topological and topological-electronic correlations in amorphous silicon. <b>2008</b> , 354, 3480-3485	17
1246	Two-dimensional supramolecular nanopatterns formed by the coadsorption of guanine and uracil at the liquid/solid interface. <b>2008</b> , 130, 695-702	67
1245	Optical excitation of deep defect levels in insulators within many-body perturbation theory: The F center in calcium fluoride. <b>2008</b> , 77,	58
1244	Role of symmetry in the transport properties of graphene nanoribbons under bias. <b>2008</b> , 100, 206802	387
1243	Bond or cage effect: how nitrophorins transport and release nitric oxide. <b>2008</b> , 130, 1611-8	37

1242	Novel high-pressure structures of MgCO <sub>3</sub> , CaCO <sub>3</sub> and CO <sub>2</sub> and their role in Earth's lower mantle. <b>2008</b> , 273, 38-47	187
1241	Characterization of leached layers on olivine and pyroxenes using high-resolution XPS and density functional calculations. <b>2008</b> , 72, 69-86	56
1240	Fe <sub>4</sub> cluster adsorbed on single-wall carbon nanotubes: A density functional study. <b>2008</b> , 42, 83-89	10
1239	Theoretical study of acetylene adsorption on armchair nanotubes. <b>2008</b> , 42, 322-328	7
1238	First-principles study of substituents effect on molecular junctions: Towards molecular rectification. <b>2008</b> , 42, 638-642	23
1237	Correlation effects in CrZinc chalcogenides. <b>2008</b> , 44, 303-309	7
1236	The use of quantum chemical methods in corrosion inhibitor studies. <b>2008</b> , 50, 2981-2992	872
1235	Quantum-interference-controlled molecular electronics. <b>2008</b> , 8, 3257-61	213
1234	An ab initio study on energy gap of bilayer graphene nanoribbons with armchair edges. <b>2008</b> , 92, 223106	53
1233	Prediction of very large values of magnetoresistance in a graphene nanoribbon device. <b>2008</b> , 3, 408-12	682
1232	Self-assembly of long chain alkanes and their derivatives on graphite. <b>2008</b> , 128, 124709	86
1231	Negative differential resistance in carbon atomic wire-carbon nanotube junctions. <b>2008</b> , 8, 2900-5	152
1230	The influence of pressure on the structure and dynamics of hydrogen bonds in zoisite and clinozoisite. <b>2008</b> , 35, 25-35	12
1229	Predictive first-principles simulations of strain-induced phenomena at water-silica nanotube interfaces. <b>2008</b> , 129, 011101	7
1228	The SIESTA method; developments and applicability. <i>Journal of Physics Condensed Matter</i> , <b>2008</b> , 20, 064208	364
1227	Nanoscale high energetic materials: a polymeric nitrogen chain N(8) confined inside a carbon nanotube. <b>2008</b> , 100, 196401	90
1226	Atomistic origin of urbach tails in amorphous silicon. <b>2008</b> , 100, 206403	95
1225	Anomalous conductance oscillations and half-metallicity in atomic Ag-O chains. <b>2008</b> , 101, 096804	13

1224	Threshold defect production in silicon determined by density functional theory molecular dynamics simulations. <b>2008</b> , 78,	120
1223	Nonmagnetic $\delta$ -FeN thin films epitaxially grown on Cu(001): Electronic structure and thermal stability. <b>2008</b> , 78,	36
1222	Theoretical study of migration processes in bulk diamond. <b>2008</b> , 17, 1225-1228	5
1221	An atomistic model and key parameters for devising single molecular nanowire sensors. <b>2008</b> , 10, 828-33	1
1220	Raman spectroscopy of charge transfer interactions between single wall carbon nanotubes and [FeFe] hydrogenase. <b>2008</b> , 5454-61	11
1219	Rectification in donor-acceptor molecular junctions. <i>Journal of Physics Condensed Matter</i> , <b>2008</b> , 20, 374106	22
1218	Ab initio calculations of structural and energetic properties of defects in gallium nitride. <b>2008</b> , 103, 123529	13
1217	Photoabsorption in sodium clusters on the basis of time-dependent density-functional theory. <b>2008</b> , 128, 014707	25
1216	Local properties at interfaces in nanodielectrics: An ab initio computational study. <b>2008</b> , 15, 170-177	28
1215	Polarizability of molecular chains: A self-interaction correction approach. <b>2008</b> , 77,	53
1214	Pulling the C60 molecule on a Si(001) surface with an STM tip: A theoretical study. <b>2008</b> , 77,	14
1213	A microscopic study of the deoxyhemoglobin-catalyzed generation of nitric oxide from nitrite anion. <b>2008</b> , 47, 9793-802	59
1212	First principles calculations using density matrix divide-and-conquer within the SIESTA methodology. <i>Journal of Physics Condensed Matter</i> , <b>2008</b> , 20, 294208	1.8 11
1211	Low-symmetry structures of Au <sub>32</sub> Z (Z = +1, 0, -1) clusters. <b>2008</b> , 112, 353-7	47
1210	BristedEvansPolanyi Relation of Multistep Reactions and Volcano Curve in Heterogeneous Catalysis. <b>2008</b> , 112, 1308-1311	146
1209	Systematic study on quantum confinement and waveguide effects for elastic and inelastic currents in atomic gold wire: importance of the phase factor for modeling electrodes. <b>2008</b> , 8, 6-12	20
1208	Bimetallic FeNi Cluster Alloys: Stability of Core(Fe)Shell(Ni) Arrays and Their Role Played in the Structure and Magnetic Behavior. <b>2008</b> , 112, 6729-6739	19
1207	Electronic properties of bulk and thin film SrRuO <sub>3</sub> : Search for the metal-insulator transition. <b>2008</b> , 78,	124

1206	Piezoelectricity of ZnO and its nanostructures. <b>2008,</b>	12
1205	Prediction of ultra-high aspect ratio nanowires from self-assembly. <b>2008, 8, 2697-705</b>	8
1204	Chain Growth Mechanism in Fischer-Tropsch Synthesis: A DFT Study of C-C Coupling over Ru, Fe, Rh, and Re Surfaces. <b>2008, 112, 6082-6086</b>	101
1203	Crystallographic and Electronic Structure of Self-Assembled DIP Monolayers on Au(111) Substrates. <b>2008, 112, 7168-7172</b>	38
1202	Symmetry controlled spin polarized conductance in au nanowires. <b>2008, 130, 9897-903</b>	20
1201	Search for ferromagnetism in SnO <sub>2</sub> doped with transition metals (V, Mn, Fe, and Co). <i>Journal of Physics Condensed Matter</i> , <b>2008, 20, 045214</b>	1.8 55
1200	Effect of h-BN Additive on Hydrogen Sorption by Ti under Mechanical Treatment in H <sub>2</sub> /He Flow. <b>2008, 112, 5869-5879</b>	10
1199	One-dimensional iron-cyclopentadienyl sandwich molecular wire with half metallic, negative differential resistance and high-spin filter efficiency properties. <b>2008, 130, 4023-7</b>	164
1198	Nexafs Study of Nitric Oxide Layers Adsorbed from a Nitrite Solution onto a Pt(111) Surface. <b>2008, 112, 10161-10166</b>	5
1197	Contrast in the Electronic and Magnetic Properties of Doped Carbon and Boron Nitride Nanotubes: A First-Principles Study. <b>2008, 112, 3464-3472</b>	11
1196	Magnetic structure of the large-spin Mn <sup>10</sup> and Mn <sup>19</sup> complexes: a theoretical complement to an experimental milestone. <b>2008, 130, 7420-6</b>	90
1195	First-principles investigations of elastic properties and energetics of antiferroelectric and ferroelectric phases of PbZrO <sub>3</sub> . <b>2008, 77,</b>	25
1194	Ices of CO <sub>2</sub> /H <sub>2</sub> O mixtures. Reflection-absorption IR spectroscopy and theoretical calculations. <b>2008, 112, 457-65</b>	19
1193	Functionalized Nanopore-Embedded Electrodes for Rapid DNA Sequencing. <b>2008, 112, 3456-3459</b>	65
1192	Quantum Interference: The Structural Dependence of Electron Transmission through Model Systems and Cross-Conjugated Molecules. <b>2008, 112, 16991-16998</b>	54
1191	Scanning tunneling microscopy images of alkane derivatives on graphite: role of electronic effects. <b>2008, 8, 3160-5</b>	77
1190	Density-functional study of edge stress in graphene. <b>2008, 78,</b>	68
1189	Electronic structure calculations of liquid-solid interfaces: Combination of density functional theory and modified Poisson-Boltzmann theory. <b>2008, 77,</b>	236

1188	Pseudo-atomic orbitals as basis sets for the O(N) DFT code CONQUEST. <i>Journal of Physics Condensed Matter</i> , <b>2008</b> , 20, 294206	1.8	29
1187	Defect-induced ferromagnetism in Mn-doped Cu <sub>2</sub> O. <i>Journal of Physics Condensed Matter</i> , <b>2008</b> , 20, 215218		9
1186	Adsorption Kinetics of Hydrogen Sulfide and Thiols on GaAs (001) Surfaces in a Vacuum. <b>2008</b> , 112, 3726-3733		32
1185	Pressure-induced deformation of the C <sub>60</sub> fullerene in Rb <sub>6</sub> C <sub>60</sub> and Cs <sub>6</sub> C <sub>60</sub> . <b>2008</b> , 77,		22
1184	Magnetic states at the oxygen surfaces of ZnO and Co-doped ZnO. <b>2008</b> , 101, 067206		71
1183	Comprehensive mechanism and structure-sensitivity of ethanol oxidation on platinum: new transition-state searching method for resolving the complex reaction network. <b>2008</b> , 130, 10996-1004		338
1182	Boroxol Rings in Liquid and Vitreous B <sub>2</sub> O <sub>3</sub> from First Principles. <b>2008</b> , 101, 065504		118
1181	Phonon transmission through defects in carbon nanotubes from first principles. <b>2008</b> , 77,		90
1180	Tuning the gap in bilayer graphene using chemical functionalization: Density functional calculations. <b>2008</b> , 78,		167
1179	Applications of atomistic calculations to chemical gas sensing. <b>2008</b> ,		
1178	Electronic energy levels of weakly coupled nanostructures: C <sub>60</sub> -metal interfaces. <b>2008</b> , 101, 026804		95
1177	Structure and dynamics of Cu(I) binding in copper chaperones Atox1 and CopZ: a computer simulation study. <b>2008</b> , 112, 4583-93		26
1176	Electronic and optical properties of ordered B <sub>x</sub> Zn <sub>1-x</sub> Se alloys by the FPLAPW method. <i>Journal of Physics Condensed Matter</i> , <b>2008</b> , 20, 075205	1.8	19
1175	Linearly scaling 3D fragment method for large-scale electronic structure calculations. <b>2008</b> ,		3
1174	Analysis of the electronic structure of liquid rubidium by the methods of ab initio molecular dynamics, linear muffin-tin orbitals and recursion. <i>Journal of Physics Condensed Matter</i> , <b>2008</b> , 20, 114104 <sup>1.8</sup>		8
1173	Conductivity of liquid Al, Na, Pb and Mn calculated from first principles. <b>2008</b> , 98, 062001		
1172	DFT calculation of crystallographic properties of dioctahedral 2:1 phyllosilicates. <b>2008</b> , 43, 351-361		35
1171	A theoretical view of unimolecular rectification. <i>Journal of Physics Condensed Matter</i> , <b>2008</b> , 20, 374105	1.8	48

1170	Channeling of protons through carbon nanotubes. <b>2008</b> , 133, 012015		5
1169	Understanding the disorder of the DNA base cytosine on the Au(111) surface. <b>2008</b> , 129, 184707		51
1168	Non-trivial length dependence of the conductance and negative differential resistance in atomic molecular wires. <b>2008</b> , 19, 455203		76
1167	Structural, Electronic Properties and Chemical Bonding of Borate $\text{Li}_4\text{CaB}_2\text{O}_6$ under High Pressure: an Ab Initio Investigation. <b>2008</b> , 25, 552-555		5
1166	A density-functional study of the structures, binding energies and magnetic moments of the clusters Mo(N) (N = 2-13), Mo(12)Fe, Mo(12)Co and Mo(12)Ni. <b>2008</b> , 19, 145704		19
1165	Effects of hydroxyl group distribution on the reactivity, stability and optical properties of fullerenols. <b>2008</b> , 19, 365703		31
1164	Efficient solution of Poisson's equation using discrete variable representation basis sets for Car-Parrinello ab initio molecular dynamics simulations with cluster boundary conditions. <b>2008</b> , 129, 224108		13
1163	A dynamic scheduler for balancing HPC applications. <b>2008</b> ,		20
1162	Density kernel optimization in the ONETEP code. <i>Journal of Physics Condensed Matter</i> , <b>2008</b> , 20, 294207	1.8	29
1161	THEORETICAL STUDY OF THE ELECTRON TRANSPORT THROUGH THE CYSTEINE AMINO ACID NANOMOLECULAR WIRE. <b>2008</b> , 07, 95-102		2
1160	Ab Initio Study on Hypothetical Silver Nitride. <b>2008</b> , 25, 2154-2157		17
1159	Ferrocene-1,1'-dithiol as molecular wire between Ag electrodes: the role of surface defects. <b>2008</b> , 128, 064704		9
1158	The structural, thermodynamical, elastic, and vibrational properties of LaBi. <i>Journal of Physics Condensed Matter</i> , <b>2008</b> , 20, 345202	1.8	6
1157	The energetics of tetrahydrocarbazole aromatization over Pd(111): a computational analysis. <b>2008</b> , 128, 105104		9
1156	Study on the maximum accuracy of the pseudopotential density functional method with localized atomic orbitals versus plane-wave basis sets. <b>2008</b> , 128, 044102		9
1155	Benchmark density functional theory calculations for nanoscale conductance. <b>2008</b> , 128, 114714		99
1154	Ab initio investigations of the transport properties of Haeckelite nanotubes. <i>Journal of Physics Condensed Matter</i> , <b>2008</b> , 20, 415207	1.8	5
1153	Adiabatic intramolecular movements for water systems. <b>2008</b> , 128, 104311		2



1152	First-principles study of the structural and electronic properties of (100)GeTe(M)O <sub>2</sub> interfaces (M=Al, La, or Hf). <b>2008</b> , 92, 242101		66
1151	Rotational dynamics and polymerization of C <sub>60</sub> in C <sub>60</sub> -cubane crystals: a molecular dynamics study. <b>2008</b> , 129, 064506		10
1150	Energy alignment induced negative differential resistance: the role of hybrid states in aromatic molecular devices. <b>2008</b> , 129, 074710		15
1149	Structure and reactions of carbon and hydrogen on Ru(0001): a scanning tunneling microscopy study. <b>2008</b> , 129, 244103		15
1148	Linear-scaling total-energy calculations with the tight-binding Korringa-Kohn-Rostoker Green function method. <b>2008</b> , 88, 2807-2815		4
1147	Representations of the occupation number matrix on the LDA/GGA+U method. <i>Journal of Physics Condensed Matter</i> , <b>2008</b> , 20, 325205	1.8	26
1146	Towards a linear-scaling algorithm for electronic structure calculations with the tight-binding Korringa-Kohn-Rostoker Green function method. <i>Journal of Physics Condensed Matter</i> , <b>2008</b> , 20, 294215	1.8	24
1145	The structure and properties of small Pd <sup>d</sup> clusters. <b>2008</b> , 19, 205701		17
1144	Elimination, in electronic structure calculations, of redundant orbital products. <b>2008</b> , 128, 034108		21
1143	Nonadiabatic effects on surfaces: Kohn anomaly, electronic damping of adsorbate vibrations, and local heating of single molecules. <i>Journal of Physics Condensed Matter</i> , <b>2008</b> , 20, 224015	1.8	7
1142	Diffusion mechanisms taking place at the early stages of cobalt deposition on Au(111). <i>Journal of Physics Condensed Matter</i> , <b>2008</b> , 20, 265010	1.8	3
1141	Theoretical modelling of tip effects in the pushing manipulation of C(60) on the Si(001) surface. <b>2008</b> , 19, 235702		13
1140	Interface dipole formation of different ZnPcCl(8) phases on Ag(111) observed by Kelvin probe force microscopy. <b>2008</b> , 19, 305501		16
1139	Polymerization of Silicon-Doped Heterofullerenes: an Ab Initio Study. <b>2008</b> , 25, 246-249		3
1138	A model of a tunable quantum dot in a semiconducting carbon nanotube. <b>2008</b> , 23, 085024		3
1137	Elastic properties of amorphous boron suboxide based solids studied using ab initio molecular dynamics. <i>Journal of Physics Condensed Matter</i> , <b>2008</b> , 20, 195203	1.8	17
1136	Adsorption of metal impurities on H-terminated Si surfaces and their influence on the wet chemical etching of Si. <i>Journal of Physics Condensed Matter</i> , <b>2008</b> , 20, 485005	1.8	7
1135	Theoretical study of melamine superstructures and their interaction with the Au(111) surface. <b>2008</b> , 19, 465704		35

1134	A density-functional study of the possibility of noncollinear magnetism in small Mn clusters using SIESTA and the generalized gradient approximation to exchange and correlation. <b>2008</b> , 128, 114315		20
1133	Correlation between the latent heats and cohesive energies of metal clusters. <b>2008</b> , 129, 144702		52
1132	Effect of Cu impurities on wet etching of Si(110): formation of trapezoidal hillocks. <b>2008</b> , 10, 013033		11
1131	The BN-pair impurity in carbon nanotubes and the possibility for disorder-induced frustration of gap formation. <b>2008</b> , 19, 445709		6
1130	Accuracy of order-Ndensity-functional theory calculations on DNA systems using CONQUEST. <i>Journal of Physics Condensed Matter</i> , <b>2008</b> , 20, 294201	1.8	23
1129	Surface properties of silver and aluminum nanoclusters. <b>2008</b> ,		2
1128	Ab initiomolecular dynamics simulations with linear scaling: application to liquid ethanol. <i>Journal of Physics Condensed Matter</i> , <b>2008</b> , 20, 294212	1.8	11
1127	Unique electronic band structures of hydrogen-terminated [Formula: see text] silicon nanowires. <b>2008</b> , 19, 035708		10
1126	The electronic structure of a single-walled aluminosilicate nanotube. <b>2008</b> , 19, 175702		15
1125	Inelastic electron tunnelling in saturated molecules with different functional groups: correlations and symmetry considerations from a computational study. <i>Journal of Physics Condensed Matter</i> , <b>2008</b> , 20, 374111	1.8	5
1124	Variable contact gap single-molecule conductance determination for a series of conjugated molecular bridges. <i>Journal of Physics Condensed Matter</i> , <b>2008</b> , 20, 374119	1.8	41
1123	Electrostatic versus polarization effects in the adsorption of aromatic molecules of varied polarity on an insulating hydrophobic surface. <i>Journal of Physics Condensed Matter</i> , <b>2008</b> , 20, 035215	1.8	15
1122	Ab initio study of the electron transport in dithienylethene photochromic molecules attached to gold leads. <b>2008</b> , 100, 052061		1
1121	Automatic data distribution and load balancing with space-filling curves: implementation in CONQUEST. <i>Journal of Physics Condensed Matter</i> , <b>2008</b> , 20, 275223	1.8	10
1120	Efficient ab initio method for inelastic transport in nanoscale devices: Analysis of inelastic electron tunneling spectroscopy. <b>2008</b> , 78,		39
1119	Ab initio calculations of inelastic transport in atomic/molecular junctions and waveguide effects. <i>Journal of Physics Condensed Matter</i> , <b>2008</b> , 20, 224023	1.8	4
1118	Dynamic Jahn-Teller effect in electronic transport through single C60 molecules. <b>2008</b> , 78,		47
1117	Strongly reshaped organic-metal interfaces: tetracyanoethylene on Cu(100). <b>2008</b> , 101, 216105		52

1116	Large electromechanical response in silicon nanowires predicted from first-principles electronic structure calculations. <b>2008, 77,</b>	4
1115	Interplay between structure and magnetism in hydride iron-vanadium systems. <b>2008, 78,</b>	8
1114	Kondo effect in single atom contacts: the importance of the atomic geometry. <b>2008, 101, 216802</b>	57
1113	Predicting d0 magnetism: Self-interaction correction scheme. <b>2008, 78,</b>	113
1112	Unification of the phonon mode behavior in semiconductor alloys: Theory and ab initio calculations. <b>2008, 77,</b>	30
1111	Contact dependence of the conductance of H2 molecular junctions from first principles. <b>2008, 77,</b>	10
1110	Ab initio study of decohesion properties in oxide/metal systems. <b>2008, 78,</b>	31
1109	Covalentlike electronic effects in metallic liquids using an orbital-free ab initio method. <b>2008, 77,</b>	8
1108	Charge relaxation resistance at atomic scale: An ab initio calculation. <b>2008, 77,</b>	9
1107	Symmetry of the phosphorus donor in diamond from first principles. <b>2008, 78,</b>	11
1106	First-principles calculations of structural changes in B2O3 glass under pressure. <b>2008, 78,</b>	20
1105	Origin of torsion-induced conductance oscillations in carbon nanotubes. <b>2008, 78,</b>	30
1104	Balancing HPC applications through smart allocation of resources in MT processors. <b>2008,</b>	8
1103	p-type Fermi level pinning at a Si:Al2O3 model interface. <b>2008, 93, 122905</b>	25
1102	Fluorination-induced magnetism in boron nitride nanotubes from ab initio calculations. <b>2008, 92, 102515</b>	48
1101	Possibility of collinear magnetic order in frustrated free-standing Fe2Cr4 clusters. <b>2008, 77,</b>	8
1100	Formation of silicon-fullerene-linked nanowires inside carbon nanotubes: A molecular-dynamics and first-principles study. <b>2008, 77,</b>	7
1099	A possible anthracene-based optical molecular switch driven by a reversible photodimerization reaction. <b>2008, 93, 013113</b>	64

1098	Geometry and diameter dependence of the electronic and physical properties of GaN nanowires from first principles. <b>2008</b> , 77,	77
1097	Stability and bonding properties of finite single-walled carbon nanotubes adsorbed on Si(001). <b>2008</b> , 92, 093109	5
1096	Effects of self-interaction corrections on the transport properties of phenyl-based molecular junctions. <b>2008</b> , 77,	114
1095	Vertical manipulation of a molecule with chemical forces. <b>2008</b> , 77,	7
1094	Structural phase transitions in high-pressure wurtzite to rocksalt phase in GaN and SiC. <b>2008</b> , 92, 241909	17
1093	First-principles modeling of strain in perovskite ferroelectric thin films. <b>2008</b> , 81, 607-622	12
1092	Numerical characterization of the Ga interstitial self-diffusion mechanisms in GaAs. <b>2008</b> , 103, 113502	9
1091	First-principles study for transport properties of armchair carbon nanotubes with a double vacancy under strain. <b>2008</b> , 103, 113714	5
1090	Reliability study of La2O3 capped HfSiON high-permittivity n-type metal-oxide-semiconductor field-effect transistor devices with tantalum-rich electrodes. <b>2008</b> , 104, 044512	10
1089	Indirect-to-direct band gap transitions in phosphorus adsorbed <112> silicon nanowires. <b>2008</b> , 93, 173108	18
1088	Tunable electronic band structures of hydrogen-terminated <112> silicon nanowires. <b>2008</b> , 92, 203109	21
1087	Germanium MOSFET Devices: Advances in Materials Understanding, Process Development, and Electrical Performance. <b>2008</b> , 155, H552	200
1086	Magnetic properties of carbon nanotube terminally connecting metal molecular complexes. <b>2008</b> , 92, 081907	3
1085	Photoabsorption spectra of small fullerenes and Si-heterofullerenes. <b>2008</b> , 128, 154307	21
1084	Compositional ordering and quantum transport in Mo6S9 nanowires: Ab initio calculations. <b>2008</b> , 77,	15
1083	Comparative ab initio study of the structural, electronic, and magnetic trends of isoelectronic late 3d and 4d transition metal clusters. <b>2008</b> , 78,	56
1082	Melting-point depression by insoluble impurities: a finite size effect. <b>2008</b> , 101, 023401	45
1081	Edge chemistry engineering of graphene nanoribbon transistors: A computational study. <b>2008</b> ,	9

1080	Zone-center instability of C(5,0) carbon nanotubes inside AlPO <sub>4</sub> channels. <b>2008, 77,</b>	3
1079	Transport properties of single vacancies in nanotubes. <b>2008, 77,</b>	32
1078	Conductance of a copper-nanotube bundle interface: Impact of interface geometry and wave-function interference. <b>2008, 77,</b>	10
1077	Lead-molecule coupling effects on the distortion-dependent conductance of carbon nanotubes. <b>2008, 77,</b>	3
1076	Divide-and-conquer density functional theory on hierarchical real-space grids: Parallel implementation and applications. <b>2008, 77,</b>	58
1075	Sequence dependent electron transport in wet DNA: ab initio and molecular dynamics studies. <b>2008, 101, 176805</b>	34
1074	Tailoring the Fermi level of the leads in molecular-electronic devices. <b>2008, 78,</b>	7
1073	Electronic processes in fast thermite chemical reactions: a first-principles molecular dynamics study. <b>2008, 77, 066103</b>	64
1072	Quantum confinement and electronic properties of tapered silicon nanowires. <b>2008, 100, 246804</b>	64
1071	Stress enhanced self-diffusion in Si: Entropy effect in anisotropic elastic environment. <b>2008, 92, 152110</b>	6
1070	Manipulating magnetism and conductance of an adatom-molecule junction on a metal surface: An ab initio study. <b>2008, 78,</b>	11
1069	Rayleigh-Schrödinger many-body perturbation theory for density functionals: A unified treatment of one- and two-electron perturbations. <b>2008, 78,</b>	22
1068	Cleaving-temperature dependence of layered-oxide surfaces. <b>2008, 101, 216103</b>	24
1067	Magnetism induced by single carbon vacancies in a three-dimensional graphitic network. <b>2008, 77,</b>	61
1066	Effect of quantization of vibrations on the structural properties of crystals. <b>2008, 78,</b>	7
1065	Thermal conduction mechanisms in boron nitride nanotubes: Few-shell versus all-shell conduction. <b>2008, 78,</b>	17
1064	Modeling realistic tip structures: Scanning tunneling microscopy of NO adsorption on Rh(111). <b>2008, 78,</b>	15
1063	Effective Hamiltonian for FeAs-based superconductors. <b>2008, 78,</b>	25

1062	First-principles nonequilibrium analysis of STM-induced molecular negative-differential resistance on Si(100). <b>2008</b> , 78,	23
1061	Cluster-surface and cluster-cluster interactions: Ab initio calculations and modeling of asymptotic van der Waals forces. <b>2008</b> , 78,	23
1060	Quasiatomic orbitals for ab initio tight-binding analysis. <b>2008</b> , 78,	77
1059	Spin currents in rough graphene nanoribbons: universal fluctuations and spin injection. <b>2008</b> , 100, 177207	240
1058	Conformational change of tetrahydroxyquinone molecules deposited on Ag(111). <b>2008</b> , 77,	14
1057	Transforming carbon nanotubes by silylation: an ab initio study. <b>2008</b> , 100, 236102	11
1056	Electronic and optical properties of polyicosahedral Si nanostructures: A first-principles study. <b>2008</b> , 77,	11
1055	Quantum conductance of 4,4-bipyridine molecular junctions: Role of electrode work function and local d band. <b>2008</b> , 78,	14
1054	Theory of the electronic structure of alternating MgB <sub>2</sub> and graphene layered structures. <b>2008</b> , 77,	10
1053	Engineering the magnetic structure of Fe'clusters by Mn alloying. <b>2008</b> , 19, 245701	13
1052	The influence of surface roughness on electrical conductance of thin Cu films: An ab initio study. <b>2008</b> , 103, 113705	98
1051	First-principles determination of the effects of intermolecular interactions on the electronic transport through molecular monolayers. <b>2008</b> , 78,	12
1050	First-principles study of adsorption, diffusion, and charge stability of metal adatoms on alkali halide surfaces. <b>2008</b> , 78,	11
1049	High-pressure stability of Cs <sub>6</sub> C <sub>60</sub> . <b>2008</b> , 77,	16
1048	Characteristic vibrational modes of a single vacancy in a zigzag carbon nanotube. <b>2008</b> , 77,	9
1047	High-pressure electronic structure and phase transitions in monoclinic InSe: X-ray diffraction, Raman spectroscopy, and density functional theory. <b>2008</b> , 77,	31
1046	Mechanism of fullerene hydrogenation by polyamines: Ab initio density functional calculations. <b>2008</b> , 78,	28
1045	Preserved conductance in covalently functionalized silicon nanowires. <b>2008</b> , 100, 046802	22

1044	Mn-doped silicon nanowires: First-principles calculations. <b>2008</b> , 78,	13
1043	Possible electric-field-induced one-dimensional excitonic insulators in pairs of carbon nanotubes. <b>2008</b> , 78,	4
1042	Nonlinear effect in conductance of a finite-length armchair single-wall carbon nanotube due to presence of a single impurity. <b>2008</b> , 129, 012010	
1041	Electronic structure of Al <sub>6</sub> Mg <sub>4</sub> Cu quasicrystals. <b>2008</b> , 98, 062006	
1040	Atomic, electronic, and transport properties of quasi-one-dimensional nanostructures. <b>2008</b> ,	
1039	Structural, wetting, and electronic properties of metal clusters adsorbed on carbon nanotubes. <b>2008</b> , 104, 013509	11
1038	Quenching of local magnetic moment in oxygen adsorbed graphene nanoribbons. <b>2008</b> , 128, 201101	29
1037	Variable atomic radii for continuum-solvent electrostatics calculation. <b>2008</b> , 129, 014509	10
1036	Molecular dynamic simulation of the melting process in Ni <sub>3</sub> Al alloy. <b>2008</b> , 98, 042026	
1035	The role of ammonia in sulfuric acid ion induced nucleation. <b>2008</b> , 8, 2859-2867	79
1034	Coexistence of superconductivity and antiferromagnetism in CeRhIn <sub>5</sub> ; model Hamiltonian and ab-initio calculations. <b>2008</b> , 121, 052008	
1033	Simulation of liquid Rb by the methods of classical and first-principle molecular dynamics and statistical geometrical analysis of the atomic structure models using the Voronoi-Delaunay method. <b>2008</b> , 98, 042023	
1032	Theory of nonequilibrium transient transport in nanostructures. <b>2008</b> , 5, 1094	
1031	Zr-metal adhesion on graphenic nanostructures. <b>2008</b> , 93, 053101	10
1030	WATER-AMMONIUM ICES AND THE ELUSIVE 6.85 TH BAND. <b>2009</b> , 703, L178-L182	13
1029	Static and dynamic properties of hydrogenated amorphous silicon with voids. <b>2009</b> , 79,	21
1028	Magnetic and structural properties of Mn adatoms on copper nitride over Cu(100). <b>2009</b> , 79,	6
1027	Charge transport through O-deficient Au-MgO-Au junctions. <b>2009</b> , 80,	4

1026	Effective Coulomb interactions within BEDT-TTF dimers. <b>2009</b> , 80,	35
1025	Oxide superlattices with alternating p and n interfaces. <b>2009</b> , 80,	59
1024	Anomalous electron-phonon interaction in doped LaFeAsO: First-principles calculations. <b>2009</b> , 79,	29
1023	Oscillation of dynamic conductance of Al-Cn-Al structures: Nonequilibrium Green's function and density functional theory study. <b>2009</b> , 79,	24
1022	Electronic structure models of phosphorus doped silicon. <b>2009</b> , 79,	39
1021	Stability of $GaxAs_{x-4}$ gallium arsenide fullerenes. <b>2009</b> , 79,	3
1020	Model of impurity segregation in graphene nanoribbons. <b>2009</b> , 80,	14
1019	Green's function method for elimination of the spurious multipole interaction in the surface/interface slab model. <b>2009</b> , 80,	60
1018	Electron transport across carbon nanotube junctions decorated with Au nanoparticles: Density functional calculations. <b>2009</b> , 79,	19
1017	Charge transfer and screening effects in polyynes encapsulated inside single-wall carbon nanotubes. <b>2009</b> , 80,	29
1016	Resonant electronic states and $I/V$ curves of Fe/MgO/Fe(100) tunnel junctions. <b>2009</b> , 79,	53
1015	Ge-H empirical potential and simulation of Si epitaxy on Ge(100) by chemical vapor deposition from $SiH_4$ . <b>2009</b> , 79,	6
1014	Andreev reflection through Fano resonances in molecular wires. <b>2009</b> , 79,	19
1013	Interface states in carbon nanotube junctions: Rolling up graphene. <b>2009</b> , 80,	22
1012	FIRST PRINCIPLES CALCULATIONS OF ELASTIC CONSTANTS FOR DEFECTED $Na_{1/2}Bi_{1/2}TiO_3$ . <b>2009</b> , 108, 21-36	9
1011	A density-functional study of the vertical ionization potentials of the cluster $Mn_{13}$ . <b>2009</b> , 131, 046101	5
1010	Stone-Wales defects created by low energy recoils in single-walled silicon carbide nanotubes. <b>2009</b> , 106, 084305	15
1009	Stacking of polycyclic aromatic hydrocarbons as prototype for graphene multilayers, studied using density functional theory augmented with a dispersion term. <b>2009</b> , 131, 194702	41



1008	Switching a single spin on metal surfaces by a STM Tip: Ab Initio studies. <b>2009</b> , 103, 057202	52
1007	Defect states in carbon nanotubes and related band structure engineering: A first-principles study. <b>2009</b> , 105, 024312	9
1006	A first principles study on tunneling current through Si/SiO <sub>2</sub> /Si structures. <b>2009</b> , 105, 083702	3
1005	A theoretical study of the initial oxidation of the GaAs(001)- $\sqrt{2}\times\sqrt{2}$ surface. <b>2009</b> , 95, 253504	29
1004	Resonant spin-filtering in cobalt decorated nanotubes. <b>2009</b> , 94, 173103	10
1003	Real space first-principles derived semiempirical pseudopotentials applied to tunneling magnetoresistance. <b>2009</b> , 105, 093709	3
1002	Electronic structures of BC <sub>3</sub> nanoribbons. <b>2009</b> , 94, 073111	50
1001	Structural and electronic properties of oxidized sodium clusters: A combined photoelectron and density functional study. <b>2009</b> , 131, 204313	11
1000	Destruction of graphene by metal adatoms. <b>2009</b> , 95, 023109	97
999	Mo <sub>4</sub> Fe <sub>x</sub> nanoalloy: Structural transition and electronic structure of interest in spintronics. <b>2009</b> , 79, 79,	13
998	Ohmic contacts on silicon carbide: The first monolayer and its electronic effect. <b>2009</b> , 80,	54
997	Doping of C <sub>60</sub> -induced electronic states in BN nanopeapods: Ab initio simulations. <b>2009</b> , 80,	5
996	Pb chains on reconstructed Si(335) surface. <b>2009</b> , 79,	16
995	Cooperative mechanism for anchoring highly polar molecules at an ionic surface. <b>2009</b> , 80,	27
994	First-principles calculation of atomic force in the LSDA+U formalism. <b>2009</b> , 80,	6
993	Shape-tunable electronic properties of monohydride and trihydride [112]-oriented Si nanowires. <b>2009</b> , 80,	10
992	Influence of carbon on the kinetics of He migration and clustering in $\alpha$ -Fe from first principles. <b>2009</b> , 80,	39
991	Genetic algorithm and first-principles DFT study of the high-pressure molecular $\beta$ phase of nitrogen. <b>2009</b> , 80,	12

990	F4TCNQ on Cu, Ag, and Au as prototypical example for a strong organic acceptor on coinage metals. <b>2009</b> , 79,	108
989	Computational study of boron nitride nanotube synthesis: How catalyst morphology stabilizes the boron nitride bond. <b>2009</b> , 80,	16
988	Anisotropic magnetoresistance in atomic chains of iridium and platinum from first principles. <b>2009</b> , 79,	21
987	Role of van der Waals forces in the adsorption and diffusion of organic molecules on an insulating surface. <b>2009</b> , 80,	38
986	Organic molecule assembled between carbon nanotubes: A highly efficient switch device. <b>2009</b> , 79,	34
985	Significant negative differential resistance predicted in scanning tunneling spectroscopy for a C60 monolayer on a metal surface. <b>2009</b> , 80,	6
984	Hydrogen-induced disintegration of fullerenes and nanotubes: An ab initio study. <b>2009</b> , 80,	17
983	Reaction and incorporation of H <sub>2</sub> molecules inside single-wall carbon nanotubes through multivacancy defects. <b>2009</b> , 80,	15
982	Polymeric nitrogen in a graphene matrix: An ab initio study. <b>2009</b> , 80,	26
981	Effects of structural relaxation on calculations of the interface and transport properties of Fe/MgO(001) tunnel junctions. <b>2009</b> , 79,	22
980	Atomistic theory for the damping of vibrational modes in monoatomic gold chains. <b>2009</b> , 80,	17
979	Tuning the conductance of molecular junctions: Transparent versus tunneling regimes. <b>2009</b> , 80,	11
978	Simulating STM transport in alkanes from first principles. <b>2009</b> , 79,	23
977	In and Si adatoms on Si(111)5 $\times$ 5-Au: Scanning tunneling microscopy and first-principles density functional calculations. <b>2009</b> , 80,	12
976	Defect-enhanced charge transfer by ion-solid interactions in SiC using large-scale ab initio molecular dynamics simulations. <b>2009</b> , 103, 027405	66
975	MgN: A possible material for spintronic applications. <b>2009</b> , 80,	28
974	Solid phases of phosphorus carbide: An ab initio study. <b>2009</b> , 79,	34
973	Localized atomic basis set in the projector augmented wave method. <b>2009</b> , 80,	232

972	Ab initio study of thiophene chemisorption on Si(111)( $\sqrt{3}\times\sqrt{3}$ ). <b>2009</b> , 80,	7
971	Nonequilibrium Green's function study of Pd <sub>4</sub> -cluster-functionalized carbon nanotubes as hydrogen sensors. <b>2009</b> , 79,	17
970	Electrostatic and dynamical effects of an aqueous solution on the zero-bias conductance of a single molecule: A first-principles study. <b>2009</b> , 80,	12
969	A density-functional study of the structures and electronic properties of neutral, anionic, and endohedrally doped In(x)P(x) clusters. <b>2009</b> , 131, 074504	7
968	Threshold displacement energy in GaN: Ab initio molecular dynamics study. <b>2009</b> , 105, 123527	70
967	Ni@B80: A single molecular magnetic switch. <b>2009</b> , 95, 133115	19
966	Metallization induced by nitrogen atom adsorption on silicon nanofilms and nanowires. <b>2009</b> , 94, 113101	4
965	Magnetism of hexagonal closed-packed Ni nanowires from ab initio calculations. <b>2009</b> , 105, 103906	6
964	Effects of the orbital self-interaction in both strongly and weakly correlated systems. <b>2009</b> , 130, 054903	20
963	Electronic effects on melting: comparison of aluminum cluster anions and cations. <b>2009</b> , 131, 044307	47
962	Glissile dislocations with transient cores in silicon. <b>2009</b> , 103, 065505	36
961	Surface-decorated silicon nanowires: a route to high-ZT thermoelectrics. <b>2009</b> , 103, 055502	132
960	Structural instability of single wall carbon nanotube edges from first principles. <b>2009</b> , 95, 153104	5
959	An understanding and implications of the coverage of surface free sites in heterogeneous catalysis. <b>2009</b> , 130, 224701	20
958	Automatic detection of parallel applications computation phases. <b>2009</b> ,	39
957	Adverse effects of asymmetric contacts on single molecule conductances of HS(CH <sub>2</sub> ) <sub>n</sub> COOH in nanoelectrical junctions. <b>2009</b> , 20, 125203	34
956	Electrostatic condition for the termination of the opposite face of the slab in density functional theory simulations of semiconductor surfaces. <b>2009</b> , 105, 113701	40
955	Effects of spin-orbit coupling on the conductance of molecules contacted with gold electrodes. <i>Journal of Physics Condensed Matter</i> , <b>2009</b> , 21, 335301	1.8 6

954	Core structure of screw dislocations in hcp Ti: an ab initio DFT study. <b>2009</b> , 100, 329-332		15
953	X-ray absorption near edge structure/electron energy loss near edge structure calculation using the supercell orthogonalized linear combination of atomic orbitals method. <i>Journal of Physics Condensed Matter</i> , <b>2009</b> , 21, 104202	1.8	21
952	Computer Simulation Methods for Defect Configurations and Nanoscale Structures. <b>2009</b> , 107-127		
951	Dependence of Conductance of Corrugated Graphene Quantum Dot on Geometrical Features. <b>2009</b> , 52, 960-964		2
950	Molecular Beam Epitaxy study of a common a-GeO <sub>2</sub> interfacial passivation layer for Ge- and GaAs-based MOS heterostructures. <b>2009</b> , 1155, 1		2
949	A dramatic effect of water on single molecule conductance.. <b>2009</b> , 1154, 1		
948	How silylene defects at (100) Si surfaces can account for the anomalous features observed via x-ray photoelectron spectroscopy. <b>2009</b> , 130, 184702		6
947	The spin filter effect of iron-cyclopentadienyl multidecker clusters: the role of the electrode band structure and the coupling strength. <b>2009</b> , 20, 385401		32
946	Controlling electronic structures by irradiation in single-walled SiC nanotubes: a first-principles molecular dynamics study. <b>2009</b> , 20, 075708		20
945	Negative differential resistance behaviour in OPE molecular devices with semiconductor electrodes. <b>2009</b> , 42, 175104		10
944	First-principles Study of Electron Transport Through Oligoacenes. <b>2009</b> , 22, 7-12		4
943	Effects of hydrogen impurities on Ge 1k Mn x semiconductors. <b>2009</b> , 87, 47001		3
942	Atomistic modeling of amorphous silicon carbide: an approximate first-principles study in constrained solution space. <i>Journal of Physics Condensed Matter</i> , <b>2009</b> , 21, 265801	1.8	5
941	Ab initio molecular dynamics simulation of a pressure induced zinc blende to rocksalt phase transition in SiC. <i>Journal of Physics Condensed Matter</i> , <b>2009</b> , 21, 245801	1.8	8
940	First-principles calculations: half-metallic Au-V(Cr) quantum wires as spin filters. <b>2009</b> , 20, 095201		25
939	Magnetic states for V(001) bcc surface: An ab initio study. <b>2009</b> , 105, 07C301		1
938	Effects of hydrogen impurities on Mn <sub>x</sub> Si <sub>1-x</sub> semiconductors. <b>2009</b> , 105, 07C512		1
937	Spin-filtering effect in the transport through a single-molecule magnet Mn <sub>12</sub> bridged between metallic electrodes. <b>2009</b> , 105, 07E309		22

936	Numerical evaluation of electron repulsion integrals for pseudoatomic orbitals and their derivatives. <b>2009</b> , 130, 124114		12
935	Partitioning scheme for density functional calculations of extended systems. <b>2009</b> , 130, 144104		15
934	Transitions between semiconductor and metal induced by mixed deformation in carbon nanotube devices. <b>2009</b> , 94, 183506		27
933	First-principles study of structure and quantum transport properties of C20 fullerene. <b>2009</b> , 131, 024311		53
932	Electronic structure of poly(azomethine) thin films. <b>2009</b> , 131, 024901		5
931	Efficient organometallic spin filter based on Europium-cyclooctatetraene wire. <b>2009</b> , 131, 104704		40
930	Toward accurate reaction energetics for molecular line growth at surface: Quantum Monte Carlo and density functional theory calculations. <b>2009</b> , 131, 214708		15
929	Spin-polarized transport and the electronic structure of the metallic antiferromagnet Fe(thiazole)(2)Cl(2). <b>2009</b> , 131, 204702		14
928	The size effects of electrodes in molecular devices: an ab initio study on the transport properties of C(60). <i>Journal of Physics Condensed Matter</i> , <b>2009</b> , 21, 145502	1.8	15
927	Including dispersion interactions in the ONETEP program for linear-scaling density functional theory calculations. <b>2009</b> , 465, 669-683		33
926	ACTION-DERIVED AB INITIO MOLECULAR DYNAMICS. <b>2009</b> , 01, 469-482		4
925	Structure and Stability of Hydrogen Clathrates of Ammonia Borane. <b>2009</b> , 1216, 1		1
924	Electronic transport calculations for rough interfaces in Al, Cu, Ag, and Au. <i>Journal of Physics Condensed Matter</i> , <b>2009</b> , 21, 315001	1.8	5
923	Balancing Intermolecular and Molecule-Substrate Interactions in Supramolecular Assemblies. <b>2009</b> , 19, 259-264		55
922	Customized Electronic Coupling in Self-Assembled Donor-Acceptor Nanostructures. <b>2009</b> , 19, 3567-3573		50
921	Conformational Tuning of Magnetic Interactions in Metal-DNA Complexes. <b>2009</b> , 121, 5077-5081		27
920	Thermally stable solids based on endohedrally doped ZnS clusters. <b>2009</b> , 15, 5138-44		16
919	Is it possible to dope single-walled carbon nanotubes and graphene with sulfur?. <b>2009</b> , 10, 715-22		199

918	Modelling the two-dimensional polymerization of 1,4-benzene diboronic acid on a Ag surface. <b>2009</b> , 10, 2480-5	14
917	Theoretical study on hydrogen-bond effects in IR spectra of high- and low-temperature phases of nitric acid dihydrate. <b>2009</b> , 10, 3229-38	2
916	Syntheses, Structure and Photoluminescence Properties of Silver(I) Complexes with Naphthalene Iminoimides. <b>2009</b> , 2009, 2817-2824	8
915	Aten--an application for the creation, editing, and visualization of coordinates for glasses, liquids, crystals, and molecules. <b>2010</b> , 31, 639-48	38
914	Conformational tuning of magnetic interactions in metal-DNA complexes. <b>2009</b> , 48, 4977-81	60
913	First-principles identification of two- and four-membered-ring hybrid structures of silica nanorings. <b>2009</b> , 373, 4376-4380	1
912	Simple and accurate model for voltage-dependent resistance of metallic carbon nanotube interconnects: An ab initio study. <b>2009</b> , 374, 297-304	22
911	Ab initio calculations of NO <sub>2</sub> and SO <sub>2</sub> chemisorption onto non-polar ZnO surfaces. <b>2009</b> , 142, 179-184	70
910	An effective Hamiltonian for sulfur adsorption at Au(100) surface. <b>2009</b> , 603, 1150-1155	6
909	Density functional study of the adsorption of aspirin on the hydroxylated (0 0 1) $\beta$ -quartz surface. <b>2009</b> , 603, 2502-2506	27
908	On the hydrogen addition to graphene. <b>2009</b> , 907, 93-103	55
907	Collagen and component polypeptides: Low frequency and amide vibrations. <b>2009</b> , 355, 141-148	20
906	Solvothermal synthesis of MnF <sub>2</sub> nanocrystals and the first-principle study of its electronic structure. <b>2009</b> , 70, 609-615	11
905	A web-deployed interface for performing ab initio molecular dynamics, optimization, and electronic structure in Fireball. <b>2009</b> , 180, 418-426	3
904	Optimal Fourier filtering of a function that is strictly confined within a sphere. <b>2009</b> , 180, 1134-1136	1
903	QWalk: A quantum Monte Carlo program for electronic structure. <b>2009</b> , 228, 3390-3404	123
902	The Electronic and Magnetic Properties of a Few Transition-Metal Clusters. <b>2009</b> , 20, 355-364	15
901	Two-center overlap integrals, three dimensional adaptive integration, and prolate ellipsoidal coordinates. <b>2009</b> , 46, 97-107	3

900	First-principles calculation on the conductance of ruthenium-quasi cumulene-ruthenium molecular junctions. <b>2009</b> , 4, 398-402	
899	Studies on structural defects in carbon nanotubes. <b>2009</b> , 4, 297-306	12
898	Electronic properties of boron nanotubes with axial strain. <b>2009</b> , 4, 383-388	5
897	Exploring at nanoscale from first principles. <b>2009</b> , 4, 256-268	
896	Magnetism in carbon nanoscrolls: Quasi-half-metals and half-metals in pristine hydrocarbons. <b>2009</b> , 2, 844-850	10
895	Study of the adsorption step in the oxidative dehydrogenation of propane on V(2)O(5) (001) using calculations of electronic density of states. <b>2009</b> , 1, 308-14	4
894	Uniform linear chains of group 11 atoms: do they have a bias towards a Peierls distortion?. <b>2009</b> , 123, 85-92	3
893	Vacancies in magnesium silicide: Stoichiometric vacancies preferred?. <b>2009</b> , 246, 1587-1589	9
892	Lattice vibrations in graphene nanoribbons from density functional theory. <b>2009</b> , 246, 2577-2580	5
891	Prochiral guanine adsorption on Au111: an entropy-stabilized intermixed guanine-quartet chiral structure. <b>2009</b> , 5, 1952-6	58
890	Reconstruction of the (011) surface on $\beta$ -quartz: A semiclassical Ab initio molecular dynamics study. <b>2009</b> , 109, 50-64	16
889	1D lead iodide crystals encapsulated within single walled carbon nanotubes. <b>2009</b> , 109, 171-175	4
888	Theoretical investigation of the stability, electronic and magnetic properties of thiolated single-wall carbon nanotubes. <b>2009</b> , 109, 772-781	26
887	A theoretical and experimental study on manipulating the structure and properties of carbon nanotubes using substitutional dopants. <b>2009</b> , 109, 97-118	64
886	First-principles study of the structure and the electronic structure of yttrium aluminum garnet Y3Al5O12. <b>2009</b> , 109, 1991-1998	36
885	Observation of the smallest metal nanotube with a square cross-section. <b>2009</b> , 4, 149-52	46
884	Theoretical demonstration of symmetric curves in asymmetric molecular junction of monothiolate alkane. <b>2009</b> , 40, 773-775	2
883	Improved calculation of Si sputter yield via first principles derived interatomic potential. <b>2009</b> , 267, 1061-1066	7

882	1,3-diphenyltriazene as a possible optical molecular switch: A first-principles study. <b>2009</b> , 404, 3462-3465	14
881	Fe/ZnSe/Fe junctions: Interplay between interface structure and tunneling magnetoresistance. <b>2009</b> , 404, 2841-2844	2
880	The sign preference in sulfuric acid nucleation. <b>2009</b> , 901, 169-173	27
879	Crystal structure and hydroxyl group vibrational frequencies of phyllosilicates by DFT methods. <b>2009</b> , 912, 82-87	23
878	Application of time-dependent density-functional theory to molecules and nanostructures. <b>2009</b> , 914, 115-129	12
877	Modeling complexes of NH <sub>3</sub> molecules confined in C <sub>60</sub> fullerene. <b>2009</b> , 913, 54-57	25
876	Metal-containing amorphous carbon (a-C:Ag) and AlN (AlN:Ag) metallo-dielectric nanocomposites. <b>2009</b> , 518, 1508-1511	16
875	Electronic and optical properties of single-layered silicon sheets. <b>2009</b> , 149, 153-155	35
874	Tuning the magnetic and transport properties of boron-nitride nanotubes via oxygen-doping. <b>2009</b> , 149, 486-490	33
873	Microscopic origin of current degradation of fully-sealed carbon-nanotube field emission display. <b>2009</b> , 149, 670-672	9
872	Electronic transport properties of a diarylethene-based molecular switch with single-walled carbon nanotube electrodes: The effect of chirality. <b>2009</b> , 149, 928-931	28
871	Mn clusterisation in. <b>2009</b> , 149, 1368-1372	
870	Lattice dynamical properties of , , and compounds. <b>2009</b> , 149, 1843-1848	28
869	Early stages of vanadium deposition on Si(1 1 1)-7 × 7. <b>2009</b> , 603, 835-838	
868	Adsorption of Si on Ag(001) from ab initio study. <b>2009</b> , 603, 2021-2029	6
867	Computational study of the surface properties of aluminum nanoparticles. <b>2009</b> , 603, 2042-2046	52
866	A DFT study of the transition metal promotion effect on ethylene chemisorption on Co(0 0 0 1). <b>2009</b> , 603, 2752-2758	17
865	First principles calculations of the adsorption and diffusion of Y on the Si(001)-c(4×4) surface. <b>2009</b> , 603, 3414-3419	4




864	A first-principles study of the structural and electronic properties of III $\nu$ /thermal oxide interfaces. <b>2009</b> , 86, 1747-1750	14
863	Carbon nanotubes interacting with vitamins: First principles calculations. <b>2009</b> , 40, 877-879	20
862	Properties of bcc metals by tight-binding total energy simulations. <b>2009</b> , 163, 8-16	4
861	Simultaneous adsorption of Cd <sup>2+</sup> and phenol on modified N-doped carbon nanotubes: experimental and DFT studies. <b>2009</b> , 334, 124-31	55
860	Efficient O(N) integration for all-electron electronic structure calculation using numeric basis functions. <b>2009</b> , 228, 8367-8379	34 <sup>2</sup>
859	First-principles study of the switching characteristics of the phenoxynaphthacenequinone-based optical molecular switch with carbon nanotube electrodes. <b>2009</b> , 41, 474-478	11
858	Effects of hydrogen atoms on the electronic structure and transport properties of silicon monatomic chains. <b>2009</b> , 41, 865-869	3
857	Ab initio investigation of the possibility of formation of endohedral complexes between H <sub>2</sub> molecules and B-, N- and Si-doped C <sub>60</sub> fullerenes. <b>2009</b> , 41, 1406-1409	24
856	First-principles simulation of the encapsulation of molecular hydrogen in C <sub>120</sub> nanocapsules. <b>2009</b> , 41, 1433-1438	24
855	Interaction of alkanethiols with single-walled carbon nanotubes: First-principles calculations. <b>2009</b> , 41, 1696-1700	9
854	A self-consistent and environment-dependent Hamiltonian for large-scale simulations of complex nanostructures. <b>2009</b> , 42, 1-16	16
853	Effect of torsion angle on electronic transport through different anchoring groups in molecular junction. <b>2009</b> , 373, 3787-3794	14
852	Quantum chemical studies of spin crossover polymers: Periodic DFT approach. <b>2009</b> , 28, 1955-1957	11
851	CrAs(001)/AlAs(001) heterogeneous junction as a spin current diode predicted by first-principles calculations. <b>2009</b> , 321, 312-315	8
850	Investigation of pressure effects on. <b>2009</b> , 321, 2575-2577	3
849	Ab initio approach to the effect of Fe on the diffusion in hcp Zr II: The energy barriers. <b>2009</b> , 392, 100-104	23
848	Influence of elastic properties on superplasticity in doped yttria-stabilized zirconia. <b>2009</b> , 70, 15-19	10
847	A first-principles study on the structural, elastic, vibrational, and thermodynamical properties of BaX (X=S, Se, and Te). <b>2009</b> , 70, 371-378	36

846	Linear-scaling density-functional theory with tens of thousands of atoms: Expanding the scope and scale of calculations with ONETEP. <b>2009</b> , 180, 1041-1053	110
845	Fitting sparse multidimensional data with low-dimensional terms. <b>2009</b> , 180, 2002-2012	43
844	Plato: A localised orbital based density functional theory code. <b>2009</b> , 180, 2616-2621	25
843	Theoretical prediction of ring structures for ZnS quantum dots. <b>2009</b> , 467, 365-368	8
842	Interplay of covalent bonding and correlation effects at molecule-metal contacts. <b>2009</b> , 478, 191-194	2
841	Theoretical investigations of the experimentally observed selectivity of a cobalt imprinted polymer. <b>2009</b> , 25, 558-62	14
840	First-principles study of the switching characteristics of the 15,16-dinitrile DDP/CPD-based optical molecular switch with carbon nanotube electrodes. <b>2009</b> , 9, 1213-1216	10
839	Ab initio study of the structural stability of fcc-CH <sub>x</sub> phases. <b>2009</b> , 47, 1637-1642	4
838	Enhanced spin-valve effect in magnetically doped carbon nanotubes. <b>2009</b> , 47, 2533-2537	18
837	Geometrical indications of adsorbed hydrogen atoms on graphite producing star and ellipsoidal like features in scanning tunneling microscopy images: Ab initio study. <b>2009</b> , 47, 3306-3312	25
836	Ab initio modeling of glass corrosion: Hydroxylation and chemisorption of oxalic acid at diopside and hercynite surfaces. <b>2009</b> , 57, 5303-5313	5
835	Deduction of a three-phase model for the (BB)R30°-Cu <sub>2</sub> Si/Cu(111) surface alloy. <b>2009</b> , 256, 636-639	5
834	Topics in the theory of amorphous materials. <b>2009</b> , 68, 1-21	96
833	Defect-induced ferromagnetism in fullerenes. <b>2009</b> , 68, 529-535	33
832	First-principles study for transport properties of defective carbon nanotubes with oxygen adsorption. <b>2009</b> , 69, 375-382	10
831	A practical first-principles band-theory approach to the study of correlated materials. <b>2009</b> , 71, 139-183	40
830	Electronic properties and quantum transport in Graphene-based nanostructures. <b>2009</b> , 72, 1-24	144
829	First-principles calculations of circular dichroism of ligand-protected gold nanoparticles. <b>2009</b> , 52, 179-182	18

828	Density functional study of the cysteine adsorption on Au nanoclusters. <b>2009</b> , 52, 123-126		11
827	Theoretical study of the coadsorption of CO and O <sub>2</sub> on doped cationic gold clusters MA <sub>n</sub> + (M = Ti, Fe, Au; n = 1, 6, 7). <b>2009</b> , 52, 135-138		13
826	Structural and electronic properties of PtPd and PtNi nanoalloys. <b>2009</b> , 52, 127-130		28
825	Atomic-scale X-ray structural analysis of self-assembled monolayers on Silicon. <b>2009</b> , 167, 33-39		5
824	Transport properties of copper phthalocyanine based organic electronic devices. <b>2009</b> , 180, 117-134		18
823	Divacancies in graphitic boron nitride sheets. <b>2009</b> , 86, 46002		41
822	Transport properties of T-shaped and crossed junctions based on graphene nanoribbons. <b>2009</b> , 20, 055202		31
821	Chemical functionalization of graphene. <i>Journal of Physics Condensed Matter</i> , <b>2009</b> , 21, 344205	1.8	286
820	Ab initio studies of electronic properties of bare GaN(0001) surface. <b>2009</b> , 106, 054901		37
819	Tuning the electronic structure of graphene by molecular charge transfer: a computational study. <b>2009</b> , 4, 855-60		162
818	Improving gas sensing properties of graphene by introducing dopants and defects: a first-principles study. <b>2009</b> , 20, 185504		732
817	First-principles study of quantum tunneling from nanostructures: Current in a single-walled carbon nanotube electron source. <b>2009</b> , 80,		16
816	Carbon nanotubes on partially depassivated n-doped Si(100)(2x1):H substrates. <b>2009</b> , 80,		8
815	Quantum Monte Carlo calculations of the energy-level alignment at hybrid interfaces: Role of many-body effects. <b>2009</b> , 79,		12
814	Structural and electronic properties of poly(3-hexylthiophene) π-stacked crystals. <b>2009</b> , 79,		52
813	A first-principle study of the structural and lattice dynamical properties of CaX (X=S, Se, and Te). <b>2009</b> , 29, 187-203		13
812	A first-principles study of π-conjugated thiol phenothiazine derivatives adsorbed on Au(111) surface. <b>2009</b> , 7,		
811	Excited states of biological chromophores studied using many-body perturbation theory: Effects of resonant-antiresonant coupling and dynamical screening. <b>2009</b> , 80,		80

810	Silicon nanocrystallites in a SiO <sub>2</sub> matrix: Role of disorder and size. <b>2009</b> , 79,	55
809	Exploring the tilt-angle dependence of electron tunneling across molecular junctions of self-assembled alkanethiols. <b>2009</b> , 3, 2073-80	49
808	A mixed-valent pentanuclear Cu(II)(4)Cu(I) compound containing a radical-anion ligand. <b>2009</b> , 48, 10643-51	17
807	Efficient spin transitions in inelastic electron tunneling spectroscopy. <b>2009</b> , 103, 176601	98
806	Metallic and ferromagnetic edges in molybdenum disulfide nanoribbons. <b>2009</b> , 20, 325703	164
805	Passing current through touching molecules. <b>2009</b> , 103, 206803	95
804	Oxygen Adsorption on CdSe Surfaces: Case Study of Asymmetric Anisotropic Growth through ab Initio Computations. <b>2009</b> , 113, 1863-1871	14
803	Length dependence of conductance in aromatic single-molecule junctions. <b>2009</b> , 9, 3949-53	135
802	How Potentials of Zero Charge and Potentials for Water Oxidation to OH(ads) on Pt(111) Electrodes Vary With Coverage. <b>2009</b> , 113, 17484-17492	50
801	Conformational dynamics of metal-binding domains in Wilson disease protein: molecular insights into selective copper transfer. <b>2009</b> , 48, 5849-63	21
800	Encapsulation of the Fullerene Derivative [6,6]-Phenyl-C61-Butyric Acid Methyl Ester inside Micellar Structures. <b>2009</b> , 113, 13677-13682	9
799	Breaking mechanism of single molecular junctions formed by octanedithiol molecules and Au electrodes. <b>2009</b> , 131, 16418-22	20
798	Electron doping and magnetic moment formation in N- and C-doped MgO. <b>2009</b> , 94, 252505	70
797	Electronic structures of silicon nanoribbons. <b>2009</b> , 95, 083115	259
796	Ab initio study of a TiO <sub>2</sub> /LaAlO <sub>3</sub> heterostructure. <b>2009</b> , 167, 012060	3
795	Effect of the surrounding oxide on the photoabsorption spectra of Si nanocrystals. <b>2009</b> , 79,	20
794	Disorder enhances thermoelectric figure of merit in armchair graphane nanoribbons. <b>2009</b> , 95, 192114	114
793	Effect of oxygen on single-wall silicon carbide nanotubes studied by first-principles calculations. <b>2009</b> , 80,	30

792	A first-principles divide-and-conquer approach for electronic structure of large systems and its application to graphene nanoribbons. <i>Journal of Physics Condensed Matter</i> , <b>2009</b> , 21, 235501	1.8	20
791	Ab initio study of the elastic properties of single and polycrystal TiO(2), ZrO(2) and HfO(2) in the cotunnite structure. <i>Journal of Physics Condensed Matter</i> , <b>2009</b> , 21, 015501	1.8	49
790	Modifications in graphene electron states due to a deposited lattice of Au nanoparticles: Density functional calculations. <b>2009</b> , 80,		17
789	Ab initio study of confinement and surface effects in hexagonal AlN nanotubes. <b>2009</b> , 45, 305-309		20
788	Structure, thermodynamic and transport properties of CaAl <sub>2</sub> Si <sub>2</sub> O <sub>8</sub> liquid. Part I: Molecular dynamics simulations. <b>2009</b> , 73, 6918-6936		36
787	Structural characteristics of Cu <sub>x</sub> Zr <sub>100-x</sub> metallic glasses by Molecular Dynamics Simulations. <b>2009</b> , 483, 658-661		39
786	Optical properties and critical points in ordered Be <sub>x</sub> Zn <sub>1-x</sub> Se alloys. <b>2009</b> , 480, 717-722		7
785	Exploiting the Variational Principle. <b>2003</b> , 79-95		1
784	Controlled Electron Transport in Single Molecules. <b>2004</b> , 13-20		
783	Electron Transport in Carbon Nanotube Shuttles and Telescopes. <b>2004</b> , 89-94		
782	Theory of Adsorption and Manipulation of C <sub>60</sub> on the Si(001) Surface. <b>2007</b> , 601-618		
781	Recent Computational Developments in Quantum Conductance and Field Emission of Carbon Nanotubes. <b>2007</b> , 31-35		
780	Electronic Transport in Nanowires at Different Length Scales. <b>2008</b> , 404-420		
779	Enhancing effect of dimethylamine in sulfuric acid nucleation in the presence of water  computational study.		
778	References. 153-161		
777	Stability and magnetism of fcc single-crystal nickel nanowires by first principles calculations. <b>2011</b> , 60, 037504		
776	Electronic and optical properties of zigzag graphene nanoribbon with Stone-Wales defect. <b>2011</b> , 60, 017102		5
775	Selection Rule of Inelastic Electron Tunneling Spectroscopy Probed by Isotope Substitution. <b>2011</b> , 32, 374-380		

- 774 The Phonon Percolation Scheme for Alloys: Extension to the Entire Lattice Dynamics and Pressure Dependence. **2011**, 50, 05FE02
- 773 Ab initio Phonons in Kesterite and Stannite-Type  $\text{Cu}_2\text{ZnSnSe}_4$ . **2011**, 50, 05FE04
- 772 An Introduction to Linear-Scaling Ab Initio Calculations. **2012**, 1-35
- 771 New insights into nocturnal nucleation. **2012**, 1-35 1
- 770 The surface effect on the p-type conductivity of Li-doped ZnO film. **2012**, 61, 157301 1
- 769 Kohn-Sham LCAO Method for Periodic Systems. **2012**, 251-301
- 768 High-Performance Computing for Theoretical Study of Nanoscale and Molecular Interconnects. **2012**, 78-97
- 767 Interface Electronic Differences Between Epitaxial Graphene Systems Grown on the Si and the C Face of SiC. **2012**, 51-56
- 766 Nanoparticle morphology and aspect ratio effects in Ag/PVDF nanocomposites. **2012**, 9-19
- 765 First-Principles Simulations of Electronic Transport in Dangling-Bond Wires. **2013**, 137-147
- 764 Adsorption of Benzene on 4H-SiC (0001) Surface: First Principles Calculations. **2012**, 122, 1049-1051
- 763 First-principles calculations of the electron transport through  $\text{Si}_4$  cluster. **2013**, 62, 140504 4
- 762 Electronic structure and spin-polarization of boron-nitride nanoflake. **2013**, 62, 057302 1
- 761 First-principles calculations of the electronic transport in Au-Si-Au junctions. **2013**, 62, 107401 5
- 760 Reinforcement Application. **2013**, 205-226
- 759 Novel Electronic Properties of Silicon Nanostructures. **2014**, 31-63
- 758 RESEARCH NOTES AND DEVELOPMENTS IN MATERIALS CHEMISTRY AND PHYSICS. **2013**,
- 757 Predictive Engineering of Semiconductor-Oxide Interfaces. **2014**, 45-61

- 756 First-Principles Modelling of Vibrational Modes in Defective Oxides and Correlation with IETS. **2014**, 35-60
- 755 Theoretical Methods. **2014**, 9-34
- 754 Magnetic Properties of Gated Graphene Nanostructures. **2014**, 111-144 0
- 753 Manifestations of the Quantum Confinement Effect in the Phototransport Properties of Ensembles of Semiconductor Quantum Dots. **2014**, 335-408 1
- 752 Born-Oppenheimer Approximation. **2015**, 3-11
- 751 Molecular dynamics studies of interaction between hydrogen and carbon nano-carriers. **2014**, 3, 329-344 3
- 750 Structure and Vibrational Spectra?. **2015**,
- 749 Electronic Structure of Sodium Thiogermanate. **2015**, 05, 31-39 1
- 748 Molecular Dynamics Simulation: From *Ab Initio* to *Coarse Grained* **2015**, 1-61
- 747 First-Principles Methods. **2015**, 39-61
- 746 First-Principles Simulations of Bulk Crystal and Nanolayer Properties. **2015**, 113-214
- 745 Boron and Metal Diborides. **2015**, 217-251
- 744 Mechanochemistry at Silicon Surfaces. **2015**, 247-274
- 743 Material modeling for large scale and complex nanostructures: A semi-empirical Hamiltonian method. **2015**, 64, 187302
- 742 Introduction to first-principles simulation package ABACUS based on systematically improvable atomic orbitals. **2015**, 64, 187104 2
- 741 Electronic transport properties of oligo phenylene ethynylene molecule modified by the (CH<sub>3</sub>)<sub>2</sub> and (NH<sub>2</sub>)<sub>2</sub> groups. **2016**, 65, 073102
- 740 Encyclopedia of Nanotechnology. **2016**, 1084-1101
- 739 Atomic scale piezoelectricity and giant piezoelectric resistance effect in gallium nitride tunnel junctions under compressive strain. **2016**, 65, 107701 1

- 738 Exact Exchange Scheme in the Parallel r-Space Implementation of the Kohn-Sham Realization of the Density Functional Theory. **2016**, 130, 1236-1238
- 737 Morphology and Stability of the Diamond/BN (001) and (111) Interfaces Based on Ab Initio Studies. **2016**, 130, 1220-1223
- 736 Ab Initio Calculations and Kinetic Process Simulations of Nitrogen-Doped Graphene. **2017**, 61-69
- 735 Silicene Nanoribbons and Nanopores for Nanoelectronic Devices and Applications. **2017**, 39-69
- 734 Effect of Boron (Nitrogen)-Divacancy Complex Defects on the Electronic Properties of Graphene Nanoribbon. **2017**, 06, 19-25 1
- 733 Design and electronic transport properties of organic thiophene molecular rectifier with the graphene electrodes. **2017**, 66, 098501 4
- 732 Band Engineering of Dangling-Bond Wires on the Si(100)H Surface. **2017**, 83-93
- 731 The Study of Magnetic Molecules Containing Cr<sup>9</sup> Chromium-Based Rings within Density Functional Theory. **2017**, 131, 961-963
- 730 Sensing properties of doped zigzag CNT and BNNT towards CO: A first principles study. **2017**,
- 729 Electronic and Optical Properties of Heterostructures based on Indium Chalcogenides. **2017**, 132, 319-321
- 728 Silicon nanoparticles with zinblend structure. **2017**, 247-270
- 727 Real-time time dependent density functional theory with numerical atomic orbital basis set: methodology and applications. **2018**, 67, 120201 2
- 726 Hidrojen depolama malzemeleri için MgH<sub>2</sub>'nin yapısal ve elektronik özellikleri. 451-461 0
- 725 Relationship between the Geometrical Structure of a Tip Apex of a Scanning Probe Microscope and the Intensity of the Signal in Inelastic Electron Tunneling Spectroscopy. **2018**, 61, 651-656
- 724 Nanoscale fracture of defective popgraphene monolayer.
- 723 Thermal spin transport properties in a hybrid structure of single-walled carbon nanotubes and zigzag-edge boron nitride nanoribbons. **2019**, 68, 057301 0
- 722 Surface Adsorption Model Calculation Database and Its Application to Activity Prediction of Heterogeneous Catalysts. **2019**, 18, 251-253 1
- 721 Importance of Atomic-Like Basis Set Optimization for DFT Modelling of Nanomaterials. **2019**, 11, 44-50 0



- 720 Sensing Volatile Organic Compounds by Phthalocyanines with Metal Centers: Exploring the Mechanism with Measurements and Modelling. **2019**, 33-45
- 719 Characterizing modulated structures with first-principles calculations: a unified superspace scheme of ordering in mullite. **2019**, 75, 260-272 1
- 718 Density functional theory calculations of the radial breathing mode in graphene quantum dots. **2019**, 13, 1 1
- 717 Electronic Properties of Hydrogenated Hexagonal Boron Nitride (h-BN): DFT Study. **2019**, 4, 72-79 1
- 716 Dynamical continuum simulation of condensed matter from first principles. **2019**, 1,
- 715 Control of charge state of dopants in insulating crystals: Case study of Ti-doped sapphire. **2020**, 2, 2
- 714 Influence of He<sup>+</sup>-ion beam induced effect on ultrafast quantum spin-state switching dynamics in exchange bias CoMn FM/AFM systems. **2020**, 34, 2050294
- 713 New RTDs with enhanced operation based on black phosphorus-graphene heterostructures and a semianalytical vdW tunneling model. **2021**, 20, 70-80
- 712 Humidity Sensing Properties of Halogenated Graphene: A Comparison of Fluorinated Graphene and Chlorinated Graphene. **2020**, 0
- 711 Quantum transport simulations of a monolayer all-inorganic perovskite transistor. **2020**, 53, 455104 2
- 710 Naphthylene-1D and 2D carbon allotropes based on the fusion of phenyl- and naphthyl-like groups. **2020**, 4, 1
- 709 Effect of Atomic Interface on Tunnel Barrier in Ferroelectric HfO<sub>2</sub> Tunnel Junctions. **2020**,
- 708 Computational Auxiliary for the Progress of Sodium-Ion Solid-State Electrolytes. **2021**, 7
- 707 Adsorption and diffusion of magnesium on nitrogen-doped MoC monolayer. **2021**, 27, 334
- 706 Adsorption characteristics of citric acid on Fe<sub>3</sub>O<sub>4</sub> (001), (011), and (111) surfaces. **2021**, 27, 332
- 705 From Zero- to One-Dimensional, Opportunities and Caveats of Hybrid Iodobismuthates for Optoelectronic Applications. **2021**, 60, 17123-17131 5
- 704 Metallic core [Ni<sub>6</sub>IIICr<sub>III</sub>] as an example of centered heterometallic rings displaying quantum effects. **2021**, 544, 168701
- 703 Simulation and fabrication of an ammonia gas sensor based on PEDOT:PSS. **2021**, ahead-of-print, 0

702	Phase transition impact on electronic and optical properties of Fe-doped MoSe <sub>2</sub> monolayer via N <sub>2</sub> O adsorption. <b>2021</b> , 160, 107083	2
701	ab initio study of Mn-based systems for oxidative degradation. <b>2021</b> , 291, 132706	0
700	Tuning the Rashba spin splitting in Janus MoSeTe and WSeTe van der Waals heterostructures by vertical strain. <b>2021</b> , 544, 168721	1
699	DFT-Based Studies on Carbon Adsorption on the wz-GaN Surfaces and the Influence of Point Defects on the Stability of the Diamond-GaN Interfaces. <b>2021</b> , 14,	
698	ZnS/ZnO nanosheets obtained by thermal treatment of ZnS/ethylenediamine as a Z-scheme photocatalyst for H <sub>2</sub> generation and Cr(VI) reduction. <b>2021</b> , 151773	5
697	First-Principles Modeling of Interface Effects in Oxides. <b>2020</b> , 1119-1149	
696	First-Principles Simulations of Bulk Crystal and Nanolayer Properties. <b>2020</b> , 123-219	
695	Conformation and Quantum-Interference-Enhanced Thermoelectric Properties of Diphenyl Diketopyrrolopyrrole Derivatives. <b>2021</b> , 6, 470-476	3
694	The nature of the hydrogen interaction on the unreconstructed platinum (110) surface: ab-initio study. <b>2021</b> , 96, 025707	2
693	First-Principles Investigation of Photoisomeric Switching of Vibrational Heat Current across Molecular Junctions. <b>2020</b> , 14,	0
692	Nanowire reconstruction under external magnetic fields. <b>2020</b> , 153, 244106	
691	The Effects of Boron-Doping on the Electronic Properties of Blue Phosphorene. <b>2021</b> , 10, 41-47	
690	Predicting activity and activation factor of catalytic reactions using machine learning. <b>2022</b> , 217-229	
689	Interference effects in one-dimensional moiré crystals. <b>2022</b> , 186, 416-422	0
688	First-principles calculations of nickel, cadmium, and lead nanoclusters adsorption on single-wall (10,0) boron-nitride nanotube. <b>2022</b> , 573, 151547	0
687	Janus In <sub>2</sub> SeTe for photovoltaic device applications from first-principles study. <b>2022</b> , 553, 111384	1
686	Tunneling FET based on defect-free, vacancy-defected, and passivated monolayer PtSe <sub>2</sub> channel: A first principles study. <b>2022</b> , 138, 106258	0
685	Electronic and Optical Properties of Carbon Nanotubes Directed to Their Applications in Solar Cells. <b>2020</b> , 341-349	3

- 684 First principles study of optical properties of 2D PtP2 and PtAs2 monolayers. **2020**,
- 683 Study of effect of hydrostatic pressure on structural, electronic and magnetic properties of In<sub>0.75</sub>Cr<sub>0.25</sub>P. **2020**,
- 682 Inter-Layer interaction induced electronic properties in partially oxidized transition metal dichalcogenides. **2020**,
- 681 An unintrusive approach to the computation of derivatives: Applications in nanoscale thermal transport. **2020**, 181-217
- 680 Open-Science Platform for Computational Materials Science: AiiDA and the Materials Cloud. **2020**, 1813-1835 1
- 679 2D and 1D heterostructures based on ZT-MoSe<sub>2</sub> and PdSe<sub>2</sub>. **2020**,
- 678 C<sub>20</sub> FULLERENE CCl<sub>3</sub> ADSORPSİYONUNUN TEORİK OLARAK İNCELENMESİ **2020**, 8, 141-149
- 677 Theoretical study on strain-controllable gradient Schottky barrier of dumbbell-shape graphene nanoribbon for highly sensitive strain sensors. **2021**,
- 676 All-electron real-time and imaginary-time time-dependent density functional theory within a numeric atom-centered basis function framework. **2021**, 155, 154801 3
- 675 An Ab Initio Study of Lithization of Two-Dimensional Silicon-Carbon Anode Material for Lithium-Ion Batteries. **2021**, 14, 1
- 674 Inq, a Modern GPU-Accelerated Computational Framework for (Time-Dependent) Density Functional Theory. **2021**, 1
- 673 Freezing the conductance of platinum(II) complexes by quantum interference effect. **2021**, 1
- 672 Validity of the on-site spin-orbit coupling approximation. **2021**, 104, 1
- 671 Ab initio simulations of black and blue phosphorene functionalised with chemical groups for biomolecule anchoring. **2021**, 27, 349
- 670 Enhanced thermoelectric properties in Sb/Ge core/shell nanowires through vacancy modulation. **2021**, 11, 21921
- 669 High-Performance Computing for Theoretical Study of Nanoscale and Molecular Interconnects. 513-532
- 668 Single Molecule Vibrational Spectroscopy of Interfacial Water. **2018**, 73-82
- 667 Frontiers in surface analysis: Experiments and modeling. **2007**, 391-414

666	Properties of ferroelectric ultrathin films from first principles. <b>2006</b> , 137-145		
665	Ab initio investigation of topological phase transitions induced by pressure in trilayer van der Waals structures: the example of h-BN/SnTe/h-BN. <i>Journal of Physics Condensed Matter</i> , <b>2021</b> , 33, 025003	1.8	0
664	Ab-initio quantum transport with a basis of unit-cell restricted Bloch functions and the NEGF formalism. <b>2020</b> ,		
663	Femtosecond fragmentation of CS <sub>2</sub> after sulfur 1s ionization: interplay between Auger cascade decay, charge delocalization, and nuclear motion. <b>2020</b> , 53, 244007		0
662	Engineering ferromagnetic lines in graphene by local oxidation and hydrogenation using nanoscale lithography. <b>2021</b> , 54, 074002		0
661	Imaginary-time time-dependent density functional theory for periodic systems. <i>Journal of Physics Condensed Matter</i> , <b>2020</b> ,	1.8	1
660	Spin transport through metal-dichalcogenides layers: a study from first-principles calculations. <i>Journal of Physics Condensed Matter</i> , <b>2021</b> , 33, 065505	1.8	1
659	The transport properties of Cl-decorated arsenene controlled by electric field. <b>2020</b> , 2, 045001		
658	Atomistic Asymmetric Effect on the Performance of HfO <sub>2</sub> -Based Ferroelectric Tunnel Junctions. <b>2020</b> , 14,		0
657	Prediction of formation energies of large-scale disordered systems via active-learning-based executions of ab initio local-energy calculations: A case study on a Fe random grain boundary model with millions of atoms. <b>2020</b> , 4,		1
656	Parallel Implementation of Large-Scale Linear Scaling Density Functional Theory Calculations With Numerical Atomic Orbitals in HONPAS. <b>2020</b> , 8, 589910		0
655	Computational Modeling of Environmental Co-exposure on Oil-Derived Hydrocarbon Overload by Using Substrate-Specific Transport Protein (TodX) with Graphene Nanostructures. <b>2020</b> , 20, 2308-2325		1
654	. <b>2021</b> , 1-1		0
653	Experimental and density functional theory computational studies on highly sensitive ethanol gas sensor based on Au-decorated ZnO nanoparticles. <b>2022</b> , 741, 139014		0
652	High-performance sub-10 nm monolayer black arsenic phosphorus tunneling transistors. <b>2022</b> , 576, 151705		3
651	Empathes: A general code for nudged elastic band transition states search. <b>2022</b> , 271, 108224		0
650	Coherent spin transport in a natural metalloprotein molecule. <b>2021</b> , 130, 184301		1
649	Predicting Finite-Bias Tunneling Current Properties from Zero-Bias Features: The Frontier Orbital Bias Dependence at an Exemplar Case of DNA Nucleotides in a Nanogap. <b>2021</b> , 11,		1

- 648 Ligand Impact of Silicanes as Anode Materials for Lithium-Ion Batteries. 0
- 647 Capturing the Rotation of One Molecular Crank by Single-Molecule Conductance. **2021**, 21, 9729-9735 1
- 646 Large-area nanoengineering of graphene corrugations for visible-frequency graphene plasmons. **2021**, 3 3
- 645 Electron-phonon coupling of Fe-atom electron states on MgO/Ag(100). **2021**, 104, 0
- 644 Externally controlled and switchable two-dimensional electron gas at the Rashba interface between ferroelectrics and heavy d metals. **2021**, 3, 0
- 643 Multi-wavelength emission through self-induced defects in GaZnO microrods. **2021**, 162693
- 642 Two-dimensional metal carbides for electro- and photocatalytic CO<sub>2</sub> reduction: Review. **2021**, 55, 101814 2
- 641 Site-dependent spin-polarized tunneling via hybrid interface states on molecule/ferromagnet surface. **2021**, 115071
- 640 Electronic structure and charge compensation in Au<sub>x</sub>Ag<sub>25-x</sub>SR181 (x = 0, 12, 13, 25), AuAg<sub>12</sub>Au<sub>12</sub>SR181 and AgAu<sub>12</sub>Ag<sub>12</sub>SR181 clusters. **2021**, 23, 1
- 639 Exotic Spintronic Properties of Transition-Metal Monolayers on Graphyne. 2100287
- 638 Numerical integration of quantum time evolution in a curved manifold. **2021**, 3, 0
- 637 IrRep: symmetry eigenvalues and irreducible representations of ab initio band structures. **2021**, 108226 1
- 636 Robustness of the chiral-icosahedral golden shell I-Au in multi-shell structures. **2021**, 155, 204307 0
- 635 Substitution effect on electronic and optical properties of Tetraphenyldipyranilidene; A theoretical study. **2021**, 162, 110504 0
- 634 Magnetically Recyclable FeO@TMU-32 Metal-Organic Framework Photocatalyst for Tetracycline Degradation Under Visible Light. **2021**, 60, 17997-18005 1
- 633 Theoretical Design of thermal spin molecular logic gates by using a combinational molecular junction. 0
- 632 Laser desorption/ionization time-of-flight mass spectrometry of yttrium(III) chloride.
- 631 Three-zone model for Ti, Al co-doped ZnO films deposited by magnetron sputtering. **2021**, 28, 101595

630	Light-activated interlayer contraction in two-dimensional perovskites for high-efficiency solar cells. <b>2021</b> ,	15
629	C-doping Anisotropy Effects on Borophene Electronic Transport. <i>Journal of Physics Condensed Matter</i> , <b>2021</b> ,	1.8
628	Bias-induced reconstruction of hybrid interface states in magnetic molecular junctions.	0
627	Twist-Dependent Electron Charge Transfer and Transport in Phosphorene-Graphene Heterobilayers. <b>2021</b> , 125, 25886-25897	
626	Calculation of Energy Level Alignment and Interface Electronic Structure in Molecular Junctions beyond DFT. <b>2021</b> , 125, 25825-25831	1
625	On the doping of the Ga <sub>12</sub> As <sub>12</sub> cluster with groups p and d atomic impurities. <b>2021</b> , 140, 1	0
624	Edge-Mediated Annihilation of Vacancy Clusters in Monolayer Molybdenum Diselenide (MoSe <sub>2</sub> ) under Electron Beam Irradiation. <b>2021</b> , e2105194	0
623	Using static linear response theory to describe field emission field enhancement and a field-induced insulator-conductor transition. <b>2021</b> , 39, 060601	1
622	Cysteine Adsorption on Twisted-Bilayer Graphene.	1
621	CO Adsorption Enhanced by Tuning the Layer Charge in a Clay Mineral. <b>2021</b> ,	6
620	Piezoelectricity of Janus BiTeX (X = Cl, Br, I) Monolayer: A First-Principles Study. <b>2021</b> , 1-5	0
619	Mixed magnetic edge states in graphene quantum dots. <b>2022</b> , 5, 014001	
618	Edge engineered Graphene Nanoribbons as Nanoscale Interconnect: DFT Analysis. <b>2022</b> , 1-1	4
617	A ReaxFF potential for Al - ZnO systems.	
616	The effects of Co/Ni-vacancy complex defects on the electronic and transport properties of armchair silicene nanoribbon. <b>2022</b> , 96, 1	
615	Band-engineered Zn <sub>2</sub> TiO <sub>4</sub> nanowires for hydrogen generation from water using visible light: A first-principles study. <b>2022</b> , 12, 015201	0
614	Large-Scale First-Principles Calculation Technique for Nanoarchitectonics: Local Orbital and Linear-Scaling DFT Methods with the CONQUEST Code. <b>2022</b> , 303-317	
613	Reversible surface reconstruction of Na <sub>3</sub> NiCO <sub>3</sub> PO <sub>4</sub> : A battery type electrode for pseudocapacitor applications. <b>2022</b> , 520, 230903	0

612	Magnetically responsive hydrophobic pockets for on/off drug release. <b>2022</b> , 23, 100702	1
611	Spin transport properties of boron nitride nanotubes: A DFT study. <b>2022</b> , 30, e00636	
610	Attached two folded graphene nanoribbons as sensitive gas sensor. <b>2022</b> , 628, 413630	
609	Group three nitride clusters as promising components for nanoelectronics. <b>2022</b> , 23, 100751	1
608	An ab initio study of the interaction of graphene and silicene with one-, two-, and three-layer planar silicon carbide. <b>2022</b> , 138, 115120	0
607	Electronic and transport property of two-dimensional boron phosphide sheet.. <b>2021</b> , 112, 108117	0
606	N-Doped Zigzag Graphene Nanoribbons For Nanoscale Interconnects. <b>2020</b> ,	1
605	High Throughput Investigation of an Emergent and Naturally Abundant 2D Material: Clinocllore.	0
604	Ultra Small Fluorine Carbon Nanoclusters.	1
603	Unconventional Metallicity in Graphene Nanoribbons with Armchair Edges. 2100392	0
602	Single-molecule magnet Mn <sub>12</sub> on GaAs-supported graphene: Gate field effects from first principles. <b>2022</b> , 105,	1
601	Modeling of the Point Defect Migration across the AlN/GaN Interfaces-Ab Initio Study.. <b>2022</b> , 15,	1
600	Impact of Mn- and Fe-Doping on Electronic and Magnetic Properties of MoX <sub>2</sub> (X = S, Se) Monolayer. <b>2022</b> , 1-8	3
599	The Impact of the Surface Modification on Tin-Doped Indium Oxide Nanocomposite Properties.. <b>2022</b> , 12,	0
598	Current spin polarization of a platform molecule with compression effect.	0
597	Atomistic insight into the formation dynamics of charged point defects: A classical molecular dynamics study of F <sup>+</sup> -centers in NaCl. <b>2022</b> , 6,	0
596	Effect of crystallographic orientations on transport properties of methylthiol-terminated permethyloligosilane molecular junction.	0
595	Unraveling Heat Transport and Dissipation in Suspended MoSe from Bulk to Monolayer.. <b>2022</b> , e2108352	1

594	Polaron Induced Conductance Switching in Conjugated Oligophenylene: A First-Principles Analysis.. <b>2022,</b>	
593	Controlled growth of Gd-Pt surface alloys on Pt(111). <b>2022,</b> 105,	
592	Spin-orbit induced equilibrium spin currents in materials. <b>2022,</b> 105,	
591	Metal-Organic Frameworks for NO Adsorption and Their Applications in Separation, Sensing, Catalysis, and Biology.. <b>2022,</b> e2105484	3
590	Ultrafast nonadiabatic dynamics of EDNA upon low energy proton irradiation. <b>2022,</b> 120, 043702	0
589	Spin Current Sensing for Selective Detection of Explosive Molecules.. <b>2022,</b>	0
588	Exceptional phonon point versus free phonon coupling in ZnBeTe under pressure: an experimental and ab initio Raman study.. <b>2022,</b> 12, 753	1
587	Tin carbide monolayers decorated with alkali metal atoms for hydrogen storage. <b>2022,</b>	1
586	Phase Properties of Different HfO <sub>2</sub> Polymorphs: A DFT-Based Study. <b>2022,</b> 12, 90	2
585	Band gap, effective masses, and energy level alignment of 2D and 3D halide perovskites and heterostructures using DFT-1/2. <b>2022,</b> 6,	3
584	Forces from Stochastic Density Functional Theory under Nonorthogonal Atom-Centered Basis Sets.. <b>2022,</b>	0
583	Adsorption of diatomic gas molecules on transition-metal-decorated GeC monolayers. 1	0
582	Effects of non-essential protein on D-glucose to control diabetes: DFT approach.. <b>2022,</b> 28, 42	0
581	Computation and Simulation. <b>2022,</b> 355-395	
580	Janus 2H-VSSe monolayer: Two-dimensional valleytronic semiconductor with nonvolatile valley polarization.. <i>Journal of Physics Condensed Matter,</i> <b>2022,</b>	1.8
579	Strain and electric field-modulated indirect-to-direct band transition of monolayer GaInS <sub>2</sub> . <b>2022,</b> 21, 227	0
578	Thermoelectric Enhancement in Single Organic Radical Molecules.. <b>2022,</b>	2
577	First-Principles Molecular Dynamics Insight into the Atomic Level Degradation Pathway of Phosphorene.. <b>2022,</b> 7, 696-704	3



- 576 Effect of Impurity Adsorption on the Electronic and Transport Properties of Graphene Nanogaps.. **2022**, 15,
- 575 Structural and electronic properties of nonconventional  $\beta$ -graphyne nanocarbons. **2022**, 6, 0
- 574 Electronic, Optical, and Magnetic Properties of Doped Triangular MoS<sub>2</sub> Quantum Dots: A Density Functional Theory Approach. 2100509 2
- 573 Spin-dependent electron transport analysis of benzyl alcohol and p-cresol based single molecular junction: a DFT-NEGF approach. **2022**, 33, 9490
- 572 Molecular Modelling of Optical Biosensor Phosphorene-Thioguanine for Optimal Drug Delivery in Leukemia Treatment.. **2022**, 14, 1
- 571 Effect of Substitution of Pb for Mg on the Photovoltaic Properties of Methyl-Ammonium Lead Iodide Perovskites. 2100509 0
- 570 The vibrational and thermodynamic properties of hydrogen adsorbed on the Pt(100) surface: a theoretical study. **2022**, 97, 035701
- 569 Tracking photocarrier-enhanced electron-phonon coupling in nonequilibrium. **2022**, 7, 1
- 568 The special case of the spectral emission of a Tb<sup>3+</sup> mono metal complex.. **2021**,
- 567 Spin transport characteristics and photoelectric properties of magnetic semiconductor NiBr<sub>2</sub> monolayer. **2022**,
- 566 Insights into Effects of Metal Cations on the Adsorption of Benzotriazole on Halloysite Nanotubes: An Experimental and DFT Study. **2022**, 126, 2920-2929 0
- 565 Field-Effect Transistor Based on MoSi<sub>2</sub>N<sub>4</sub> and WSi<sub>2</sub>N<sub>4</sub> Monolayers Under Biaxial Strain: A Computational Study of the Electronic Properties. **2022**, 69, 863-869 3
- 564 Density functional theory study of the selective oxidation of 5-Hydroxymethylfurfural (HMF) to 5-Hydroxymethyl-2-furancarboxylic acid (HMFA) on the Silver oxide surface (001). **2022**, 519, 112117 0
- 563 The electronic structure and chemical bonding in MgPbP<sub>2</sub>.
- 562 Computational Methods for Charge Density Waves in 2D Materials.. **2022**, 12, 0
- 561 Multi-pathway mechanism of polydopamine film formation at vertically aligned diamondised boron-doped carbon nanowalls. **2022**, 409, 140000 0
- 560 A new salt-inclusion compound, |Ag<sub>4</sub>Br|[B<sub>7</sub>O<sub>12</sub>], with a novel type of the porous double-layered borate anion and strong anharmonicity of the guest sublattice. **2022**, 125, 106831 1
- 559 Structural, elastic, and optical properties of silicon carbide nanotubes using DFT. **2022**, 344, 114672 0

- 558 Ionically selective carbon nanotubes for hydrogen electrocatalysis in the hydrogen-bromine redox flow battery. **2022**, 24, 100937
- 557 Electron and proton conducting framework organic salt single crystals. **2022**, 308, 122903
- 556 First-principles insight into the interfacial properties of epitaxial Bi<sub>2</sub>O<sub>2</sub>X (X = S, Se, Te) on SrTiO<sub>3</sub> substrates. **2022**, 163, 110601 2
- 555 Molecular dynamics study of phonon and thermoelectric properties of hydrogen-passivated silicon carbide nanotubes. **2022**, 198, 110899 0
- 554 Physisorption and chemisorption of CO on Fe-MIL-88B derivatives: Impact of the functional groups on the electronic properties and adsorption tendency - A theoretical investigation.. **2022**, 112, 108124 1
- 553 Efficient and accurate atomistic modeling of dopant migration using deep neural network. **2022**, 143, 106513 0
- 552 Methylphenidate adsorption onto graphene derivatives: theory and experiment. 2
- 551 Real-space density kernel method for Kohn-Sham density functional theory calculations at high temperature.. **2022**, 156, 094105
- 550 Ab initio DFT simulation of electronic and magnetic properties of Ti and FeTi clusters.. **2022**, 28, 56
- 549 Molecular design of benzo[c][1,2,5]thiadiazole or thieno[3,4-d]pyridazine-based auxiliary acceptors through different anchoring groups in D-π-A framework: A DFT/TD-DFT study.. **2022**, 113, 108148 0
- 548 Precise control of single-phenanthrene junction conductance. **2022**, 21, 71 1
- 547 Structural and bonding properties of small hydrocarbons inside Ca(squarate)-metal organic framework: ab-initio study.
- 546 Structural analysis based on unsupervised learning: Search for a characteristic low-dimensional space by local structures in atomistic simulations. **2022**, 105, 0
- 545 Band offset and leakage current in fluorine doped Si/HfO<sub>2</sub>/SiO<sub>2</sub> gate stack of metal oxide semiconductor field effect transistors: An ab initio investigation. **2022**, 746, 139116
- 544 The influence of tungsten oxide concentration on a carbon surface for capacitance improvement in energy storage devices: A combined experimental and theoretical study. **2022**, 164, 110610 0
- 543 Magnetic Interactions Between Radical Pairs in Chiral Graphene Nanoribbons.. **2021**, 6
- 542 A new aggregation induced emission enhancement (AIEE) dye which self-assembles to panchromatic fluorescent flowers and has application in sensing dichromate ions.. **2022**, 0
- 541 DFT-NEGF simulation study of Co<sub>2</sub>FeAl-MgO-Co<sub>2</sub>FeAl magnetic tunnel junctions under biaxial strain. **2022**, 1-1

540	Biosensing Properties of Zinc Oxide Nanoribbons toward Creatine: A First-Principles Study. <b>2022</b> , 1-1	1
539	Theoretical studies of gas-phase decomposition of single-source precursors. <b>2022</b> , 123-161	
538	Na Adsorption on Para Boron-Doped AGNR for Sodium-Ion Batteries (SIBs): A First Principles Analysis. <b>2022</b> , 51, 2095-2106	0
537	Density Functional Tight Binding Calculations for Probing Electronic-Excited States of Large Systems. <b>2022</b> , 45-79	
536	Enhanced emission directivity from asymmetrically strained colloidal quantum dots.. <b>2022</b> , 8, eabl8219	2
535	X-ray Induced Fragmentation of Protonated Cystine.. <b>2022</b> ,	0
534	Investigation of Atomic Layer Futuristic Memory Devices of Binary Chalcogenides WX <sub>2</sub> (X = S and Se): First-Principles Study. <b>2022</b> ,	
533	Giant tunneling magnetoresistance and electroresistance in Hg <sub>2</sub> Se <sub>3</sub> -based van der Waals multiferroic tunnel junctions. <b>2022</b> , 105,	0
532	NH <sub>3</sub> capture and detection by metal-decorated germanene: a DFT study. 1	4
531	Competition between Ta-Ta and Te-Te bonding leading to the commensurate charge density wave in TaTe <sub>4</sub> . <b>2022</b> , 105,	0
530	From 2D to 3D: Bridging Self-Assembled Monolayers to a Substrate-Induced Polymorph in a Molecular Semiconductor. <b>2022</b> , 34, 2238-2248	2
529	Strain modulating electronic band gaps and SQ efficiencies of semiconductor 2D PdQ (Q = S, Se) monolayer.. <b>2022</b> , 12, 2964	1
528	Prospect of DFT Utilization in Polymer-Graphene Composites for Electromagnetic Interference Shielding Application: A Review.. <b>2022</b> , 14,	0
527	Crystal Structures and Fluorescent Properties of Two Distinct 2D Ag(I)/Cd(II) Coordination Polymers Based on Isonicotinic Acid Derivative and Dipyridyl Coligand. <b>2022</b> , 48, 118-126	
526	Moiré-induced topology and flat bands in twisted bilayer WSe <sub>2</sub> : A first-principles study. <b>2022</b> , 105,	1
525	Mechanism of length-induced magnetism in polyacene molecules. <b>2022</b> , 105,	0
524	SAFETY PROFILE AND PREVENTION OF COGNITIVE DEFICIT IN ALZHEIMER'S DISEASE MODEL OF GRAPHENE FAMILY NANOMATERIALS, TUCUMA OIL (Astrocaryum vulgare) AND ITS SYNERGISMS. <b>2022</b> , 10, 267-303	
523	Electronic properties of germanene on pristine and defective MoS <sub>2</sub> : A first-principles study. <b>2022</b> , 105,	

- 522 Mode-locked erbium-doped fiber laser based on a mechanically exfoliated ReS<sub>2</sub> saturable absorber onto D-shaped optical fiber. **2022**, 12, 1657 3
- 521 Interlayer hybridization in graphene quasicrystal and other bilayer graphene systems. **2022**, 105, 0
- 520 Atomically Sharp Lateral Superlattice Heterojunctions Built-in Nitrogen-doped Nanoporous Graphene.. **2022**, e2110099 1
- 519 Numerical analysis of electronic state of CNT/BNNT heterojunction. **2022**, 2207, 012038
- 518 DFT+ $\sigma$  method for electron correlation effects at transition metal surfaces. **2022**, 105, 1
- 517 Moiré-induced band-gap opening in one-dimensional superlattices of carbon nanotubes on hexagonal boron nitride. **2022**, 105, 0
- 516 Effective Inhibition of Carbon Steel Corrosion by Waterborne Polyurethane Based on N-tert-Butyl Diethanolamine in 2M HCl: Experimental and Computational Findings. **2022**, 15, 1939 0
- 515 Scaling Behavior of Magnetoresistance with the Layer Number in CrI<sub>3</sub> Magnetic Tunnel Junctions. **2022**, 17, 2
- 514 Thermoelectric properties of organic thin films enhanced by  $\pi$ -stacking. **2022**, 4, 024002 1
- 513 Localized  $\pi$ -Surface States on 2D Molybdenum Disulfide from Carbene-Functionalization as a Qubit Design Strategy. 0
- 512 Arsenene nanotubes adsorbed with various non-metallic atoms: Chemical bonding, odd-even effect, and electronic transport. **2022**, 207217 1
- 511 Low-resistance contact in MoSe<sub>2</sub> -based solid-state thermionic devices. **2022**, 105, 0
- 510 Computational Modeling on Binding Interactions of Cyclodextrins with the Human Multidrug Resistance P-glycoprotein Toward Efficient Drug-Delivery System Applications.. **2022**, 1
- 509 The structure and properties of a carbon nanotube (7, 7) with a vacancy defect. **2022**, 12, 32-36 0
- 508 The Li stance on precipitation in Al $\pi$ -based alloys: an investigation by X-ray Raman spectroscopy. **2022**, 57, 6157-6166 1
- 507  $\pi$ -magnetism and spin-dependent transport in boron pair doped armchair graphene nanoribbons. **2022**, 120, 132406 2
- 506 Degradation Chemistry and Kinetic Stabilization of Magnetic CrI<sub>3</sub>.. **2022**, 3
- 505 Gate- versus defect-induced voltage drop and negative differential resistance in vertical graphene heterostructures. **2022**, 8, 0

504	Electron Transport in N-functionalised Armchair Graphene Nanoribbons: Computational Insight. <b>2022</b> , 1221, 012053	
503	Multiferroic van der Waals heterostructure FeCl <sub>2</sub> /Sc <sub>2</sub> CO <sub>2</sub> : Nonvolatile electrically switchable electronic and spintronic properties. <b>2022</b> , 105,	3
502	Tuning the size of skyrmion by strain at the Co/Pt interfaces.. <b>2022</b> , 25, 104039	1
501	Unveiling Unintentional Fluorine Doping in TMDs During the Reactive Ion Etching: Root Cause Analysis, Physical Insights, and Solution. <b>2022</b> , 69, 1956-1963	
500	Ab Initio Simulation of Amorphous Materials. <b>2022</b> , 30-59	0
499	Enhancement in magnetization of two-dimensional cobalt telluride and its magnetic field-assisted photocatalytic activity. <b>2022</b> , 128, 1	2
498	Giant Tunneling Electroresistance Induced by Interfacial Doping in Pt/BaTiO <sub>3</sub> /Pt Ferroelectric Tunnel Junctions. <b>2022</b> , 17,	2
497	Enhanced reversible hydrogen storage performance of light metal-decorated boron-doped siligene: A DFT study. <b>2022</b> ,	0
496	Shape-Controlled Photochemical Synthesis of Noble Metal Nanocrystals Based on Reduced Graphene Oxide.. <b>2022</b> ,	0
495	Bidirectional Hydrogen Electrocatalysis on Epitaxial Graphene.. <b>2022</b> , 7, 13221-13227	1
494	Prediction, determination and stability of the mixed NaBr <sub>2</sub> Br crystal structure. <b>2022</b> , 123124	
493	Theoretical investigation on un-doped and doped TiO <sub>2</sub> for solar cell application. <b>2022</b> , 97, 055806	
492	Spin transport properties and nanodevice simulations of NiI <sub>2</sub> monolayer. <b>2022</b> , 115262	1
491	Carbon Vacancy Assisted Contact Resistance Engineering in Graphene FETs. <b>2022</b> , 69, 2066-2073	4
490	A DFT theoretical and experimental study about tetracycline adsorption onto magnetic graphene oxide. <b>2022</b> , 353, 118837	3
489	Insight into structural, electronic, and chemical bonding properties of PEO-PEG-LiI polymer electrolyte: A first-principles investigation. <b>2022</b> , 1211, 113667	
488	The piezoelectricity of 2D Janus ZnBrI: Multiscale prediction. <b>2022</b> , 794, 139506	0
487	Ferromagnetism in V and Cr doped ScN diluted magnetic semiconductor in B3 phase: A DFT study. <b>2022</b> , 347, 114724	

- 486 A DFT investigation on the mechanical and structural properties of halogen- and metal-adsorbed silicene nanosheets. **2022**, 283, 126029 1
- 485 Hollow structures of Ti O systems with m  $\mathbb{Z}$ n: A density functional theoretical study. **2022**, 164, 110646 0
- 484 Interaction of primary precipitates in reduced  $\alpha$ -activation ferritic/martensitic steel F82H with hydrogen atoms: Atomistic calculation based on the density functional theory. **2022**, 31, 101157
- 483 Transverse electronic transport through nucleobase-pairs of a DNA wire. **2022**, 24, 100834 1
- 482 Investigation of electronic stabilities and properties of Mn-doped Janus WSSe monolayer. **2022**, 31, e00677 0
- 481 Study of the structural stability and electronic properties of the C-doped boron nanomaterials. **2022**, 350, 114773
- 480 Effect of oxygen impurities on the electronic and mechanical properties of penta-graphene sheet. 1-8
- 479 The spin-dependent properties of silicon carbide/graphene nanoribbons junctions with vacancy defects.. **2021**, 11, 23879
- 478 Half-metallic porphyrin-based molecular junctions for spintronic applications. **2021**, 104, 1
- 477 Complex band structure with non-orthogonal basis set: analytical properties and implementation in the SIESTA code. *Journal of Physics Condensed Matter*, **2021**, 1.8 0
- 476 Emergence and Tuning of Multiple Flat Bands in Twisted Bilayer  $\mathbb{E}$ Graphyne.. **2021**, 12, 12283-12291 0
- 475 Theoretical study of electronic properties and chemical stability of cubic phase zirconia nanowires. **2021**, 96, 125879 0
- 474 Band Structure and Energy Level Alignment of Chiral Graphene Nanoribbons on Silver Surfaces.. **2021**, 11, 1
- 473 Semiconductor nanochannels in metallic carbon nanotubes by thermomechanical chirality alteration.. **2021**, 374, 1616-1620 8
- 472 Graphene and NTCDAs adsorbed on Ag(111): Temperature-dependent binding distance and phonon coupling to the interface state. **2021**, 104, 1
- 471 Magnetically Collected Platinum/Nickel Alloy Nanoparticles as Catalysts for Hydrogen Evolution. **2021**, 4, 12957-12965 2
- 470 Single cycloparaphenylene molecule devices: Achieving large conductance modulation via tuning radial  $\mathbb{E}$ conjugation.. **2021**, 7, eabk3095 2
- 469 Modeling charge transport in gold nanogranular films. **2021**, 5,

- 468 Optical property analysis of transition and alkaline metal doped MoS<sub>2</sub> bulk layers for photo-sensor applications. **2021**,
- 467 New van der Waals Heterostructures Based on Borophene and Rhenium Sulfide/Selenide for Photovoltaics: An Ab Initio Study. **2021**, 11, 11636
- 466 A 3D Lead Iodide Hybrid Based on a 2D Perovskite Subnetwork. **2021**, 11, 1570 1
- 465 Structural and Electronic Property Analysis of Transition and Alkaline Metal Doped MoS<sub>2</sub> Bulk Layers for Photo-Sensor Applications. **2021**,
- 464 Mixing ReaxFF parameters for transition metal oxides using force-matching method.. **2021**, 28, 8
- 463 Quantum transport simulation of the two-dimensional GaSb transistors. **2021**, 42, 122001 0
- 462 Distinguishing between Similar Mini-proteins with Single-Molecule Nanopore Sensing: A Computational Study. 1
- 461 Multi-Component Self-Assembled Molecular-Electronic Films: Towards New High-Performance Thermoelectric Systems. 3
- 460 Defect-Induced Different Band Alignment and Transport of All-Phosphorene Devices from First Principles. 0
- 459 Penta-belt: a new carbon nanobelt. **2022**, 133055
- 458 Spin-Crossover in Supramolecular Iron(II)-2,6-bis(1-Pyrazol-1-yl)pyridine Complexes: Toward Spin-State Switchable Single-Molecule Junctions.. **2022**, 7, 13654-13666 0
- 457 Penta-SiCN: A Highly Auxetic Monolayer. 2
- 456 Insight into the Effect of Iodine Doping Soft Carbon and Iodine Functional Separator for Li-S Batteries. 0
- 455 Deep Potentials for Materials Science. 6
- 454 Theoretical probing the anchoring properties of BNP2 monolayer for lithium-sulfur batteries. **2022**, 153393 1
- 453 Tuning temperature-dependent of thermal conductivity and heat capacity of two-dimensional GeC compared to Graphene and Germanene: Effects of magnetic field. **2022**, 638, 413921
- 452 Structural and optical behavior of single-walled and multi-walled boron nitride nanotubes. **2022**, 1262, 133069 1
- 451 Effect of vacancy defects on electronic structure and ferromagnetism in pristine In<sub>2</sub>O<sub>3</sub> nanostructures: An experimental study and first-principles modeling. **2022**, 152, 111853

450 Chapter 4. Computer Modelling. 148-179

449 Table\_1.docx. 2020,

448 Data\_Sheet\_1.PDF. 2020,

447 Electronic Band Tuning and Multivalley Raman Scattering in Monolayer Transition Metal Dichalcogenides at High Pressures.. 2022,

3

446 Nanovectorization of Ivermectin to avoid overdose of drugs.. 2022, 1-14

445 Role of Channel Inversion in Ambient Degradation of Phosphorene FETs. 2022, 1-6

444 Excellent Optoelectronic and Thermoelectric Properties of Two-Dimensional Transition Metal Dinitride Hfn<sub>2</sub>.

443 Highly Sensitive and Low-Power Consumption Metalloporphyrin-Based Junctions for CO<sub>x</sub> Detection with Excellent Recovery.

0

442 A first principle study on spin-dependent transport properties of graphite nanostructures. 2022,

441 Spin Filtering and Negative Differential Resistance in Paqr-Zgnr Junctions.

440 Investigation of Sensing Properties of NO<sub>x</sub> Adsorbed Gas Molecules on Fe-doped MoSe<sub>2</sub> Monolayer. 2022, 1-1

0

439 Impact of Adsorption of Straight Chain Alcohol Molecules on the Optical Properties of Calcite (10.4) Surface.. 2022, 12,

438 Calculated characterisation of a sensitive gas sensor based on PEDOT:PSS.

437 Enhancing the Photocatalytic Hydrogen Evolution Performance of the CsPbI<sub>3</sub>/MoS<sub>2</sub> Heterostructure with Interfacial Defect Engineering.. 2022, 4007-4014

1

436 Insights into the NaCl-Induced Formation of Soluble Humins during Fructose Dehydration to 5-Hydroxymethylfurfural. 2022, 61, 5786-5796

2

435 Engineering the band gap of BN and BC<sub>2</sub>N nanotubes based on T-graphene sheets using a transverse electric field: Density functional theory study. 2022, 207244

0


434 Computational and performance studies of Ag<sub>2</sub>Sb<sub>2</sub>S<sub>3</sub> quantum dot-sensitised solar cells. 1-11

433 Interlaboratory Study on Sb<sub>2</sub>S<sub>3</sub> Interplay between Structure, Dielectric Function and Amorphous-to-Crystalline Phase Change for Photonics. 2022, 104377

3



- 432 On the Role of Collective Electrostatic Effects in Electronic Level Pinning and Work Function Changes by Molecular Adlayers: The Case of Partially Fluorinated DNTTs Adsorbed Flat-Lying on Various Metals and Hetero-Structures. 2200361
- 431 Magnetization in CNT induced by nitrogen doping and enhanced by transversal electric field application. 1 0
- 430 Transition Metal Atoms Anchored on CuPS3 Monolayer for Enhancing Catalytic Performance of Hydrogen Evolution Reactions. 1 0
- 429 Accurate and efficient molecular dynamics based on machine learning and non von Neumann architecture. 2022, 8, 1
- 428 Computational Design of  $\text{Bi-AsP/AsP}$  Vertical Two-Dimensional Homo Junction for Photovoltaic Applications. 2022, 12, 1662
- 427 Emergence of topological and trivial interface states in VSe2 films coupled to Bi2Se3. 2022, 105,
- 426 Application of atomic simulation for studying hydrogen embrittlement phenomena and mechanism in iron-based alloys. 2022, 1
- 425 Optoelectronic features of NbCu3Q4 (Q= S, Se) for p-type transparent conducting application: DFT and HSE06. 2022, 169297 0
- 424 Gate-Tuned Gas Molecule Sensitivity of a Two-Dimensional Semiconductor.. 2022, 2
- 423 A powerful approach to develop nitrogen-doped graphene sheets: theoretical and experimental framework. 1
- 422 The Origin of the Thermo-chromic Property Changes in Doped Vanadium Dioxide.. 2022, 0
- 421 Two orthorhombic superhard carbon allotropes: Hcc-C14 and DHcc-C20. 2022, 126, 109065 0
- 420 A DFT study of the electronic and optical properties of four 2D thin films. 2022, 286, 126158 0
- 419 Determining the diffusion behavior of point defects in zirconium by a multiscale modelling approach. 2022, 566, 153772 0
- 418 Optoelectronic and vibrational properties of chalcogenides VCu3Q4 (Q= Se, Te) for potential p-type transparent conducting materials: HSE06 approach. 2022, 312, 123190 0
- 417 Design of Molecular Positive Electronic Transition Device. 2021, 18, 1714-1723
- 416 Interface layer DFT study of first transition series XO oxides (X= Ti, Cr, Mn, Fe, Co, Ni, Cu and Zn). 2022, 0
- 415 Capacity development of Pd doped Si2BN nanotube for hydrogen storage. 2022, 0

- 414 Adsorption and sensing behaviors of SF<sub>6</sub> decomposed species on pristine and Ru/Ti-modified stanene monolayer: A first-principles study. **2022**, 115307
- 413 Ab-initio study of formamidinium lead halide (FAPbX<sub>3</sub>, X = Br, Cl) perovskite monolayers. **2022**,
- 412 Molecular rectification assisted by spin-polarized hybrid interfacial states. **2022**, 128200
- 411  **2017**, 0
- 410 Exploring the CO<sub>2</sub> conversion into hydrocarbons via a photocatalytic process onto . **2022**, 324, 124440 0
- 409 Influence of magnetite incorporation into chitosan on the adsorption of the methotrexate and in vitro cytotoxicity.. **2022**, 1
- 408 Inelastic scattering of electrons in water from first principles: cross sections and inelastic mean free path for use in Monte Carlo track-structure simulations of biological damage. **2022**, 9, 2
- 407 Vibrational Enthalpies of Solid Crystalline Materials. **2022**, 3, 319-326
- 406 Transport properties of blue phosphorene nanoribbons in the presence of pollutant molecules. **2022**, 207257
- 405 Selective and sensitive toxic gas sensors mechanism in 2D Janus MoSSe monolayer. 1
- 404 Rational Design of Dynamic Z-Scheme Heterojunction Composites for Photocatalytic Cr(VI) Reduction and H<sub>2</sub> Production: An Experimental and Computational Study.
- 403 Highly Sensitive, Selective and Low-Power Consumption MetalloporphyrinBased Junctions for Nitrogen Monoxide Detection with Excellent Recovery. 0
- 402 Photoconductance from the Bent-to-Planar Photocycle between Ground and Excited States in Single-Molecule Junctions. 1
- 401 Microstructure Evolution and Its Correlation with Performance in Nitrogen-Containing Porous Carbon Prepared by Polypyrrole Carbonization: Insights from Hybrid Calculations. **2022**, 15, 3705 0
- 400 DFT+\$U\$ within the framework of linear combination of numerical atomic orbitals. 0
- 399 Fe- and Co-based magnetic tunnel junctions with AlN and ZnO spacers. **2022**, 105,
- 398 Unveiling Temperature-Dependence Mechanisms of Perpendicular Magnetic Anisotropy at Fe / MgO Interfaces. **2022**, 17, 1
- 397 KSSOLV 2.0: An efficient MATLAB toolbox for solving the Kohn-Sham equations with plane-wave basis set. **2022**, 108424 2

- 396 Oxidation of two-dimensional electrides: Structural transition and the formation of half-metallic channels protected by oxide layers. **2022**, 105,
- 395 Synthesis and Characterization of Biotene: A New 2D Natural Oxide From Biotite. 2201667 ○
- 394 First-Principles Study of Electronic and Optical Properties of Tri-Layered van der Waals Heterostructures Based on Blue Phosphorus and Zinc Oxide. **2022**, 6, 163
- 393 Quantum hybridization negative differential resistance from non-toxic halide perovskite nanowire heterojunctions and its strain control. **2022**, 9, 1
- 392 Spin-Transport through Van der Waals Heterojunctions Based on 2D-Ferromagnet and Transition Metal Dichalcogenides: A Study from First-Principles Calculations. 2200178 ○
- 391 A DFT study of the adsorption and surface enhanced Raman spectroscopy of pyridine on Au<sub>20</sub>, Ag<sub>20</sub>, and bimetallic Ag<sub>8</sub>Au<sub>12</sub> clusters. **2022**, 115, 108234 1
- 390 First Principle Contemplation of Carbon Peapod (C<sub>20</sub>@CNT) Junction. **2021**,
- 389 Tuning the Carrier Mobility and Electronic Structure of Graphene Nanoribbons Using Stone-Wales Defects.
- 388 Computational Investigation of Magnetic Properties of (Fe)-doped-MoSe<sub>2</sub> Monolayer through Spin Angle Rotation. **2022**, 1-1
- 387 Unrevealing the interaction between O<sub>2</sub> molecules and poly(3-hexylthiophene-2,5-diyl) (P3HT). **2022**, 12, 18578-18584
- 386 Morphology-Controlling Hydrothermal Synthesis of H-Wo<sub>3</sub> for Photocatalytic Degradation of 1,2,4-Trichlorobenzene.
- 385 Predicting the Materials Properties Using a 3D Graph Neural Network With Invariant Representation. **2022**, 10, 62440-62449 ○
- 384 Prediction of Shockley-Read-Hall Centers in Strained Layer Superlattices for Mid-Wave Infrared Photodetectors.
- 383 Nonequilibrium Charge-Density-Wave Melting in 1T-TaS<sub>2</sub> Triggered by Electronic Excitation: A Real-Time Time-Dependent Density Functional Theory Study. 5711-5718 ○
- 382 Real-time first-principles calculations of ultrafast carrier dynamics of SnSe/TiO<sub>2</sub> heterojunction under Li<sup>+</sup> implantation. *Journal of Physics Condensed Matter*, 1.8
- 381 Structural and Electronic Properties of  $\beta$ -MnO<sub>2</sub> Compound Under High Pressure for Energy Storage Devices. **2022**, 12, 155-167
- 380 Recent Advances in Density Functional Theory and Molecular Dynamics Simulation of Mechanical, Interfacial, and Thermal Properties of Natural Gas Hydrates in Canada. ○
- 379 Electrical transport and NDR property on the cis-trans photo-isomerization of (1R,3S)-2,2-dimethyl-3-(2-methylprop-1-en-1-yl)cyclopropanecarboxylate as an optical molecular switch; A DFT-NEGF study. **2022**, 139818 ○

- 378 Functional Carbon and Silicon Monolayers in Biphenylene Network. 2
- 377 Novel Van Der Waals Heterostructures Based on Borophene, Graphene-like GaN and ZnO for Nanoelectronics: A First Principles Study. **2022**, 15, 4084 0
- 376 Layered Gallium Sulfide Optical Properties from Monolayer to CVD Crystalline Thin Films. 0
- 375 Pyrene Substituted Phthalonitrile Derivative As a Fluorescent Sensor For Detection of Fe<sup>3+</sup> Ions in Solutions. 0
- 374 Elasticity of two-dimensional ferroelectrics across their paraelectric phase transformation. **2022**, 105, 2
- 373 Crucial role of vibrational entropy in the Si(111) surface structure stability. **2022**, 105, 0
- 372 The Role of Zr on Monoclinic and Orthorhombic Hf<sub>x</sub>Zr<sub>1-x</sub>O<sub>2</sub> Systems: A First-Principles Study. **2022**, 15, 4175 1
- 371 Prominent Electrode Material for Na-, K-, and Mg-ion Batteries: 2D Sb Monolayer. 0
- 370 Dynamic control of octahedral rotation in perovskites by defect engineering. **2022**, 105, 0
- 369 Microscopic theory of ionic motion in solids. **2022**, 105, 0
- 368 TPV radical-based multifunctional molecular spintronic device: A first-principles study. **2022**, 115345 0
- 367 Multifunctional molecular spintronic device based on zigzag-edged trigonal graphene: A first-principles study. **2022**, 445, 128244 0
- 366 Amorphous BC5 from first principles calculations. **2022**, 592, 121743 1
- 365 High throughput investigation of an emergent and naturally abundant 2D material: Clinocllore. **2022**, 599, 153959 2
- 364 In Silico Study of Adsorption of Oxide Gases by Mn<sub>4</sub> (M = Be, Mg) Monolayers. 0
- 363 Tuning Electronic, Magnetic and Transport properties of SnS<sub>2</sub> 2D-material by rare-earth metal (Y) doping for sensing application: Ab-initio Modelling. **2022**, 0
- 362 Effects of 3d transition metal impurities and vacancy defects on electronic and magnetic properties of pentagonal Pd<sub>2</sub>S<sub>4</sub>: competition between exchange splitting and crystal fields. **2022**, 12, 0
- 361 Graph representation-based machine learning framework for predicting electronic band structures of quantum-confined nanostructures. 1

- 360 Magneto-optical Kerr effect in surface engineered 2D hexagonal boron nitride. **2022**, 12,
- 359 Electronic and magnetic properties of tripentaphene nanoribbons. **2022**, 6, 0
- 358 2,7- and 4,9-Dialkynyldihydropyrene Molecular Switches: Syntheses, Properties, and Charge Transport in Single-Molecule Junctions. 2
- 357 Theory of polar domains in moiré heterostructures. **2022**, 105, 0
- 356 Electronic structure and optical properties of Fe incorporated TiO<sub>2</sub> by ab initio calculations.
- 355 Understanding of the Electrochemical Behavior of Lithium at Bilayer-Patched Epitaxial Graphene/4H-SiC. **2022**, 12, 2229 1
- 354 Rational design of intrinsic and defective BGe monolayer as the anode material for Li-ion batteries. **2022**, 123418 0
- 353 The Impact of Interface Defects on Thermal Boundary Resistance at a Si|C interface.
- 352 Modulation of the Electronic and Magnetic Properties of Pyridinic N-Doped Graphene with Ni/Cr.
- 351 Magnetically textured superconductivity in elemental rhenium. **2022**, 106,
- 350 Proposal for All-Electrical Spin Manipulation and Detection for a Single Molecule on Boron-Substituted Graphene. **2022**, 129,
- 349 First-principles calculation of gate-tunable ferromagnetism in magic-angle twisted bilayer graphene under pressure. *Journal of Physics Condensed Matter*, **2022**, 34, 385501 1.8
- 348 Biogenic Synthesis and antibiofilm efficacy of iron nanoparticles via computer simulation. **2022**, 10, 1-10
- 347 Adhesion and Electron Properties of Quasi-2D Mo<sub>2</sub>C, Ti<sub>2</sub>C, and V<sub>2</sub>C MXene Flakes after Van Der Waals Adsorption of Alcohol Molecules: Influence of Humidity. **2022**, 10, 159 2
- 346 Piezoresistive Memories Based on Two-Dimensional Nano-Scale Electromechanical Systems. **2022**, 12, 968
- 345 Room-temperature logic-in-memory operations in single-metallofullerene devices. 1
- 344 Ab Initio Properties of Hybrid Cove-Edged Graphene Nanoribbons as Metallic Electrodes for Peptide Sequencing via Transverse Tunneling Current.
- 343 Adsorption of CO<sub>2</sub>, H<sub>2</sub>O, H<sub>2</sub>S, NH<sub>3</sub> and NO<sub>2</sub> on germanane nanosheet: A density functional study. **2022**, 1214, 113799 0

- 342 The thermal spin molecular logic gates modulated by light. **2022**, 560, 169680
- 341 Phenyl- and naphthyl-type heteroatom substitution blocks in naphthylene- $\pi$ A DFT study. **2022**, 213, 111578
- 340 Metallic Penta-BN<sub>2</sub> monolayer: A novel platform for non-lithium-ion batteries with high capacity and splendid cyclicality. **2022**, 149, 106849 ○
- 339 Defected NiFe layered double hydroxides on N-doped carbon nanotubes as efficient bifunctional electrocatalyst for rechargeable zinc-air batteries. **2022**, 601, 154253 1
- 338 Rational design of dynamic Z-scheme heterojunction composites for photocatalytic Cr(VI) reduction and H<sub>2</sub> production: an experimental and computational study. **2022**, 12, 100363 ○
- 337 Bilayer armchair graphene nanoribbon photodetector with Stone-Wales defect: A computational study. **2022**, 150, 106918 ○
- 336 Thermoelectric Transport in Noble Metals Monolayers: A First Principles Study. **2020**,
- 335 Tuning the Topological Band Gap of Bismuthene with Silicon-based Substrates.
- 334 Spin Transport Properties of Carbon Nanotubes by Ferromagnetic Zigzag Triangular Defects: A first-principles study. **2022**, 104074
- 333 Penta-BeP<sub>2</sub> Monolayer: A Superior Sensor for Detecting Toxic Gases in the Air with Excellent Sensitivity, Selectivity, and Reversibility. ○
- 332 Fabrication and Characterization of P3HT-Based OFETs with TPU Polymer Gate Dielectric Prepared by Electrospinning Method with Different Thicknesses.
- 331 Mechanistic study on the depolymerization of typical lignin-derived oligomers catalyzed by Pd/NbOPO<sub>4</sub>. **2022**, 528, 112500 1
- 330 PREFACE. **2003**, v-viii
- 329 Copyright Page. **2003**, iv-iv
- 328 GLOSSARY OF SYMBOLS. **2003**, ix-x
- 327 A DFT investigation on the mechanical and structural properties of silicene nanosheets under doping of transition metals. **2022**, 128, 1 ○
- 326 Adsorption of Polycyclic Aromatic Hydrocarbons and C<sub>60</sub> onto Forsterite: C-H Bond Activation by the Schottky Vacancy. **2022**, 6, 2009-2023 ○
- 325 Electronic and spintronic properties of Janus MSi<sub>2</sub>PxAsy ( M = Mo, W) monolayers. **2022**, 106, ○

- 324 Ab-initio analysis of zigzag stanene nanoribbons for lithium-ion batteries. 0
- 323 Removing the Destructive Quantum Interference in Cross Conjugation System by Structural Restraint.
- 322 Development of Classical Force Fields for Interfaces between Single Molecules and Au. **2022**, 126, 5031-5039
- 321 Deciphering the Molecular Mechanism of Substrate-Induced Assembly of Gold Nanocube Arrays toward an Accelerated Electrocatalytic Effect Employing Heterogeneous Diffusion Field Confinement. **2022**, 38, 9597-9610
- 320 An Integrated Experimental and Computational Platform to Explore Gas Hydrate Promotion, Inhibition, Rheology, and Mechanical Properties at McGill University: A Review. **2022**, 15, 5532 0
- 319 Optical spectra of zigzag graphene nanoribbons: a first-principles study. 1
- 318 Hematite Fe<sub>2</sub>O<sub>3</sub>@nitrogen-doped graphene core-shell photocatalyst for efficient cephalexin degradation under visible light irradiation. **2022**, 0
- 317 High performance computing for first-principles Kohn-Sham density functional theory towards exascale supercomputers. 0
- 316 In-situ label-free single-molecule dynamic detection of thermal-reversible reactions. **2022**, 138779
- 315 Density functional theory computation of the binding free energies between various mutations of SARS-CoV-2 RBD and human ACE2: molecular level roots of the contagiousness. **2022**, 8, e10128 1
- 314 Ultrafast modification of the electronic structure of a correlated insulator. **2022**, 4, 0
- 313 Interactions of nitric oxide molecules with pure and oxidized silver clusters Ag<sub>n</sub><sup>+</sup>/Ag<sub>n</sub>O<sup>+</sup> (n=11-13): A computational study. **2022**, 157, 074310
- 312 Polarization doping Ab initio verification of the concept: Charge conservation and nonlocality. **2022**, 132, 064301 1
- 311 Ionic forces and stress tensor in all-electron density functional theory calculations using an enriched finite-element basis. **2022**, 106, 0
- 310 Acetone and Toluene Gas Sensing by WO<sub>3</sub>: Focusing on the Selectivity from First Principle Calculations. **2022**, 12, 2696 1
- 309 Carbon-based nanostructures as a versatile platform for tunable magnetism. 5
- 308 Density Functional Theory Plus Dynamical Mean Field Theory within the Framework of Linear Combination of Numerical Atomic Orbitals: Formulation and Benchmarks.
- 307 DFT-1/2 and shell DFT-1/2 methods: electronic structure calculation for semiconductors at LDA complexity. **2022**, 34, 403001 2

- 306 Pentalene-based metallic and semiconducting nanostructures. **2022**, 115472 0
- 305 Quantum Interference-Controlled Conductance Enhancement in Stacked Graphene-like Dimers. 1
- 304 Effect of Oxygen Vacancies on Ferromagnetism of Cu-Doped BaSnO<sub>3</sub>. 0
- 303 Conductive mechanism in memristor at the thinnest limit: The case based on monolayer boron nitride. **2022**, 121, 073505 0
- 302 Water Diffusion Effects at Gold/Graphene Interfaces Supporting Surface Plasmon Polaritons. **2022**, 126, 13905-13919 0
- 301 Janus dione derivatives: Novel high-mobility hole transport materials for perovskite solar cells. **2022**, 32, 104090
- 300 Negative Differential Resistance in Spin-Crossover Molecular Devices. **2022**, 13, 7514-7520 0
- 299 Quantum Interference Controlled Spin-Polarized Electron Transmission in Graphene Nanoribbons.
- 298 Characterization and Manipulation of Intervalley Scattering Induced by an Individual Monovacancy in Graphene. **2022**, 129, 1
- 297 The effects of substrate and stacking in bilayer borophene. **2022**, 12, 1
- 296 Phonon anharmonicity in multi-layered WS<sub>2</sub> explored by first-principles and Raman studies. **2022**, 118299
- 295 Large-Scale DFT Methods for Calculations of Materials with Complex Structures. **2022**, 91, 0
- 294 Interaction of CO<sub>2</sub> with TiO<sub>2</sub>/reduced graphene oxide as superior catalysts: Dispersion-corrected density functional theory simulation. **2022**, 128, 109279
- 293 Analysis of structural, optical, electronic and transport properties in undoped, hydrogenated, doped and rotated pentahexocite systems. **2022**, 144, 115468
- 292 Determination of layer charge density in expandable phyllosilicates with alkylammonium ions: A combined experimental and theoretical assessment of the method. **2022**, 229, 106665
- 291 Effect of different dielectrics on performance of sub-5.1 nm blue phosphorus Schottky barrier field-effect transistor from quantum transport simulation. **2022**, 43, 29-35 0
- 290 Nonlinear optical properties of tin telluride topological crystalline insulator at a telecommunication wavelength. **2022**, 925, 166643 0
- 289 The Role of Cobalt Clusters (Co<sub>n</sub>, n = 1-5) Supported on Defective Graphyne for Efficient Hydrogen Adsorption: A First Principles Study. 2200354 0



288	Phosphorus and nitrogen codoped entangled carbon nanotubes forming spongy materials: Synthesis and characterization. <b>2022</b> , 129, 109317	1
287	Effect of doping on stability and electronic structure of MAPb <sub>1-x</sub> MxI <sub>3</sub> (M=Ca, Sr, Ba) perovskites. <b>2022</b> , 316, 123537	0
286	In silico study of adsorption of oxide gases by MN <sub>4</sub> (M = Be, Mg) monolayers. <b>2022</b> , 605, 154711	0
285	Metal-modified s-C <sub>3</sub> N <sub>6</sub> as a potential superior sensing medium for effective capture of toxic waste gases CO, H <sub>2</sub> S and SO <sub>2</sub> in the iron and steel industry based on first-principles investigations. <b>2022</b> , 606, 154947	1
284	Tuning the carrier mobility and electronic structure of graphene nanoribbons using Stone-Wales defects. <b>2023</b> , 201, 222-233	0
283	Experimental and theoretical investigation of structure-magnetic properties relationships in a new heteroleptic one-dimensional triple bridged azido/acetato/DMSO copper (II) coordination polymer. <b>2023</b> , 1271, 134041	0
282	Density-functional theory. <b>2023</b> , 27-65	0
281	Theoretical evaluation of charge transport properties and mobility of tetraphenyldipyranilidene derivatives in organic field-effect transistors. <b>2023</b> , 435, 114283	0
280	Effect of edge passivation on the electronic and transport properties of graphene nanogaps. <b>2022</b> ,	0
279	Tailoring optoelectronic properties and dielectric profiles of few-layers S-doped MoO <sub>3</sub> and O-doped MoS <sub>2</sub> nanosheets: a first-principles study.	0
278	Computational Simulations to Predict the Morphology of Nanostructures and Their Properties. <b>2022</b> , 267-287	0
277	Highly Interface Dependent Spin Transport In Fe-Mn(DBTAA)-Fe Single Molecule Spintronic Device.	0
276	Modulation of electronic bandgaps and subsequent implications on SQ efficiencies via strain engineering in ultrathin SnX (X = S, Se) nanowires.	0
275	Comparative Assessment of Individual and Mixture Chronic Toxicity of Glyphosate and Glufosinate Ammonium on Amphibian Tadpoles: A Multibiomarker Approach.	0
274	Spin filtering and negative differential resistance in PAQR-ZGNR junctions. <b>2023</b> , 145, 115512	0
273	Intralayer charge-transfer moiré excitons in van der Waals superlattices. <b>2022</b> , 609, 52-57	3
272	Dynamical mean-field theory for spin-dependent electron transport in spin-valve devices. <b>2022</b> , 106,	1
271	Simulation and Calculation for Predicting Structures and Properties of High-Entropy Alloys.	0

270	Resolving the Problems of the Past: Reinvestigation of the Structure of Acentric Deep UV BaB8O13 Borate. <b>2022</b> , 22, 6267-6274	0
269	Hydrogenated Carbon Monolayer in Biphenylene Network Offers a Potential Paradigm for Nanoelectronic Devices. <b>2022</b> , 126, 15491-15500	0
268	Revealing the topological phase diagram of ZrTe5 using the complex strain fields of microbubbles. <b>2022</b> , 8,	1
267	First Principle Calculation: Effect of Doped Gold Clusters with Platinum Atom on Chemical Catalysis. <b>2022</b> , 251-255	0
266	Evolution of the structural and electronic properties of AlnP13B (n = 0-3) clusters. <b>2022</b> , 141,	0
265	Impact of Carcinogenic Benzene on Electronic Properties of Mn- and Fe-Doped MoSe2 Monolayer. <b>2023</b> , 111-118	0
264	Carrier Multiplication in Transition Metal Dichalcogenides Beyond Threshold Limit. 2203400	1
263	Deterministic fabrication of 3D/2D perovskite bilayer stacks for durable and efficient solar cells. <b>2022</b> , 377, 1425-1430	17
262	Temperature-dependent micromagnetic model of the antiferromagnet Mn2Au : A multiscale approach. <b>2022</b> , 106,	1
261	Atomic-scale study of type-II Dirac semimetal PtTe2 surface. <b>2022</b> , 5, 044003	0
260	Ab Initio Analysis of Li Adsorption on Beryllium-Doped Zigzag Graphene Nanoribbon for Lithium-Ion Batteries (LIBs).	0
259	Electronic and Transport Properties of Covalent Functionalized Monolayer MoS2 by Ferrocene Derivatives.	0
258	Electronic Transport Properties and Nanodevice Designs for Monolayer MoSi2P4. <b>2022</b> , 18,	1
257	Adsorption of Selected Molecules on (TiO2)20 Nano-Clusters: A Density-Functional-Theory Study. <b>2022</b> , 2, 124-145	1
256	Engineering Transport Orbitals in Single-Molecule Junctions. <b>2022</b> , 13, 9156-9164	1
255	Healing Se Vacancies in Bi2Se3 by Ambient Gases. <b>2022</b> , 126, 16877-16884	0
254	First-Principles Investigation of the Shear Properties and Sliding Characteristics of c-ZrO2(001)/B-Al2O3(1102) Interfaces. <b>2022</b> , 12, 8869	1
253	Probing Optoelectronic and Thermoelectric Properties of Lead-Free Perovskite SnTiO3: HSE06 and Boltzmann Transport Calculations. <b>2022</b> , 12, 1317	0

252	Transferable prediction of intermolecular coupling achieved by hierarchical material representation.	0
251	Investigation of spatially localized defects in synthetic WS <sub>2</sub> monolayers. <b>2022</b> , 106,	1
250	Computation of the Binding Energies between Human ACE2 and Spike RBDs of the Original Strain, Delta and Omicron Variants of the SARS-CoV-2: A DFT Simulation Approach. 2200337	0
249	Observation of competing, correlated ground states in the flat band of rhombohedral graphite. <b>2022</b> , 8,	1
248	A comprehensive study on the processing of Co:ZnO nanostructured ceramics: Defect chemistry engineering and grain growth kinetics. <b>2022</b> ,	0
247	Hot and cold phonons in electrically biased graphene. <b>2022</b> , 106,	0
246	Almost Perfect Spin Filtering in Graphene-Based Magnetic Tunnel Junctions. <b>2022</b> , 16, 14007-14016	4
245	Experimental and theoretical study of lead sulfide nanocrystals attached to nitrogen-doped carbon nanotubes.	0
244	Vacuum barrier induced large spin polarization, giant magnetoresistance, and pure spin photocurrent in ferromagnetic zigzag graphene nanoribbons. <b>2022</b> , 55, 455302	0
243	Large Negative Poisson's Ratio and Anisotropic Mechanics in New Penta-PBN Monolayer.	0
242	Nucleobase-Bonded Graphene Nanoribbon Junctions: Electron Transport from First Principles.	0
241	Influence of CO <sub>2</sub> on Nanoconfined Water in a Clay Mineral.	2
240	Simple approach to current-induced bond weakening in ballistic conductors. <b>2022</b> , 106,	0
239	Sub-5-nm Monolayer GaSe MOSFET with Ultralow Subthreshold Swing and High On -State Current: Dielectric Layer Effects. <b>2022</b> , 18,	1
238	Non-Stoichiometric NiFeMo Solid Solutions; Tuning the Hydrogen Adsorption Energy via Molybdenum Incorporation. 2201214	0
237	Large bandgap insulating superior clay nanosheets.	1
236	Comparative assessment of individual and mixture chronic toxicity of glyphosate and glufosinate ammonium on amphibian tadpoles: A multibiomarker approach. <b>2022</b> , 309, 136554	0
235	Interactions of amine functional group with Stone-Wales defects on single-walled carbon nanotubes: A theoretical study. <b>2022</b> , 33, e00751	0

- 234 An investigation of bridge atoms effects on the thermal and electrical properties for both para and meta linked indeno-fluorene single molecules. **2022**, ○
- 233 Intermolecular coupling enhanced thermopower in single-molecule diketopyrrolopyrrole junctions. **2022**, ○
- 232 Enhancing Electron Correlation at a 3d Ferromagnetic Surface. 2205698 ○
- 231 Electronic Band Gap Tuning and Calculations of Mechanical Strength and Deformation Potential by Applying Uniaxial Strain on MX<sub>2</sub> (M = Cr, Mo, W and X = S, Se) Monolayers and Nanoribbons. ○
- 230 Controlling anisotropic properties by manipulating the orientation of chiral small molecules. 1
- 229 Electronic fingerprint mechanism of NO<sub>x</sub> sensor based on single-material SnP<sub>3</sub> logical junction. **2022**, 8, ○
- 228 Charge and Spin Current Rectification through Functionalized Boron Nitride Bilayers. **2022**, 126, 18383-18392 ○
- 227 H-Graphyne as a Promising Anode Material for Na-ion Batteries: A First-principles Study. ○
- 226 Electrical control of spin-polarized topological currents in monolayer WTe<sub>2</sub>. **2022**, 106, ○
- 225 Electric-Field Control in Phosphorene-Based Heterostructures. **2022**, 12, 3650 ○
- 224 Carrier trapping centers in a two-dimensional silica bilayer: Strongly localized shallow gap states and resonances induced by oxygen vacancies. **2022**, 106, ○
- 223 Sella, an Open-Source Automation-Friendly Molecular Saddle Point Optimizer. ○
- 222 Mechanically Tuned Thermopower of Single-Molecule Junctions. 2200700 ○
- 221 Partial Discharge Elimination in Transformer Oils by Nanofluids: From Theory to Practice. ○
- 220 Functionalized boron nitride nanotubes: First-principles calculations. **2022**, 155358 ○
- 219 Sulfur/Polyacrylonitrile-Based N-Terminated Graphene Nanoribbon Cathodes for Li-S Batteries. **2022**, 18, ○
- 218 RHOMBOHEDRAL NIOBIUM MONOXIDE: THEORETICALLY PREDICTED HIGH- PRESSURE PHASE NbO. **2022**, 63, 1639-1648 ○
- 217 Bilayer Heterostructure of Boron Nitride and Graphene for Hydrogen Storage: A First-Principles Study. **2022**, 36, 13307-13316 ○

216	A DFT study on transformation of TiN's atomic chain structure into atomic chain structures of HfN and ZrN. <b>2022</b> , 126945	0
215	Adhesion of Bis-Salphen-Based Coordination Polymers to Graphene: Insights from Free Energy Perturbation Study. <b>2022</b> , 14, 4525	0
214	Two-dimensional semiconductors of Cr <sub>3</sub> X <sub>3</sub> (X = O, S, Se, and Te) structures with large magnetic anisotropy and high Curie temperature.	0
213	Calculation of infrared spectra for adsorbed molecules from the dipole autocorrelation function. <b>2022</b> , 141,	0
212	Dynamic interplay between thionine and DNA under carbon ion irradiation:a real-time first-principles study.	0
211	Order of magnitude reduction in Joule heating of single molecular junctions between graphene electrodes. <b>2022</b> , 157, 174303	0
210	Deposition mechanism of molecular S8 on the dolomite surface. <b>2022</b> , 113930	0
209	Stability of and conduction in single-walled Si <sub>2</sub> BN nanotubes. <b>2022</b> , 6,	0
208	Thermoelectric properties and the effect of biaxial strain and external electric fields on the electronics of novel 2D Lase-like O-Pd <sub>2</sub> Q <sub>3</sub> (Q= S, Se) monolayers. <b>2022</b> , 34, 102396	0
207	Ab initio electronic stationary states for nuclear projectiles in solids. <b>2022</b> , 4,	0
206	Metal-decorated siligene as work function type sensor for NH <sub>3</sub> detection: A DFT approach. <b>2022</b> , 155541	0
205	On accelerating a multilevel correction adaptive finite element method for Kohn-Sham equation. <b>2023</b> , 472, 111674	0
204	Investigation and comparison of graphene nanoribbon and carbon nanotube based SARS-CoV-2 detection sensors: An ab initio study. <b>2023</b> , 648, 414438	1
203	Band structures and transport properties of broken-gap heterostructures: 2D C <sub>3</sub> N/MX case. <b>2023</b> , 202, 119-127	1
202	Band-gap engineering and optoelectronic properties of 2D WSi <sub>2</sub> N <sub>4</sub> nanosheets: A first principle calculations. <b>2023</b> , 146, 115530	0
201	Highly Thermoelectric Efficient Armchair Silicene Nanoribbons With Silicon Adatom Defects. <b>2022</b> , 1-7	0
200	Investigating the Infrared (IR) Absorption and Optoelectronic Properties of Mn-doped MoSe <sub>2</sub> ML by Adsorption of NO <sub>x</sub> Gas Molecules. <b>2022</b> , 1-1	0
199	The bonding of H in Zr under strain. <b>2023</b> , 573, 154124	0

- 198 Charge Transport Models for Amorphous Chalcogenides. **2023**, 1451-1489 ○
- 197 Ab initio Methods for Electronic Transport in Semiconductors and Nanostructures. **2023**, 1515-1558 ○
- 196 Ge136 type-II clathrate as precursor for the synthesis of metastable germanium polymorphs: A computational study. **2022**, 106, ○
- 195 Multifunctional 2D g-C4N3/MoS2 vdW Heterostructure-Based Nanodevices: Spin Filtering and Gas Sensing Properties. ○
- 194 How graphenic are graphynes? Evidence for low-lying correlated gapped states in graphynes. 1
- 193 Functionalized electrodes embedded in nanopores: read-out enhancement?. ○
- 192 Resonantly Enhanced Electromigration Forces for Adsorbates on Graphene. **2022**, 129, ○
- 191 Investigation of Interferences in Carbon Dioxide through Multidimensional Molecular-Frame High-Harmonic Spectroscopy. ○
- 190 Tight-Binding Models, Their Applications to Device Modeling, and Deployment to a Global Community. **2023**, 1601-1640 ○
- 189 Machine learning approach for screening alloy surfaces for stability in catalytic reaction conditions. **2023**, 5, 015002 ○
- 188 Annealing Rate as a Crucial Parameter Controlling the Photoelectrochemical Properties of AuCu Mosaic Core-Shell Nanoparticles. ○
- 187 Prediction of Diamene-Based Chemosensors. **2022**, 10, 480 ○
- 186 Two-dimensional Multi-Component Quasicrystal as Bi-functional Electrocatalysts for Alkaline Oxygen and Hydrogen Evolution Reactions. ○
- 185 Adsorption Mechanism and Optical Behaviors of Typical Volatile Organic Compounds on Pristine and Cu/Ni-Modified C 3 N Monolayer: A First-Principles Study. 2200611 ○
- 184 Bis(Vinylenedithio)-Tetrathiafulvalene-Based Coordination Networks. ○
- 183 Linking optical and electronic properties to photoresponse of heterojunctions based on titania nanotubes and chromium, molybdenum, and tungsten oxides. **2022**, 134, 113183 1
- 182 Electronic and magnetic properties of stacked graphene quantum dots. **2022**, 109550 ○
- 181 Direct calculation of the ionic mobility in superionic conductors. **2022**, 12, ○

- 180 Role of oxygen vacancy ordering on structure and reactivity of iron-doped Sr-based perovskites: A computational study. **2022**, 123734 ○
- 179 Vacancy-Mediated Anomalous Emission Characteristics of Size-Confined Semiconducting CoTe<sub>2</sub>. ○
- 178 Quantum capacitance of multi-layered  $\beta$  borophene: A DFT study. **2023**, 439, 141589 ○
- 177 Crystalline multilayer graphene nanoflakes synthesized by catalytic chemical vapor deposition using reduced nanostructured hematite as catalyst precursor and 1,2-dichlorobenzene and benzylamine mixture as carbon source. **2023**, 203, 813-826 ○
- 176 Variation in gold monolayer properties on interaction with DNA/RNA nucleobases useful for DNA sensing. **2023**, 288, 116152 ○
- 175 Thermoelectric performance and optoelectronic properties of Janus monolayer of ZrXY(X'=O, S) (Y'=S, Se). **2023**, 218, 111993 ○
- 174 Selective sensing of DNA/RNA nucleobases by metal-functionalized silicon nanowires: A DFT approach. **2023**, 36, 102529 ○
- 173 Non-invasive improvement of machining by reversible electrochemical doping: A proof of principle with computational modeling on the example of lithiation of TiO<sub>2</sub>. **2023**, 295, 127183 ○
- 172 Excellent thermoelectric properties of monolayer MoS<sub>2</sub>-MoSe<sub>2</sub> aperiodic superlattices. **2023**, 612, 155914 1
- 171 Adsorption behavior of methylene blue on graphene and hexagonal boron nitride monolayers in aqueous solution: A first-principles treatment. **2023**, 174, 111151 ○
- 170 SPIN: [S]imple [P]ython [I]pywidgets [N]otebook interface to obtain the optoelectronic properties of materials employing DFT. **2023**, 284, 108614 ○
- 169 Structural and Binding energy of Aun+1 and PtAun (n =1-9) Clusters. **2022**, 340-344 ○
- 168 Chemical properties of Bimetallic (Au+Pt) using Density Functional Theory. **2022**, 314-318 ○
- 167 Controlling the Spin States of FeTBrPP on Au(111). ○
- 166 Bimetallic NiM/C (M = Cu and Mo) Catalysts for the Hydrogen Oxidation Reaction: Deciphering the Role of Unintentional Surface Oxides in the Activity Enhancement. **2022**, 12, 15341-15351 ○
- 165 Spin-Polarized Resonant Tunneling in Antiferromagnetic Heterojunctions of Graphene Nanoribbons with 3d Adatoms. **2022**, 18, ○
- 164 Band-Gap Engineering: Lithium Effect on the Electronic Properties of Hydrogenated 3C-SiC (1 1 0) Surfaces. **2022**, 8, 247 ○
- 163 The Electronic and Structural Properties of NaxSy Nanoclusters. **2022**, 17, 429-437 ○

- 162 First-Principles Prediction of New 2D p-SiPN: A Wide Bandgap Semiconductor. **2022**, 12, 4068 ○
- 161 Theoretical Approach for Electron Dynamics and Ultrafast Spectroscopy (EDUS). ○
- 160 Phase transition hysteresis at the antiferroelectric-ferroelectric boundary in  $\text{PbZr}_{1-x}\text{Ti}_x\text{O}_3$ . **2022**, 106, ○
- 159 Large Scale Quantum Chemistry with Tensor Processing Units. ○
- 158 Transition metals doped (3,3) armchair boron nitride nanosheet as dilute magnetic semiconductor materials for the spintronic application. ○
- 157 Ab Initio Investigation of the Hydrogen Interaction on Two Dimensional Silicon Carbide. **2022**, 7, 47642-47649 ○
- 156 Stereoelectronic Effect from B-Site Dopants Stabilizes Black Phase of  $\text{CsPbI}_3$ . ○
- 155 Half-Metallic Heusler Alloy/ $\text{MoS}_2$  Based Magnetic Tunnel Junction. **2022**, 14, 55167-55173 ○
- 154 Identification of the Kirkendall effect as a mechanism responsible for thermal decomposition of the  $\text{InGaN}/\text{GaN}$  MQWs system. **2022**, 24, 123007 ○
- 153 The Effect of Y Doping on Monoclinic, Orthorhombic, and Cubic Polymorphs of  $\text{HfO}_2$ : A First Principles Study. **2022**, 12, 4324 1
- 152 Single-step extraction of small-diameter single-walled carbon nanotubes in the presence of riboflavin. 13, 1564-1571 ○
- 151 Machine Learning Aided Interpretable Approach for Single Nucleotide-Based DNA Sequencing using a Model Nanopore. **2022**, 13, 11818-11830 ○
- 150 Utilizing Ultraviolet Photons to Generate Single-Photon Emitters in Semiconductor Monolayers. ○
- 149 Density functional theory for selecting modifiers for enhanced adsorption of tetracycline in water by biochar. ○
- 148 DeePKS + ABACUS as a Bridge between Expensive Quantum Mechanical Models and Machine Learning Potentials. **2022**, 126, 9154-9164 ○
- 147 The adsorption modeling of bisphenol A derivatives on the surface of carbon materials. **2022**, 12, 316-320 ○
- 146 Hyperspectral imaging of exciton confinement within a moiré unit cell with a subnanometer electron probe. **2022**, 378, 1235-1239 1
- 145 Strain tunable quantum emission from atomic defects in hexagonal boron nitride for telecom-bands. **2022**, 12, ○



144	The Ti <sub>0.2</sub> V <sub>1.8</sub> C MXene Ink-Prepared Chemiresistor: From Theory to Tests with Humidity versus VOCs. <b>2023</b> , 11, 7	5
143	Modulating spintronic properties of transition metals doped GaN nanotubes with high Curie temperature.	0
142	Highly sensitive amphetamine drug detection based on silicon nanowires: Theoretical investigation. <b>2022</b> , 102584	0
141	Extending the applicability of popular force fields for describing water/metal interfaces: application to water/Pd(111). <b>2023</b> , 98, 015009	0
140	Morphology-controlling hydrothermal synthesis of h-WO <sub>3</sub> for photocatalytic degradation of 1,2,4-trichlorobenzene. <b>2022</b> , 168620	1
139	AtomAI framework for deep learning analysis of image and spectroscopy data in electron and scanning probe microscopy. <b>2022</b> , 4, 1101-1112	2
138	Ionic Equilibria in Polytungstate Melts. <b>2022</b> , 10, 2658	1
137	Band Gap Opening in Borophene/GaN and Borophene/ZnO Van der Waals Heterostructures Using Axial Deformation: First-Principles Study. <b>2022</b> , 15, 8921	0
136	The loss of the property of locality of the kernel in high-dimensional Gaussian process regression on the example of the fitting of molecular potential energy surfaces.	1
135	Thiosemicarbazonecopper/Halido Systems: Structure and DFT Analysis of the Magnetic Coupling. <b>2023</b> , 11, 31	0
134	Quasi-2D SnO <sub>2</sub> Thin Films for Gas Sensors: Chemoresistive Response and Temperature Effect on Adsorption of Analytes. <b>2023</b> , 16, 438	0
133	Magnetism and EPR Spectroscopy of Nanocrystalline and Amorphous TiO <sub>2</sub> : Fe upon Al Doping. <b>2023</b> , 9, 26	0
132	Vitamin C as a shelf-life extender in liposomes. 58,	0
131	Charge-induced phase transition in encapsulated HfTe <sub>2</sub> nanoribbons. <b>2023</b> , 7,	0
130	Thermoelectric Response Enhanced by Surface/Edge States in Physical Nanogaps. <b>2023</b> , 16, 660	0
129	Hydrogen adsorption on methyl-functionalized IRMOF-1 and IRMOF-18 by molecular simulation. <b>2023</b> , 142,	0
128	Highly efficient perovskite solar cells by building 2D/3D perovskite heterojunction in situ for interfacial passivation and energy level adjustment.	0
127	Electronic Origin of Laser-Induced Ferroelectricity in SrTiO <sub>3</sub> . 576-583	0

- 126 Pressure-induced reentrant Dirac semimetallic phases in twisted bilayer graphene. **2023**, 107, 0
- 125 Detection of H<sub>2</sub>S, HF and H<sub>2</sub> pollutant gases on the surface of penta-PdAs<sub>2</sub> monolayer using DFT approach. **2023**, 13, 1
- 124 Expanding gaufroyite family to Sr<sub>2</sub>MBi(REEO)<sub>3</sub>(BO<sub>3</sub>)<sub>4</sub> (M = Ca, Sr, Ba; REE = Y, Eu) borates with large second harmonic generation responses. **2023**, 0
- 123 Ab initio study of boron-rich amorphous boron carbides. 0
- 122 Effect of transition metal modification on the sensing characteristics of arsenene adsorption of nitrogenous toxic gases. **2023**, 111845 0
- 121 Controllable Low-Bias Rectifying Behaviors Induced by AA-P2 Dopants in Armchair Silicene Nanoribbons with Different Widths. **2023**, 13, 106 0
- 120 Inter and intra molecular dynamics in Poly(trimethylene 2,5-furanoate) as revealed by infrared and Broadband Dielectric Spectroscopies. **2023**, 125699 0
- 119 A Time-Dependent Random State Approach for Large-scale Density Functional Calculations. 0
- 118 Transverse Electronic Transport Properties of Single DNA Nucleobase Pairs between Different Electrode Materials. 0
- 117 Enhanced  $\pi$ -Stacking between Dipole-Bearing Single Molecules Revealed by Conductance Measurement. 0
- 116 Influence of particle size on the electrocatalytic activity and optical properties of NiO nanoparticles. **2023**, 289, 116266 0
- 115 Ab Initio Calculations of Chitosan Effects on the Electronic Properties of Unpassivated Triangular ZnO Nanowires Oriented along [0001] Directions. **2023**, 8, 2337-2343 0
- 114 Bacterial nanocellulose and long-chain fatty acids interaction. **2022**, 10, 218-249 0
- 113 Ab Initio Investigation of Boron- and Nitrogen-Doped Penta-graphene in the Presence of a Vacancy Defect. 0
- 112 Optimizing density-functional simulations for two-dimensional metals. **2022**, 6, 0
- 111 Electrical characteristics and conductive mechanisms of AlN-based memristive devices. **2022**, 18, 815-825 0
- 110 Graphene oxide and flavonoids as potential inhibitors of the spike protein of SARS-CoV-2 variants and interaction between ligands: a parallel study of molecular docking and DFT. 0
- 109 Graphitic spheres by pyrolyzing tolueneferroceneethiophene in a chemical vapor deposition experiment. **2023**, 58, 2170-2187 0

- 108 Electronic and electromechanical properties of vertical and lateral 2D heterostructures. **2023**, 51-71 ○
- 107 Electrically driven singlet-triplet transition in triangulene spin-1 chains. **2023**, 107, ○
- 106 Bifunctional Nanostructured Palladium/MoS<sub>x</sub> Electrocatalyst for Cathode Hydrogen Evolution Reaction PEM Water Electrolysis and Oxygen Reduction Reaction. 2200518 ○
- 105 Polarization Doping in a GaN-InN System Ab Initio Simulation. **2023**, 16, 1227 ○
- 104 Cs<sub>2</sub>XI<sub>2</sub>Cl<sub>2</sub> (X = Pb, Sn) All-Inorganic Layered Ruddlesden-Popper Mixed Halide Perovskite Single Junction and Tandem Solar Cells: Ultra-High Carrier Mobility and Excellent Power Conversion Efficiency. 2201050 ○
- 103 Efficient All-Electron Time-Dependent Density Functional Theory Calculations Using an Enriched Finite Element Basis. ○
- 102 Electron Transport through Nanoconfined Ferrocene Solution: Density Functional Theory-Nonequilibrium Green Function Approach. **2023**, 127, 2666-2674 ○
- 101 On-Surface Synthesis of Nanographenes and Graphene Nanoribbons on Titanium Dioxide. 1
- 100 Investigation of the electric and thermoelectric properties of metallo-phthalocyanine molecular junctions with planar and axial configuration. **2023**, ○
- 99 A comprehensive model of nitrogen-free ordered carbon quantum dots. **2023**, 18, ○
- 98 Combining multi-scale simulations and experiments to unveil the adsorption of methylene blue in graphene tridimensional-based materials. ○
- 97 Nano-ZrO<sub>2</sub>-Catalyzed Biginelli Reaction and the Synthesis of Bioactive Dihydropyrimidinones That Targets PPAR- $\gamma$  in Human Breast Cancer Cells. **2023**, 13, 228 ○
- 96 Modeling metamaterials: Planar heterostructures based on graphene, silicene, and germanene. **2023**, 27-50 ○
- 95 Electronic and magnetic properties of TATA-DNA sequence driven by chemical functionalization. ○
- 94 Investigation of thickness dependent efficiency of CsPbX<sub>3</sub> (X = I, Br) absorber layer for perovskite solar cells. **2023**, 176, 111264 ○
- 93 LAVA 1.0: A general-purpose python toolkit for calculation of material properties with LAMMPS and VASP. **2023**, 286, 108667 ○
- 92 2.5 Million-Atom Ab Initio Electronic-Structure Simulation of Complex Metallic Heterostructures with DGDFT. **2022**, ○
- 91 Comparison of three cyclodextrins to optimize bisphenol A extraction from source water: Computational, spectroscopic, and analytical studies. 2300012 ○

- 90 Ab initio comparison of spin-transport properties in MgO-spaced ferrimagnetic tunnel junctions based on Mn<sub>3</sub>Ga and Mn<sub>3</sub>Al. **2023**, 13, 025016 ○
- 89 Graphynes and Graphdiynes for Energy Storage and Catalytic Utilization: Theoretical Insights into Recent Advances. ○
- 88 Investigation of structural and electronics properties of boron co-doped silicon carbide nanoribbons. **2023**, ○
- 87 Size dependent electrocatalytic activities of h-BN for oxygen reduction reaction to water. **2023**, 158, 134713 ○
- 86 Enhanced tunneling electroresistance effect in Pt/BiAlO<sub>3</sub>/Pt ferroelectric tunnel junctions by a graphene interlayer. **2023**, 619, 156726 ○
- 85 Compatibility of DFT+U with non-collinear magnetism and spin-orbit coupling within a framework of numerical atomic orbitals. **2023**, 286, 108684 ○
- 84 Stability, mechanical and electronic properties of Occ carbon allotropes: Four new tetragonal 3D superhard carbon crystals. **2023**, 135, 109838 ○
- 83 The mechanism of carcinogenic heavy metal adsorption on a new monolayer AlP<sub>5</sub>. **2023**, 623, 157025 ○
- 82 Exploring the electronic and mechanical properties of lithium-decorated silicon carbide nanowires for energy storage. **2023**, 62, 106840 ○
- 81 Nanodevice design and electronic transport properties of Ge<sub>2</sub>Sb<sub>2</sub>-based monolayers. **2023**, 150, 115681 ○
- 80 Ab initio study of electronic and magnetic properties of zigzag and armchair AlN nanosheets. **2023**, 150, 115670 ○
- 79 Surface Li effects on the electronic properties of GaAs nanowires: A first principles approach. **2023**, 38, 102745 ○
- 78 Computational evaluation of sensing properties of a novel 2D diboron dinitride for detecting toxic gas molecules. **2023**, 161, 107446 ○
- 77 G-C<sub>3</sub>N<sub>5</sub> nanotube as a promising candidate for adsorption and inactivation of aflatoxin B<sub>1</sub>: A first-principles study. **2023**, 38, 102868 ○
- 76 Highly furosemide uptake employing magnetic graphene oxide: DFT modeling combined to experimental approach. **2023**, 379, 121652 ○
- 75 Role of environmental oxygen and water in the electronic and optical properties of sigma tellurene. **2023**, 151, 115716 ○
- 74 Boron Nitride-Graphene (BN-G) Bilayer as a Channel of Graphene Based Field Effect Transistor. **2023**, 12, 021001 ○
- 73 Adsorption of 3d transition-metal atoms on two-dimensional penta-graphene: A first-principles study. **2023**, 27, 101611 ○

72	Topological and nodal superconductor kagome magnesium triboride. <b>2023</b> , 7,	0
71	Utilization of two-dimensional multicomponent Quasicrystal for NO <sub>2</sub> gas detection. <b>2023</b> , 298, 127449	1
70	Influences of point defects on electron transport of two-dimensional gep semiconductor device. <b>2023</b> , 34, 185204	0
69	Designing sub-5 nm monolayer ALP MOSFETs. <b>2023</b> , 176, 207524	0
68	Potential application of two-dimensional PC6 monolayer as an anode material in alkali metal-ion (Li, Na, K) batteries. <b>2023</b> , 769, 139734	0
67	Device-to-Materials Pathway for Electron Traps Detection in Amorphous GeSe-Based Selectors. <b>2023</b> , 9,	0
66	Raman study of Cd <sub>1-x</sub> Zn <sub>x</sub> Te phonons and phonon polaritons Experiment and ab initio calculations. <b>2023</b> , 133, 065701	0
65	On the self-consistency of DFT-1/2. <b>2023</b> , 158, 094103	0
64	Mechanistic Insights into Plasmonic Catalysis by Dynamic Calculations: O <sub>2</sub> and N <sub>2</sub> on Au and Ag Nanoparticles. <b>2023</b> , 35, 1586-1593	0
63	Effects of Ga on the structural, mechanical and electronic properties of Ti-45Nb alloy by experiments and ab initio calculations. <b>2023</b> , 140, 105728	0
62	Unlocking the electronic, optical and transport properties of semiconductor coupled quantum dots using first principles methods.	0
61	Defect-Induced Transport Enhancement in Carbon-Boron Nitride-Carbon Heteronanotube Junctions. <b>2023</b> , 14, 2056-2064	0
60	Tuning structural and electronic properties of single-walled SiC nanotubes.	0
59	Current-driven collective dynamics of non-Hermitian edge vibrations in armchair graphene nanoribbons. <b>2023</b> , 107,	0
58	BaTiO <sub>3</sub> perovskite for optoelectronics application: A DFT study. <b>2023</b> ,	0
57	Strong field driven extreme nonlinear photoemission from individual single-walled carbon nanotubes. <b>2023</b> , 107,	0
56	Defect induced enhanced quantum capacitance in Plumbene: A first principles study. <b>2023</b> ,	0
55	Switchable Organic Low-Loss Spin Filters Based on Gold-Viologen-Gold Molecular Junctions. <b>2023</b> , 127, 4251-4257	0

- 54 Effective Hubbard Parametrization for Optimizing Electronic Bandgap of monolayer CrI<sub>3</sub>. **2022**, ○
- 53 Mixed-Valence Conductors from Ni Bis(diselenolene) Complexes with a Thiazoline Backbone. **2023**, 62, 4197-4209 ○
- 52 Pseudo-Elasticity and Variable Electro-Conductivity Mediated by Size-Dependent Deformation Twinning in Molybdenum Nanocrystals. 2206380 ○
- 51 Revealing the band structure of ZrTe<sub>5</sub> using multicarrier transport. **2023**, 107, ○
- 50 High-Capacity Ion Batteries Based on Ti<sub>2</sub>C MXene and Borophene First Principles Calculations. **2023**, 11, 95 ○
- 49 Electronic, spintronic, and piezoelectric properties of new Janus ZnAXY (A=Si, Ge, Sn, and . **2023**, 107, ○
- 48 Theoretical Investigation of Diameter Effects and Edge Configuration on the Optical Properties of Graphdiyne Nanotubes in the Presence of Electric Field. 1083 ○
- 47 Effect of nickel impurity on structural, magnetic and electronic properties of WX<sub>2</sub>MLs (X=S, Se): An ab-initio study. **2023**, ○
- 46 Estimation of electron temperature dynamics in warm dense gold using measured and DFT-calculated plasma frequency. **2023**, 98, 045813 ○
- 45 Electrical and optical properties of PbSe/PbTe heterostructures containing vacancies, doping, and alloys using first-principle calculations. **2023**, 138, ○
- 44 Full analytical solution of finite-length armchair/zigzag nanoribbons. **2023**, 107, ○
- 43 Thermal and Electrical Properties of Additively Manufactured Polymer/Boron Nitride Composite. **2023**, 15, 1214 ○
- 42 Low resistance electrical contacts to few-layered MoS<sub>2</sub> by local pressurization. **2023**, 10, 021003 ○
- 41 Electronic and optical properties of boron nitride nanoribbons exploiting DFT. **2023**, 55, ○
- 40 High-pressure studies of atomically thin van der Waals materials. **2023**, 10, 011313 ○
- 39 Intercell moiré exciton complexes in electron lattices. ○
- 38 Efficient discovery of multiple minimum action pathways using Gaussian process. **2023**, 7, 025004 ○
- 37 Role of Chalcogen Defect Introducing Metal-Induced Gap States and Its Implications for Metal/MDs Interface Chemistry. **2023**, 8, 10176-10184 ○

- 36 Massively parallel GPU enabled third-order cluster perturbation excitation energies for cost-effective large scale excitation energy calculations. **2023**, 158, 144111
- 35 Digital-to-analog converter implementation based on silicon nanowire FET.
- 34 Enhancement of Graphene Phonon Excitation by a Chemically Engineered Molecular Resonance. **2023**, 130,
- 33 Introduction. **2023**, 1-17
- 32 Activation, Transportation, and Reaction of Alkyl Radicals on a Si(111)-B Surface by a Scanning Tunneling Microscope Tip. **2023**, 127, 6002-6009
- 31 High-Performance Fe<sub>x</sub>GeTe<sub>2</sub>-Based ( $x = .$  **2023**, 19,
- 30 Anion influence on electronic and optical properties of several iodobismuthates. **2023**, 223, 112138
- 29 An Isothiazolanthrone-Based Self-Assembling Anticancer Color-Changing Dye for Concurrent Imaging and Monitoring of Cell Viability.
- 28 Substrate-Induced Changes on the Optical Properties of Single-Layer WS<sub>2</sub>. **2023**, 16, 2591
- 27 Polar meron-antimeron networks in strained and twisted bilayers. **2023**, 14,
- 26 Intercalation of CO<sub>2</sub> Selected by Type of Interlayer Cation in Dried Synthetic Hectorite. **2023**, 39, 4895-4903
- 25 Electronic, mechanical, and thermal properties of zirconium dioxide nanotube interacting with poly lactic-co-glycolic acid and chitosan as potential agents in bone tissue engineering: insights from computational approaches. 1-13
- 24 Halide Containing Short Organic Monocations in  $n = 1\bar{4}$  2D Multilayered Halide Perovskite Thin Films and Crystals. **2023**, 35, 2873-2883
- 23 Control the electronic and optical properties of AlN nanosheet by the electric field. **2023**, 11, 100423
- 22 An ab-initio study of hydrogen storage performance of Si<sub>2</sub>BN nanotubes decorated with group 8B transition metals. **2023**,
- 21 Not So Innocent After All: Interfacial Chemistry Determines Charge-Transport Efficiency in Single-Molecule Junctions..
- 20 Not So Innocent After All: Interfacial Chemistry Determines Charge-Transport Efficiency in Single-Molecule Junctions..
- 19 Metastable Polymorphic Phases in Monolayer TaTe<sub>2</sub>.

- 18 Quantum Interference and Contact Effects in the Thermoelectric Performance of Anthracene-Based Molecules. **2023**, 127, 7484-7491 ○
- 17 First-Principles Calculation of MoO<sub>2</sub> and MoO<sub>3</sub> Electronic and Optical Properties Compared with Experimental Data. **2023**, 13, 1319 ○
- 16 Stretching effects on non-adiabatic electron dynamic behavior in poly(dG)-poly(dC) DNA upon the proton irradiation. **2023**, 35, 285101 ○
- 15 Microscopic theory of spin relaxation of a single Fe adatom coupled to substrate vibrations. **2023**, 107, ○
- 14 Spectral Downshifting and Passivation Effects Using 2D Perovskite (OAm)<sub>2</sub>SnBr<sub>4</sub> Films to Enhance the Properties of Si Nanowire Solar Cells. ○
- 13 Fe<sup>III</sup>d Ferromagnetic Cyclic Coordination Cluster [Fe<sup>III</sup>4Gd<sup>III</sup>4(teaH)<sub>8</sub>(N<sub>3</sub>)<sub>8</sub>(H<sub>2</sub>O)] with Magnetic Anisotropy-Theory and Experiment. ○
- 12 Controlling Spin Interference in Single Radical Molecules. ○
- 11 Magnetic Ordering in TlGa<sub>1-x</sub>Fe<sub>x</sub>Se<sub>2</sub> Dilute Magnetic Semiconductors with Various Fe Dilution Ratios. ○
- 10 Atomic structure and peculiarities of the electronic properties of Br layers on Ag(111) at different coverages. **2023**, 122304 ○
- 9 Organic Stable Radical Oligomers as Spin Filters. ○
- 8 DFT Study of Adsorption Behavior of Nitro Species on Carbon-Doped Boron Nitride Nanoribbons for Toxic Gas Sensing. **2023**, 13, 1410 ○
- 7 Two-Dimensional Films Based on Graphene/Li<sub>4</sub>Ti<sub>5</sub>O<sub>12</sub> and Carbon Nanotube/Li<sub>4</sub>Ti<sub>5</sub>O<sub>12</sub> Nanocomposites as a Prospective Material for Lithium-Ion Batteries: Insight from Ab Initio Modeling. **2023**, 16, 3270 ○
- 6 Janus PdSTe Nanosheet as Promising Contender for Detection of Volatile Organic Compounds (VOCs) in human breath: a first principles investigation. **2023**, 143101 ○
- 5 Tuning the Sharing Modes and Composition in a Tetrahedral GeX<sub>2</sub> (X = S, Se) System via One-Dimensional Confinement. **2023**, 17, 8734-8742 ○
- 4 Structural and Electronic Properties of Small-Diameter Carbon NanoTubes: A DFT Study. **2023**, 392-402 ○
- 3 Fabrication of MoS<sub>2</sub>/Bi<sub>2</sub>S<sub>3</sub> heterostructure for photocatalytic degradation of Metronidazole and Cefalexin and antibacterial applications under NIR light: experimental and theoretical approach. **2023**, 129, ○
- 2 Mechanistic Study of Lithium-Ion Battery Cathode Recycling Using Deep Eutectic Solvents. **2023**, 11, 6914-6922 ○
- 1 Gap Opening in Graphene via Locally Introduced Electric Field. ○



